A POLYMERIC TRIPLE-LAYERED TABLET FOR STRATIFIED ZERO-ORDER DRUG RELEASE

KOVANYA MOODLEY

A dissertation submitted to the Faculty of Health Sciences, University of the Witwatersrand, in fulfilment of the requirements for the degree of Master of Pharmacy

Supervisor:

Professor Viness Pillay

Department of Pharmacy and Pharmacology, University of the Witwatersrand, South Africa

Co-Supervisors:

Dr. Yahya Essop Choonara

Department of Pharmacy and Pharmacology, University of the Witwatersrand, South Africa

Ms. Lisa Claire du Toit

Department of Pharmacy and Pharmacology, University of the Witwatersrand, South Africa

Johannesburg, 2011

DECLARATION

I, Kovanya Moodley, declare that this dissertation is my own work. It has being submitted for the degree of Master of Pharmacy in the Faculty of Health Sciences in the University of the Witwatersrand, Johannesburg. It has not been submitted before for any degree or examination at this or any other University.

…….

This 28th day of February 2012

RESEARCH OUTPUTS

1. Research Publications

Oral Drug Delivery Systems Comprising Altered Geometric Configurations for Controlled drug delivery*
Kovanya Moodley, Viness Pillay, Yahya E. Choonara, Lisa C. du Toit, Valence M.K. Ndesendo, Shivaan Cooppan, Priya Bawa and Pradeep Kumar
*Submitted to the *International Journal of Molecular Sciences*

Computational Mechanistic Characterization and Drug Release Evaluation of Novel Polymeric Triple-layered Solid Matrix Configurations for Stratified Zero-order Drug Release*
Kovanya Moodley, Viness Pillay, Yahya E. Choonara, Lisa C. du Toit, Valence M.K. Ndesendo, Pradeep Kumar, Leith Meyer, Riaz A. Khan and Nthato Chirwa
*Submitted to the *Journal of Biocompatible Polymers*

2. Conference Outputs

Intonation of diphenhydramine release from a multifaceted tablet configuration. Poster presented at Academy of Pharmaceutical and Pharmacological Sciences of South Africa, 22-26 September 2008, Magaliesburg, South Africa.
Kovanya Moodley, Thiresen Govender, Viness Pillay, Yahya E. Choonara and Lisa C. du Toit.

Development of a Novel Polymeric Triple-layered Solid Matrix for Flexible Zero-order Drug Release. Poster presented at International Conference of Pharmaceutical and Pharmacological Sciences, 23-26 September 2009, Potchefstroom, South Africa.
Kovanya Moodley, Poonam Rama, Viness Pillay, Yahya E. Choonara and Lisa C. du Toit.

Composite Polymeric Blends for Potential Zero-order Drug Release Kinetics from a Triple-layered Tablet Matrix. Poster presented at the American Academy of Pharmaceutical Sciences conference, November 2009, Los Angeles, USA.
Kovanya Moodley, Viness Pillay, Yahya E. Choonara and Lisa C. du Toit.

Matrix Tablet Configurations for Constant Multiple Drug Delivery. Poster presented at the APS UKPHARMSCI conference, September 2010, Nottingham, UK.
Kovanya Moodley, Viness Pillay, Yahya E. Choonara and Lisa C. du Toit.

PATENTS

A Polymeric Stratified Drug Release Tablet, University of the Witwatersrand, Kovanya Moodley, Viness Pillay, Yahya Essop Choonara and Lisa Claire Du Toit

Publication date: 30/07/2010

Patent Application Number: 2010/03744

ABSTRACT

Patient compliance is a major factor in achieving optimal therapeutic outcomes. Pill burden, due to multiple drug therapies, has a great detrimental impact on compliance of the patient. Dose-dependent side-effects, associated with peak-trough plasma fluctuations of drugs, also have a negative impact on patient compliance with drug therapy. It is under these circumstances that zero-order drug release kinetics proves to be ideal. This is due to the lack of peak-trough fluctuations that occur with zero-order drug release, thereby minimizing the side-effects of drug therapy. Furthermore, a drug delivery system that may deliver more than one drug at a time may be beneficial to alleviate the pill burden associated with chronic diseases or specific health conditions. Novel drug delivery systems have been developed that offer zero-order or linear drug release. Amongst such systems are multilayered tablets. However these systems generally offer the delivery of just one drug. The development of a delivery system that is able to deliver up to three drugs in a zero-order manner may prove to be significantly beneficial to greatly increase patient compliance and in turn therapeutic efficacy.

The purpose of this study was to design a novel triple-layered tablet (TLT) matrix targeted at achieving stratified zero-order drug release. The central factor for the establishment of the TLT was the selection of ideal and novel polymers that are capable of acting as superior drug release matrices. Modified polyamide 6,10 (PA6,10) and salted-out poly(lactic-co-glycolic acid) (PLGA) were employed as the outer drug-carrier matrices whereas poly(ethylene oxide) (PEO) was used as the middle layer drug matrix. Specialized granulation techniques and direct compression were employed to prepare the TLT matrices. Diphenhydramine HCl, ranitidine HCl and promethazine were chosen as model drugs for the study due to their similar high aqueous solubilities (100mg/mL). Matrix hardness, gel strength, swelling/erosion characteristics, Fourier Transform Infrared spectroscopy, Differential Scanning Calorimetry and in vitro drug release analysis employing High Performance Liquid Chromatography were performed on the TLT matrices in order to determine the physicomechanical and physicochemical nature of the TLT matrices. Computational molecular modeling (CMM) was employed to characterize the formation and dissolution of the TLT matrices. A box-Behnken experimental design was employed that resulted in the generation of 17 design formulations for ultimate optimization. In vivo animal studies were performed in the Large White Pig model to assess drug release behavior of the TLT. Ultra Performance Liquid Chromatography was employed for plasma sample analysis.

The PA 6,10 layer provided relatively linear and controlled drug release patterns with an undesirable burst release greater than 15%, which upon addition of sodium sulphate was greatly reduced. The addition of PEO to the salted-out PLGA layer greatly reduced the initial burst release that occurred when salted-out PLGA matrix was used alone. Desirable results were obtained from FTIR, hydration and swelling/erosion analysis. CMM elucidated the possible mechanism of zero-order release from respective layers. Upon completion of the Box-Behnken design analysis, an optimized TLT formulation was established according to the formulation responses selected namely the rate constants and correlation coefficients. The TLT displayed desirable near linear release of all three drugs simultaneously over 24 hours, with approximately 10%, 50% and 90% of the drugs released in 1, 10 and 24 hours. An in vitro drug release comparison performed between the optimized TLT and the commercial tablets currently used, showed an unequivocal display of superiority of the TLT in terms of linear drug release over commercial tablets. A cardiovascular related drug regimen (Adco-simvastatin®, DISPRIN CV® and Tenormin 50®) was applied to the TLT to assess the flexibility of incorporating a range of drugs. The TLT furthermore provided near linear to linear release of the therapeutic regimen over 24 hours and maintained superiority over the commercial tablets. Benchtop Magnetic Resonance Imaging, porosity analysis and Scanning Electron Microscopy was utilized for further introspective characterization of the TLT. In vivo analysis demonstrated a definite control of drug release from the TLT as compared to commercial tablets which further confirmed the advantage of the TLT.

ACKNOWLEDGEMENTS

Foremost to my parents Alan and Shareena Moodley for sacrificing in order to provide for us, and to my siblings Kody and Siara Moodley for their support.

To my family Mahadevi Reddy, Bathmadevi Naidoo, Gonadevi Anthony, Renu Pramlall, Peter Moodley and Ajeeth Pramlall for their guidance and support throughout the years.

To my supervisor, Professor Viness Pillay, for his dedication to science and continuous encouragement to push frontiers.

To my co-supervisors, Dr. Yahya Choonara and Ms Lisa du Toit, for their readiness to offer help and knowledge which greatly aided my research.

To my mentors Dr. Valence Ndesendo, Ndidi Ngwuluka and Pradeep Kumar for their wisdom and invaluable inputs to my research.

To my dearest “Majestic” alternate family Yashodan Naidoo, Kavitha Nundkwar, Natanya Moodley, Narushka Pillay, Vinodhum Pillay, Chantal Koomcaran, Shivaan Cooppan, Sambarthan Cooppan, Priyen Naidu, Firdaus Nabeemeeah, Rynae Grewan, Janine Carim, Kiren Pillay, and Taygan Pillay for the fun times and de-stressing sessions as well as the great support system they have offered me.

To my dear friends: Ameena Wadee, Derusha Frank, Thiresen Govender, Rubina Shaikh, Yusuf Dawood, Clare Dott, Thomas Tsai, Tasneem Rajan, Latavia Singh, Deshnee Naidoo and Yasien Docrat for the good times and support they have offered me both on and off campus.

To my fellow research colleagues: Caragh Murphy, Deshika Reddy, Priya Bawa, Zaheeda Khan, Pius Fasinu, Steven Mufamadi, Deanne Hazle, Nonhlanhla Masina, Sheri-lee Harrilal, Samantha Pillay, Nthato Chirwa, Felix Mashingaidze, Ahmed Seedat, Angus Hibbins and Raeesa Moosa for their advice and utmost willingness to assist me with the challenges I faced during my studies.

To Sello Ramarumo, Tebogo Chandu, Kleinbooi Mohlabi and Bafana Temba for their essential assistance with the running of the laboratories.

To the Central Animal Services at the University of the Witwatersrand for their tremendous knowledge and teachings regarding my *in vivo* studies.

To the National Research Foundation (NRF) for their financial assistance which was immensely appreciated.

To the TATA Foundation for awarding me a prestigious scholarship that greatly assisted me during my studies.

To the staff of the Department of Pharmacy and Pharmacology, Professor Michael Danckwerts, Professor Sandy Van Vuuren, Mr. David Bayever, Ms. Shirona Naidoo, Ms. Neelaveni Padayachee, Ms. Sibongile Sibambo, Ms. Neha Singh and Ms. Busi Damane for their support, assistance and insight.

DEDICATION

This dissertation is dedicated to my parents Alan and Shareena Moodley. Thank you for providing only the best for me.

TABLE OF CONTENTS

CHAPTER 3

FORMULATION, DEVELOPMENT AND CHARACTERIZATION OF NOVEL TRIPLE-LAYERED TABLETS MATRICES FOR ZERO-ORDER DRUG RELEASE

CHAPTER 5

CHARACTERIZATION AND FURTHER INTROSPECTIVE EVALUATION OF THE OPTIMIZED TRIPLE-LAYERED TABLET FORMULATION

CHAPTER 6

***IN VIVO* ASSESSMENT OF THE TRIPLE-LAYERED TABLET MATRIX IN THE LARGE WHITE PIG MODEL**

CHAPTER 7

CONCLUSIONS AND RECOMMENDATIONS

LIST OF FIGURES

LIST OF TABLES

LIST OF EQUATIONS

CHAPTER 1

INTRODUCTION

1.1. Background to the Study

Patient compliance is a major influence of therapeutic outcomes, drug treatment regimens may become complex as they require the patient to take numerous tablets up to three or four times a day and this is therefore very influential to therapeutic results. In addition, a large number of conventional tablets need to be administered up to three or four times a day. Understandably, treatment regimens that require multiple drugs to be taken often can lead to non-compliance on the part of the patient (Townsend *et al*., 2003; Apu *et al*., 2009; Phutane *et al*., 2010; Shivaraj *et al*., 2010). This poses a significant problem as the majority of treatment available is in the form of oral drug delivery (Colombo *et al*., 2009) which is the most desirable route for drug delivery and is rapidly growing (Phutane *et al*., 2010). Decreased patient compliance to treatment regimens is always present and challenging (Vermeire *et al*., 2001), this is prevalent with chronic conditions. Non-compliance has proven to be a serious problem that poses significant financial disadvantages to healthcare.

Pertinent to novel drug delivery technology is the concept of increasing patient compliance by endeavouring to simplify treatment regimens thereby improving treatment efficacy and therapeutic success. Developing Drug Delivery Systems (DDS) that reduce the number of tablets a patient is obliged to take is therefore very appropriate in this regard. Multilayered tablets that allow for sustained release of more than one drug at a time have been proven to be useful in addressing this issue (Kohlrausch, 2005).

The current standard, regarding conventional drug therapy, is first-order drug release. Most of the available drug products administered by and to patients exhibit first-order drug release kinetics. With first-order kinetics, there is a rapid disintegration of the tablet almost complete release of the drug active within 2 hours of administration. This results in initial elevated plasma levels of the drug after administration, followed by an exponential decrease. This poses a disadvantage as there will be minimal therapeutic efficacy after drug levels drop to a certain amount or drug toxicity at very high plasma levels (Landgraf *et al*., 2005). This type of drug release does not allow for appropriate plasma drug level balance. Peak-to-trough fluctuations may occur with first-order drug release that can cause dose-dependent side-effects (Shahiwala *et al*., 2004). This is poses a significant impediment that may result in a lack of patient compliance with the treatment regimen due to the side-effects that are associated with the peak-to-trough fluctuations.

Wherever applicable, a DDS should ideally exhibit zero-order drug release kinetics which allows for a constant quantity of drug to be released over an extended period of time resulting in uniform and sustained drug delivery (Ayres, 2004). Zero-order drug release can be used in antibiotic delivery, the treatment of hypertension, pain management, antidepressant delivery and numerous other conditions that require constant plasma drug levels (Landgraf *et al*., 2005).

Multilayered tablets have been developed or patented for simplifying various treatment regimens. For example, a bilayered tablet containing a statin and aspirin for the treatment of cholesterol and reducing the risk of a myocardial infarction was developed (Ullah *et al*., 1998). The tablet was comprised of two layers, one containing aspirin and the other containing a statin. The proposed function of the tablet was to minimise the interaction between the two drugs (Ullah *et al*., 1998). However the drug release kinetics achieved from the tablet did not follow zero-order.

There are several challenges that are associated with achieving zero-order drug release from the outer layers of a multilayered tablet. The outer layers are able to delay the interaction of the inner layer with the liquid medium by reducing the surface area available for release of the drug and by decreasing the penetration rate of the solvent (Efentakis *et al*., 2006). This results in zero-order drug release from the inner layer. The outer layers therefore are more exposed to the gastrointestinal environment and more susceptible to changes and degradation. Control of drug release from the outer layers is therefore challenging.

A coated platform-delivering tablet is described in a patent (Ayres, 2004, US Patent 6720005). Osmotic pumps are very good at providing zero-order drug release; the tablet had a rigid coating membrane. A laser was used to form a hole (aperture) through the coating. The tablets presented a lag time of approximately 2 hours prior to drug release due to the time taken for the gastrointestinal fluids to penetrate the semi-permeable coating membrane. This device has been widely used in providing zero- order drug release. However, there are challenges with large scale manufacturing and specialised laser equipment is needed to drill holes through the coating layer. There are various other problems associated with drug delivery from osmotic tablets such as cost of manufacture (Dash and Cudworth II, 1998; Kaushal and Garg, 2003; Ghosh and Ghosh, 2011).

Central to achieving zero-order kinetics with a DDS is the intimate selection of suitable polymeric material. There are various polymeric materials that have shown the ability to control the release of drugs (Peppas, 1997). Examples of these include poly(lactide-co-glycolide) (PLGA) which is biodegradable, polyethylene oxide (PEO) which is robust and

swells, HPMC and poly(acrylic acid) (PAA) which is hydrophilic (Jian-Hwa Guo,copyright 2001-2007). Studies have shown that the main factors affecting the release of drugs are the geometry of the tablet, the polymers used, as well as method of formulation (*Varma et al*., 2004). The suitable use of these polymers as drug carrier matrices is an essential aspect of controlled drug delivery.

Therefore the aim of this study was to develop a triple-layered tablet (TLT) containing drug in each polymeric layer with drug release from each layer ideally following zero-order kinetics. Each layer will contain one drug, therefore offering the delivery of up to three different drugs. The use of polymers such as PEO, HPMC and PLGA amongst other specialised polymers capable of providing zero-order drug release was explored for use in the design of the drug delivery system.

1.2. Rationale and Motivation for this Study

Chronic conditions such as hypertension, tuberculosis, HIV and malaria require multiple drug therapy. Adherence to therapy in these conditions by patients can be tedious therefore the TLT system may also be used to deliver drugs in a zero-order fashion all in a single dose with significant potential to reduce the associated dose-dependent side-effects that are caused by peak-to-trough fluctuations. The delivery of antidepressants may possibly also be incorporated into the TLT to provide superior plasma drug level profiles as well as reduced daily doses. Figure 1.1 illustrates the peak-to-trough fluctuations associated with general drug administration and the effect of zero-order drug release kinetics on these peak-to-trough fluctuations.

High blood pressure (hypertension) was the underlying cause of death for 56,561 Americans in 2006 and a primary or contributing cause of about 326,000 deaths. According to the South African Hypertensive Society, hypertension is prevalent in 1 in 5 adults. Hypertension is also a leading cause of death in adults aged over 55. Approximately 7 million people die every year due to cardiovascular related health conditions. In a recent South African Demographic and Health Survey, it was presented that 6.1 million South Africans have hypertension or are taking antihypertensive medication.

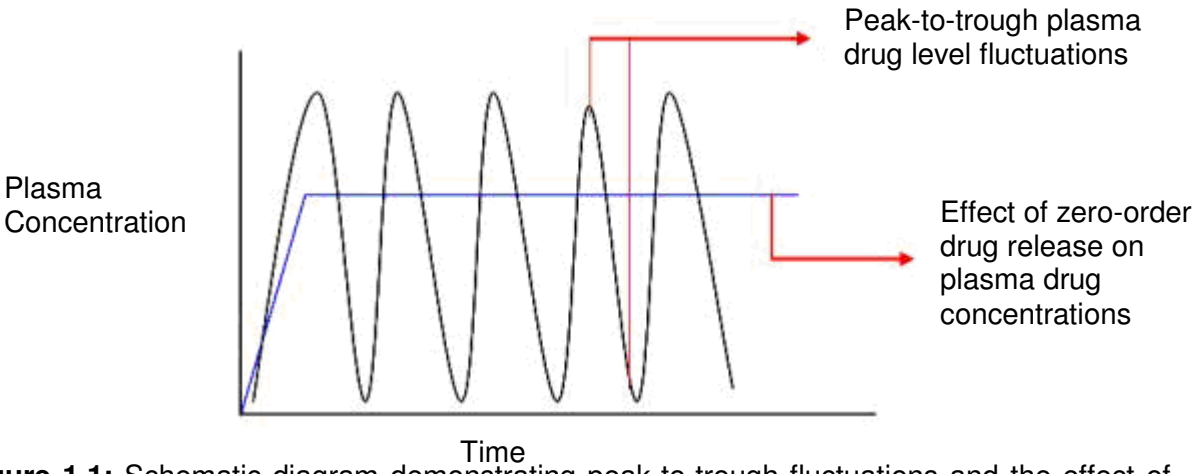

Figure 1.1: Schematic diagram demonstrating peak-to-trough fluctuations and the effect of zero-order drug release on plasma drug concentration.

Current multilayered drug delivery systems do not offer the flexibility of the delivery of three drugs in a zero-order manner. Various studies have revealed the development of multilayered tablet devices for modified drug release. The limitation however is that essentially, most of the systems developed allow for the controlled release of one drug only. This usually occurs from the middle drug loaded layer.

Hence, this study proposes a DDS, a polymeric triple layered tablet (TLT) for stratified zero-order drug release that will desirably lead to better therapeutic outcomes and increase patient compliance through overcoming the challenges associated with multiple drug treatment regimens. The main mechanism to achieve this would be providing sustained or controlled zero-order drug release. In comparison with other multilayered oral drug delivery systems that have been developed, the TLT would offer zero-order drug release from up to three tablet layers.

The aim of this study was to therefore develop a polymeric TLT that offers stratified zero-order drug release for potential use in the treatment of chronic conditions that require multiple drugs to be delivered in a zero-order manner. The TLT would be superiorly capable of improving plasma drug levels and allowing the incorporation of up to three drugs in a single DDS to enhance patient compliance.

The uniform dosing that the TLT may offer would also help to reduce the side-effects associated with the drugs by reducing peak-to-trough fluctuations. In an attempt to provide superior control of drug release from the outer layers of the TLT, the drug in the outer layers were encapsulated into a polymer matrix using direct compression and specialised granulation techniques. The effects of modifying the geometry and chemistry of the outer layers of the TLT were essentially explored. The culmination of these factors was intended for the fundamental zero-order release of each drug. Ideally when the TLT comes into

contact with the gastrointestinal environment the polymers will erode away or swell to release the drug. With polymeric matrices being the elementary backbone to the TLT formulations, various polymers or polymer combinations and specialized granulation techniques for example wet granulation were studied and utilized to aid in obtaining drug release in a zero-order manner from the outer layers of the TLT.

1.3. Novelty of the Proposed Triple-layered Tablet

- The system offers zero-order release of up to three drugs in a stratified manner from a multilayered polymeric tablet.
- Other multilayered systems that have been developed offer zero-order drug release from only one to two layers.
- The use of newly synthesized polyamide 6,10 and salted-out PLGA as rate controlling polymers in the outer layers add to the novelty of the TLT.
- The specialized granulation techniques and other approaches to achieve zero-order drug release from the outer layers enhance the novelty of the triple-layered tablet system.

1.4. Aims and Objectives of the Study

- Selection and synthesis of suitable polymers that may be employed as drug matrices for the outer layers of the proposed TLT.
- To determine the physicochemical (e.g. structural molecular variations) and physicomechanical (e.g. hardness) properties of the polymers.
- To develop a triple-layered tablet comprising formulation techniques such as specialised granulation approaches and direct compression.
- To select suitable drug actives with a high water solubility (>50mg/ml) in order to prove the capability of controlled release of highly water soluble drugs.
- To perform *in vitro* dissolution studies to determine the drug release kinetics.
- To incorporate a therapeutic drug combination into the optimized TLT to assess the flexibility to control the release of various drug classes.
- To perform *in vivo* animal studies to assess drug release kinetics and biocompatibility of the TLT in a suitable animal model.

1.5. Overview of the Dissertation

Chapter 1 introduces the challenges experienced in current drug therapies and emphasizes the rationale for the study. The aims and objectives of the study are also outlined in this Chapter.

Chapter 2 provides a detailed description of the current and novel drug delivery developments in terms of geometrically modified oral tablet-like drug delivery systems such as multilayered tablets. It is a comprehensive literature review that outlines the fields of innovation involved in developing altered and superior tablet devices for oral drug delivery and the advantages and shortfalls of such devices.

Chapter 3 contains the preliminary experimental laboratory formulation and development of a suitable feasible Triple-layered Tablet formulation. It outlines the formulation parameters, physicochemical and physicomechanical characterization, computational and molecular modelling and fundamental *in vitro* drug release analysis.

Chapter 4 demonstrates the structuring of a Box-Behnken experimental design which involved the selection of suitable formulation responses and complex *in vitro* drug release analysis and the statistical optimization of the Triple-layered Tablet.

Chapter 5 exhibits the further essential physicomechanical analysis such as porosity analysis, Scanning Electron Microscopy imaging and Magnetic Resonance Imaging that was performed on the optimized TLT. The additional incorporation of a therapeutic drug regimen into the optimized Triple-layered Tablet is also assessed and comparative analysis with conventional products is demonstrated.

Chapter 6 is an inclusive analysis of the *in vivo* drug release testing in the Large White pig model. The establishment of a suitable protocol for the administration of the Triple-layered Tablet and blood sampling is also presented.

Chapter 7 provides the conclusions for this study and recommendations for future work.

CHAPTER 2

REVIEW OF ORAL DRUG DELIVERY SYSTEMS COMPRISING ALTERED GEOMETRIC CONFIGURATIONS FOR CONTROLLED DRUG DELIVERY

2.1. Introduction

Modified or controlled release oral drug delivery systems have over the few decades been shown to offer advantages over the conventional methods (Deshpande, 1996; Green, 1996; Rubinstein *et al*., 2007; Abdul and Poddar, 2004; Yu *et al*., 2009). These include increased patient compliance (Chien, 1982; Wilding *et al*., 1991), selective pharmacological action; reduced side-effect profile and reduced dosing frequency (Fassihi *et al*., 1995). These systems may therefore have a significantly beneficial outcome in therapeutic efficacy. Controlled release offers prolonged delivery of drugs and maintenance of plasma levels to within a therapeutic range (Singh, 2000; Lingam *et al*., 2006). Furthermore, by pairing drug administration rate with drug elimination rate, steady-state plasma levels can be maintained (Shah *et al*., 1988; Hardy *et al*., 2007). Currently most drug delivery systems exhibit first-order drug release kinetics where the plasma level of the drug is extremely high after administration and then decreases exponentially. This poses disadvantages such as minimal therapeutic efficacy due to reduced drug levels; or drug toxicity which can occur at high concentrations (Landgraf *et al*., 2005). This type of drug release does not allow for appropriate plasma drug level balance.

The utilization of geometric principles has been considered and employed in order to modify drug release behavior from non-linear to zero-order or near zero-order release kinetics (Brooke *et al*., 1977; Ford *et al*., 1987; Sangalli *et al*., 1993; Siepmann *et al*., 2000; Wise, 2000; Cobby *et al*., 2006, Sakamoto *et al*., 2010). Thus far researchers have attempted to control dissolution behavior of drug delivery systems by modifying and controlling the geometry of the employed devices e.g. geometries such as spherical, cylindrical, holed cylindrical and biconvex devices were developed and investigated (Cao *et al*., 2001; Karasulu *et al*., 2003; Efentakis and Politis, 2006; Martin del Valle *et al*., 2009).

One of the principles involved in altering the geometry of tablets is to create a constant surface area for drug release to enable the achievement of zero-order kinetics (Sundy *et al*., 2004; Dash *et al*., 2010). Systems such as multilayered tablets, donut-shaped tablets, Procise®, Geomatrix® and Smartrix® technologies have been developed employing geometric manipulations (Conte *et al*., 1993; Kim, 1999; Wise, 2000; Efentakis, 2006; Yu *et al*., 2009). These geometric manipulations may also be employed to develop drug delivery systems for the treatment of specialized biological conditions where zero-order drug release is not

optimal, for example chronotherapy for heart conditions (Survase *et al*., 2007) or the scheduled treatment of asthma and inflammation (Losi *et al*., 2006). Bimodal drug release may also be desirable with drugs that have variable absorption sites along the gastro-intestinal tract (Shah, 1988; Gohel *et al*., 2009). Technologies such as the Dome Matrix® have shown promise in achieving varied drug release profiles in order to treat specific conditions (Losi *et al*., 2006). Dilacor XR™ was developed as an extended release formulation for the delivery of diltiazem hydrochloride as described by Colombo and co-workers (2000) where the geometry of the system played an important role in the release profiles of drugs (Colombo *et al*., 1989).

In addition, the polymeric materials used to construct these technologies play an important role in the functioning of these specialised systems (Efentakis, 2006; Martin del Valle *et al*., 2009). Thus far, various types of polymers have been investigated for their ability to control drug release (Brannon-Peppas, 1997; Bernkop-Schnurch *et al*., 2003; Jones, 2004; Yoo *et al*., 2006; Song *et al*., 2009).

Polymers are the essential drug carriers of multilayered matrix tablets (Efentakis *et al*., 2006) and their properties are an important factor in the behavior of these devices. In the past, polymers that were mainly employed for such purposes were the hydro-polymers (Efentakis *et al*., 2006) while currently the employed polymers range from swollen and non-swollen (Jones, 2004; Efentakis *et al*., 2006; Herrlich *et al*., 2009) porous and non-porous (Mueller and Heiber, 1983; Crotts and Park, 1995; Learoyd *et al*., 2009) to erodible or non-erodible polymers (Brannon-Peppas, 1997; Naveen, 2009; Yu *et al*., 2009).

In general, the mechanisms by which polymers perform their functions are by erosion (Heller, 1987), dissolution and swelling (Harland *et al*., 1988). Some studies have shown that drug release from hydrophilic polymer matrices exhibit a typical time-dependent profile for which the drug release becomes controlled after swelling of the polymer (Lee *et al*., 1985; Nelson *et al*., 1987; Peppas *et al*., 1989; Wilding *et al*., 1991; Narasimhan *et al*., 1997; Conte *et al*., 2000).

This chapter thus discusses the application of altered geometric technology and its role in controlled oral drug delivery, focusing primarily on the types of polymers that have been employed in developing geometrically modified systems, the interplay of system geometry and polymeric selection ultimately contributing to the type of drug release patterns that are attained.

2.2. Multilayered Tablets for Controlled Drug Delivery

Mutilayered systems (bilayered, triple-layered or quadruple-layered) are becoming increasingly recognised as controlled-release drug delivery systems (Yang *et al*., 1997; Zerbe *et al*., 2006). These systems have shown to be advantageous over typical tablet systems as depicted in Table 2.1. Namdeo (2008) expressed that multilayered tablets have demonstrated promise, possessing various benefits namely the ability to prevent interactions between drugs and excipients; providing an array of release profiles in one delivery system of either the same or different drugs; treatment for conditions that require a regimen of more than one drug; immediate drug release using a disintegrating monolithic matrix in order to achieve an initial peak in plasma drug level; delayed drug release using an eroding monolithic matrix which may deliver another active to another part of the gastrointestinal tract; providing controlled drug release using a swellable monolithic matrix; provide better control and regulation of release profiles by retarding initial burst release and providing zero-order kinetics (Namdeo, 2008).

The advantages make it apparent that multilayered tablets may play a significant role in future drug delivery trends due to the various capabilities they pose over conventional systems. It would be beneficial to focus on further modification of these systems for more improved and comprehensive drug release control that is capable of a larger scope of application in drug delivery.

Controlled-release multilayered tablets typically involve a drug core layer that is surrounded by barrier layers that may be made up of hydrophilic swellable polymers such as hydroxypropylmethylcellulose (HPMC) and poly(ethylene oxide) (PEO) or hydrophobic polymers such as ethylcellulose (EC) (Abdul *et al*., 2004.). The barrier layers minimize and therefore delay the interaction of the gastrointestinal environment with the active core, by decreasing the surface area available for drug release or by controlling the rate at which the solvent penetrates the layers (Efentakis *et al*., 2006). This allows the initial burst release to be minimized and therefore the drug release can be controlled at a near constant level while the barrier layers undergo erosion or swelling (Brannon-Peppas, 1997; Yu *et al*., 2009). The swollen barrier layers undergo erosion as time goes on, thus increasing the surface area which ultimately allows more drug to be released. Following the same principle it is possible to obtain a constant release profile as well as other types of dissolution patterns such as pulsatile or delayed delivery as well as extended drug delivery depending on the characteristics of the polymers employed. In either case the system should ideally erode completely (i.e. leaving no residue in the gastrointestinal tract after the entire amount of drug is released).

Table 2.1: Advantages of Multi-layered tablets over conventional tablets (Adapted from Namdeo, 2008).

Conventional tablet	Multilayered matrix tablets
	
Drug is released in only one kinetic model.	May be used to incorporate more than one drug and separate them if any chemical incompatibilities exist.
If more than one drug is incorporated, there is no way of avoiding chemical incompatibilities.	Drug release behavior is not restricted to one type, this system may offer varied drug release kinetics of the same or different drugs such as extended and immediate release.

The different types of multilayered tablets designs with varying drug release behavior are shown in Figure 2.1.

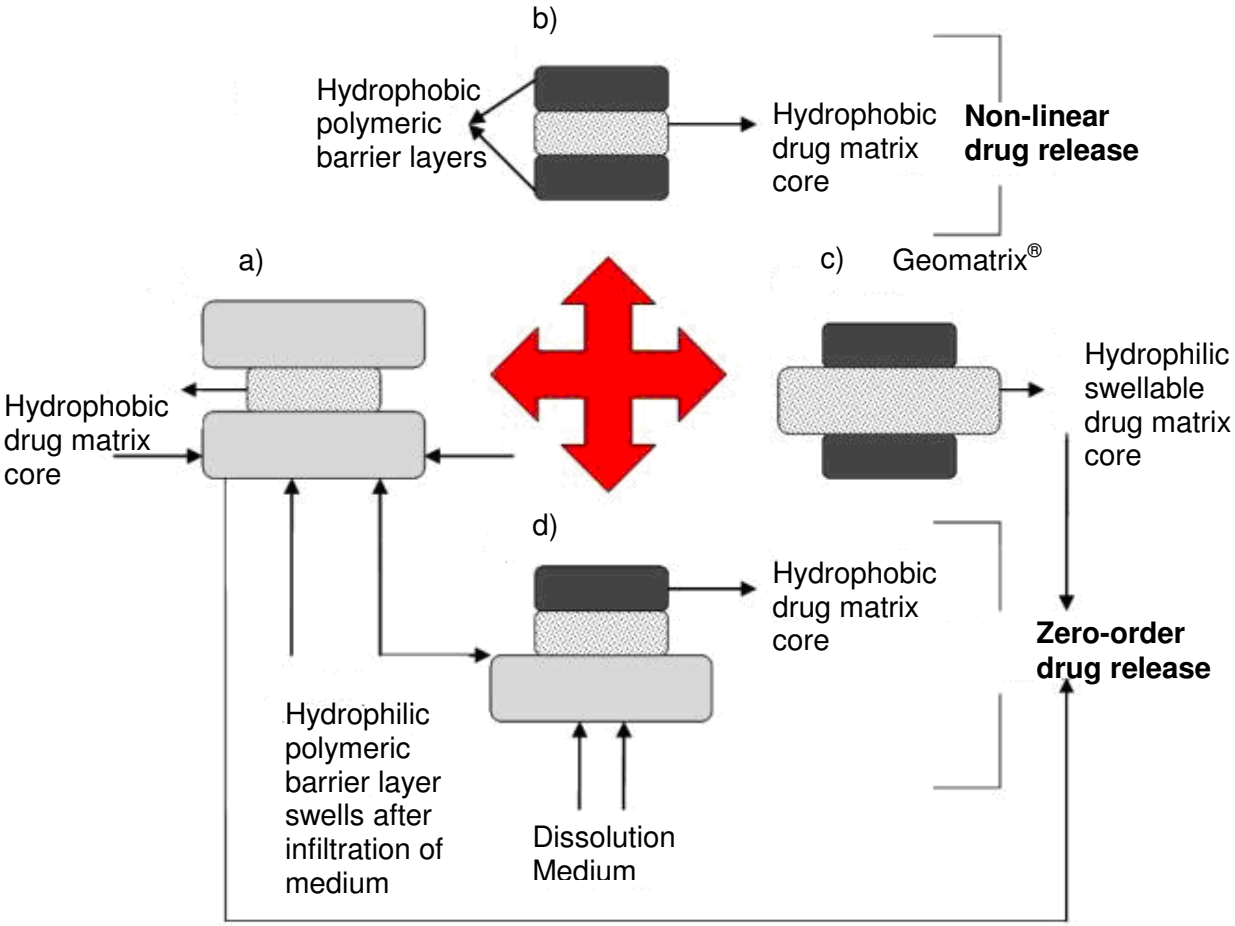

Figure 2.1: Various polymeric formulations of multilayered tablets and possible drug release behavior (adapted from Chidambaram *et al.*, 1998).

There are multilayered tablets that can provide zero-order sustained release where the tablet consists of either a hydrophilic or hydrophobic core layer with barrier layers that are press coated to the surfaces of the core layer. This leaves the sides of the core layer exposed. It

has been shown that, generally, constant drug release can be achieved when both barrier layers are hydrophilic and the core layer is hydrophobic (Qiu *et al*., 1998; Abdul *et al*., 2004). However, other factors also need to be controlled in order to achieve zero-order drug release.

2.2.1. Geomatrix® multilayer tablet technology

The Geomatrix® multilayer tablet technology was developed by Conte and co-workers (1993) for constant drug release. The technology includes triple-layered and bilayered tablets. The triple-layered tablet which is depicted in Figure 2.2 consists of an active core which is a hydrophilic matrix layer and two polymeric barrier layers on either side that are hydrophobic or semi permeable (Kim, 2005; Shionogi Pharma, 2008). The bilayered tablet consists of the drug layer and one barrier layer (Patel *et al*., 2007). The barrier layers modify the swelling rate of the active core and reduce the surface area available for diffusion of drug (Streubel *et al*., 2000; Efentakis and Peponaki, 2008). Zero-order drug release can be achieved with the Geomatrix® system (Yu *et al*., 2009) however release is limited to one drug.

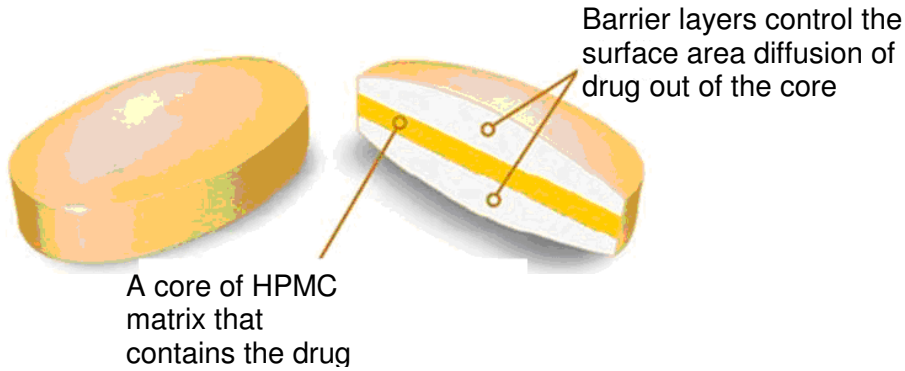

Figure 2.2: A typical Geomatrix® multilayered tablet (Source: Shionogi Pharma, Inc., 2008).

2.2.2. Sodas® multilayer tablet technology

Sodas® multilayer tablet technology (Figure 2.3) is a multilayer drug delivery system that has focused on the production of controlled release beads (Elan Drug Technologies, 2010). The Sodas® technology is characterized by its inherent flexibility that enables the production of customized dosage forms that respond directly to individual needs such as pain and blood pressure. The technology essentially leads a pursatile drug release where the drug is released in pulses that are separated by defined time intervals. Examples of this technology include Ritalin® LA and Focalin® XR. These formulations are both used to treat Attention Deficit Hyperactivity Disorder (ADHD). Furthermore, these formulations provide a once-daily pulsed profile that offers the patient efficacy throughout the day negating the need for taking the dose during working hours unlike the twice-daily dosing of the conventional immediate

release tablet. Benefits offered by the SODAS® technology include: controlled absorption with resultant reduction in peak-to-trough ratios, targeted release of the drug to specific areas within the gastrointestinal tract, absorption independent of the feeding state, suitability for use with one or more active drug candidates, a facility to produce combination dosage forms, “sprinkle dosing” by administrating the capsule contents with soft food, once or twice daily dose resembling multiple daily dose profiles.

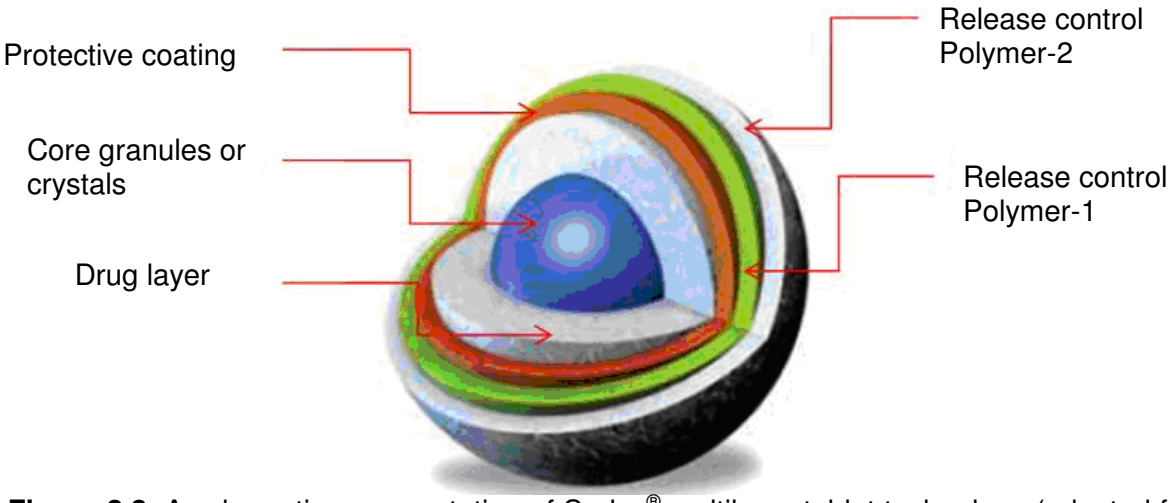

Figure 2.3: A schematic representation of Sodas® multilayer tablet technology (adapted from Elan drug technologies, 2010).

The aforementioned studies have provided practical technical ideas in the development of multilayered tablets depending on the clinical applications of these systems. The studies have also provided insight on what strategies need to be considered for further application. Table 2.2 provides the summary of the polymers influencing the behavior and release characteristics of multilayered tablets. It is observed that there are great variations of multilayered tablet technologies proving flexibility, which affords possibilities for positive research betterment. With the intuitive selection of polymers and the appropriate employment of geometric principles, multilayered tablets may emerge as the future benchmark for the treatment of chronic diseases. However the difficulties that may occur with the scale up of more intricate layered drug delivery systems may present as unfavourable to the pharmaceutical industry. The necessity of specialized equipment may add to the difficulties in commercialization of these systems.

Table 2.2: Summary of the type of polymers that influence the behavior and release characteristics of multilayered tablets.

Type of polymer used a drug carrier	Type of polymer used in barrier layers	Type/Dimensions of tablet	Drug release achieved
Hydrophilic	Hydrophilic	Bilayered	Extended release
Hydrophilc	Hydophilic	Bilayered	Lesser extent of release retardation
Hydophobic	Hydrophilic (HPMC K4M)	Triple-layered	Zero-order release
Hydrophobic (CW)	Hydrophobic (CW)	Triple-layered	Non-linear release

2.3. Factors Influencing the Rate of Drug Release from Multilayered Tablets

2.3.1. Polymers employed in multilayered tablets

Generally, a multilayered system should initially swell, then gel and ultimately slowly erode (Abdul, 2004; Yang *et al*., 2003). A study done by Efentakis and co-workers (2006) investigated the effect of polymeric substances on drug release. Hydrophilic and swellable polymers such as HPMC (Methocel K100M), microcrystalline cellulose (MC) and PEO and the hydrophobic polymer cellulose acetate propionate (CAP) were employed in this study in which venlafaxine HCl was used as a model drug. The study focused on a core tablet that contained venlafaxine HCl and Methocel K100M as the drug carrier. Bilayered and triple-layered tablets were prepared using the core tablet. The bilayer tablet consisted of a core tablet where one surface was covered with either Cellulose Acetate Pthalate (CAP) or Methocel E50LV, while both surfaces of the core tablet were covered with both of the polymers to form the triple-layered tablets. Hydrophilic polymers are employed as drug core matrices due to their swelling ability (Hongtao *et al*., 2007; Conti *et al*., 2007; Li *et al*., 2008; Barakat *et al*., 2009). The release profiles obtained showed that drug release was slower from the multilayered tablets than from the core tablet alone (Efentakis *et al*., 2006). When the core tablet came into contact with the dissolution medium, it swelled and expanded. This caused an increase in the diffusion path length for the drug and the drug release rate was therefore reduced. Upon employing HPMC as a barrier layer, the layer swelled concurrently with the core tablet, merging the core surfaces thereby enveloping part of the core, which resulted in the limiting of drug transport through the barriers (Efentakis *et al*., 2006). CAP did not swell due to its impermeability properties and therefore drug dissolution and the drug release rate was retarded. The use of HPMC or CAP in the barrier layers showed similar results in terms of retarding drug release except that HPMC showed slow erosion as opposed to CAP (Efentakis *et al*., 2006). HPMC devices, generally, presented with slower drug release when compared to CAP devices, reason being that they form a more efficient and solid barrier. Overall, the study showed that the characteristics of the polymers employed had a significant influence on the release profiles of the tablets although the choice of polymers employed in the study was conservative. Further research that focuses on the use of novel specialised polymers that are competent in providing zero-order drug release is necessitated.

A study performed by Chidambaram and co-workers (1997) assessed the behavior of layered diffusional matrices for zero-order sustained drug release. Layered tablets were formulated with a hydrophobic core layer which contained the drug; this layer typically consisted of 24% pseudoephedrine HCl, 40% carnauba wax and lactose filler. The barrier

layers were composed of either hydrophilic (HPMC K4M or K100M or microcrystalline cellulose (MCC) PH 101) or hydrophobic polymers. Three different types of matrices were formulated. In the first type, the two barrier layers were hydrophilic, in the second type, one of the barriers was hydrophobic while the other was hydrophilic and in the third type, the two barrier layers were both hydrophobic. Results showed that more desirable linear release profiles were obtained with the first and second type of matrices as depicted in Figure 2a and d, while the barrier layers in the third system needed to be manipulated in order to achieve zero-order release kinetics (Chidambaram *et al*., 1997; Qui *et al*., 1998). The proposed mechanism for the zero-order drug release from the first type of matrix was that as the hydrophilic barriers swelled and eroded the rate of diffusion of drug from the hydrophobic middle layer decreased (Chidambaram *et al*., 1997; Yang *et al*., 1998). According to the study, the release rate from the lateral surface was influenced by polymer viscosity and concentration. These factors ultimately influence diffusion path length as well as the diffusion co-efficient. The use of polymers that possess mechanical or chemical characteristics to intrinsically alter the geometry, via modification of diffusion path length, of matrices for controlled release may be an interesting perspective to study for future drug delivery research.

2.3.2. Structure of the multilayered tablet device

A study undertaken by Efentakis and co-workers (2006) illustrated that the structure of a DDS plays an important role in its drug release behavior. They found that covering a greater area of the core tablet by a barrier layer results in the retardation of drug release to a greater extent, as it forms a more efficient barrier thereby decreasing the drug release rate. Another study by Efentakis and Peponaki (2008) re-iterated the significance of structure and geometry of triple-layered tablets with isosorbide mononitrate as a model drug. The weight and thickness of the barrier layers also had a role in drug release behavior. Chidambaram and co-workers (1997) established that drug release from the surfaces of the core was dependent on the thickness of the hydrophilic barrier layers. An investigation by Streubel and co-workers (2000) looked at bimodal drug release from multilayered matrix tablets. It was discovered that by increasing the weight of the barrier layers from 50mg to 150mg it resulted in a more effective retardation of drug release, thus it was concluded that by manipulating the weight and thickness of the outer layers (Table 2.2) a desirable drug release profile of individual drugs may be achieved, thus complementing their pharmacokinetic behavior. The concept of barrier layers have proven to be beneficial in multilayered tablet designs however converting the barrier layers into additional controlled release drug matrices may prove to be beneficial for future application (Namdeo, 2008).

Zerbe and co-workers (2006) have shown that there are also complex multilayered tablet systems with layers of various shapes that are able to provide zero-order drug release. The Smartrix® tablet technology (Figure 2.3) that was developed by LTS Lohmann Therapie-Systeme employs modified geometrical shapes that compensate for the varying surface area caused by erosion or swelling (Table 2.3) (Rathbone *et al*., 2002).

The triple-layered tablet is composed of a drug core that has a specific shape. The core is enclosed between two rapidly erodible outer layers. The middle layer has a biconcave shape that the two outer layers tightly bond to after compression. The thickness of the outer layers and the shape of the drug core control the release of drug usually in a linear fashion. The Smartrix® system (as depicted in Figure 2.4) is also able to achieve bimodal drug release (Porter, 2009) as an added advantage of being flexible. This technology proves to be useful as it does not require specialised polymers to perform the desired function. The study that resulted in the development of the Smartrix® system has further emphasized the functionality of shape and geometry in altering drug release behavior and the research has demonstrated favourable outcomes. However this technology requires specialized dry tablet press machines that may pose as a disadvantage.

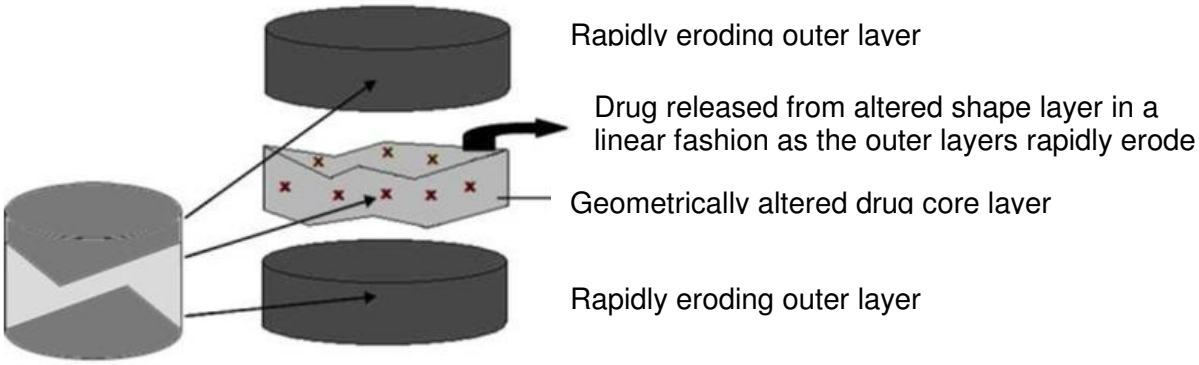

Figure 2.4: Smartrix® technology (Adapted from Rathbone *et al*., 2002).

2.4. Bilayered Tablets

Bilayered tablets have proven to be effective in delivering drugs that require a loading dose followed by a maintenance dose (Doshi *et al*., 2007; Patra *et al*., 2007; Nirmal *et al*., 2008; Kim *et al*., 2008). Commonly, in bilayered systems, one layer contains a quantity of drug for conferring immediate release, while the second layer contains a quantity of drug for extended release. The rapid release layer disintegrates immediately after administration while the matrix layer remains intact during the passage of drug through the gastrointestinal tract. The matrix erodes in a controlled fashion in order to maintain blood levels. Two drugs may also be incorporated into this delivery system for variable release profiles.

A bilayered tablet for the delivery of propranolol hydrochloride was developed by Patra and co-workers (2007). These tablets were comprised of an immediate release layer and a sustained release layer. Sodium starch glycolate was employed as the superdisintegrant in the rapid release layers of various formulations, while the polymers Eudragit RLPO, Eudragit RSPO and EC were utilised in the sustained release layers. Drug release studies illustrated that there was an initial burst release that delivered the loading dose while the rest of the drug was released over 12 hours in a sustained manner (Patra *et al*., 2007). The same concept has been demonstrated in a patent by Kim and co-workers (2008) where the system provided release of two drugs in different manners. The controlled release layer delivers metformin while the rapid release layer delivers glimepiride. The controlled release layer is made up of a mixture of hydrophobic and hydrophilic polymers, while the immediate release layer is composed of a disintegrant and glimepiride. This further enhances the positive function of these systems in treating chronic conditions such as hypertension and diabetes.

Nirmal and co-workers (2008) developed a bilayered tablet containing atorvastatin calcium for immediate release and nicotinic acid for extended release for the concurrent treatment of hypercholesterolemia. It has been shown that the combination of these two drugs results in an important reduction of low density lipoprotein cholesterol as well as desirable variations in high density lipoprotein cholesterol (Nirmal *et al*., 2008). HPMC K100M was employed as the polymeric matrix for nicotinic acid and the immediate release layer containing atorvastatin calcium was formulated using superdisintegrant croscarmellose sodium. Drug release studies were performed over 12 hours and the results indicated that these tablets were successful in delivering two types of drugs concurrently (Nirmal *et al*., 2008). This study was shown to be valuable for future application in the successful treatment of hypertension.

2.4.1 VersaTab® bilayered tablet technology

A VersaTab® bilayered tablet technology is a tablet that has been devised to result in linear drug release through controlled erosion (IntelGenx Corp, 2009). The technology designs tablets with the ability to co-release multiple drugs with different release rates. This technology is suitable for a large number of bioactives. The tablet is highly versatile with a broad range of delivery profiles and therefore endowed with improved patient compliance. Figure 2.5 displays a profile that depicts VersaTab® bilayered tablet technology firstly with one bioactive that provides controlled release and secondly with two bioactives that provides immediate release and controlled release (IntelGenx Corp, 2009).

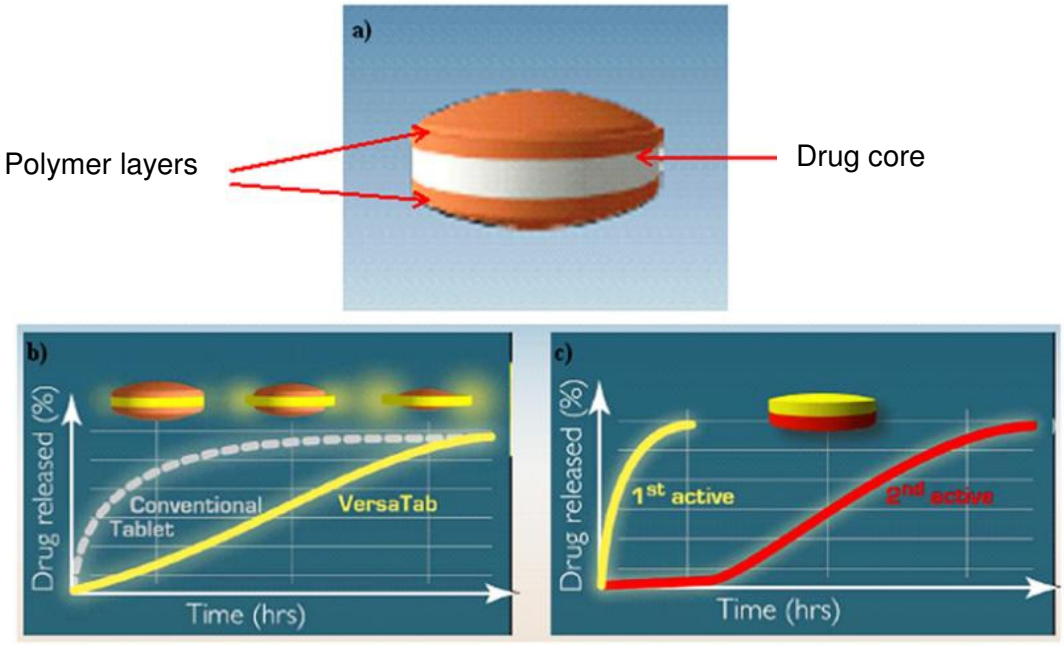

Figure 2.5: a) VersaTab® bilayered tablet; Profiles depicting VersaTab® bilayered tablet technology; b) One bioactive-controlled release and c) Two bioactives-immediate release and controlled release (Sourced from: IntelGenx Corp, Innovative Drug Delivery Solutions, 2009).

2.5. Triple-layered Tablets

Triple-layered tablets are comprised of an inner drug core layer which is sandwiched between two surrounding barrier layers (Abdul, 2004; Namdeo, 2008). These barrier layers may also contain drug and serve as matrices to release drug in various release patterns (Namdeo, 2008). The general mechanisms of action of triple-layered tablets include erosion of matrix layers, creation of a drug concentration gradient, limiting surface area of release of the swellable matrix by the barrier layers, erosion and swelling of the barrier layers to achieve a constant area for uniform drug release, as well as modification of the layers dissolution to achieve pulsatile or alternating release profiles (Efentakis, 2006; Namdeo, 2008).

Triple-layered systems have some rewards in contrast to typical systems due to the varying release pattern capability, simplicity of manufacturing, enhanced patient compliance, enhanced safety profile of drug levels and reduced cost.

2.5.1. Geolock™ technology

Geolock™ Technology is a triple-layered tablet that has been devised for chronotherapy focused-real time oral drug delivery (SkyePharma, 2010). Principally, it is a new clinically oral drug delivery technology which allows, with a high degree of precision, the timed delivery of

drugs that employs a press-coating technique. Geolock™ tablet is composed of an active drug core (middle layer) that is surrounded by two outer protective layers (Figure 2.6). The inner core can be a single or combination of drugs essentially formulated for either immediate or modified release.

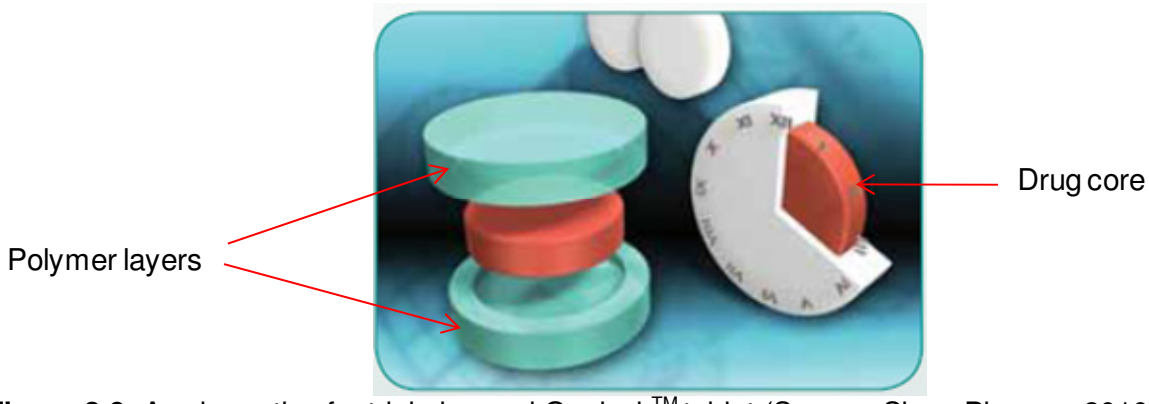

Figure 2.6: A schematic of a triple layered Geolock™ tablet (Source: SkypePharma, 2010).

2.5.2. Various drug release profiles achievable by triple-layered tablets

It has been shown that both immediate and sustained drug delivery can be obtained through a single triple-layered tablet (Abdul, 2004). In this case, there is an initial immediate rapid release of drug, which is followed by a sustained constant drug release. This type of release could be useful for drugs that need a high plasma concentration immediately for therapeutic efficacy where zero-order drug release kinetics is not required. Maggi and co-workers (1997) developed such a system where a quick/slow release of Naproxen was achieved. A multi-layered controlled release tablet containing naproxen and naproxen sodium salt was developed by Desai in 1996. The tablet composition included a layer containing naproxen which offered a delayed release of a granulated form of naproxen and another immediate release layer that contained naproxen sodium salt. This system was designed to deliver a prompt therapeutic effect while maintaining the effect for 24 hours (Desai, 1996). This type of variable release is extremely useful for the delivery of specific drugs that need both rapid and sustained release. A patent by Iyer and his co-workers (2006) reported on a triple-layered system that was comprised of a sustained release layer containing methylcobalamin while the other two immediate release layers each contained an antihypertensive, a lipid regulator or a serum homocysteine lowering agent providing a valuable combination for the treatment of hypertension. Compressed mini-tablets were designed for biphasic delivery of drugs with zero-order release kinetics (Lopes *et al.*, 2006; Iyer *et al.*, 2006). The mini-tablets were compressed within an outer filling that was composed of MCC PH102 that filled the space between the minitablets. This outer filling provided rapid drug release while the minitablets provided prolonged release (Iyer *et al.*, 2006). The mini-tablets specifically were composed of either HPMC or EC, with a diameter of 2.5mm and an approximate weight of 12mg each.

Various formulations that differed in the amount of outer filling and number of mini-tablets used were prepared. Results showed that the mini-tablets with HPMC showed the most potential for achieving zero-order drug release. Another patent by Zerbe and co-workers (2004) presented a multilayer oral system that had a matrix core that contained an NSAID for sustained release and two surrounding layers each containing an H_2–receptor antagonist. The first layer provided sustained release of the antagonist and the second layer provided a rapid release of the antagonist. This idea was developed for use in the treatment of osteoarthritis in people who are more susceptible to developing gastrointestinal adverse effects such as NSAID-induced ulcers.

Time-programmed or chronotherapeutic drug delivery can also be achieved with multi-layered tablets (Abdul *et al*., 2004). With chronotherapy, drug release is governed by time so that drug is released only when needed. This can be described as pulsatile release rather than continuous release. This type of delivery may be beneficial for preventing tolerance arising from the drug as well as in reducing the side-effects. Press coating is a good technique for producing this type of time-dependent release. With press coating, there are no specific coating solvents or equipment that is needed and therefore the manufacturing process is more efficient (Fukui *et al*., 2000). The core layer is essentially coated with polymeric barrier layers by compression. The drug is released when the barrier layers either swell or erode. The coating delays the interaction of the core with the fluid medium, which causes a lag-time before the drug is released. When the solvent penetrates the core layer, the core swells and dissolves, this causes the coating shell to break thereby rapidly releasing the drug (Abdul *et al*., 2004). This research further confirms the useful flexibility of triple-layered tablets although the application is often limited to the release of one drug.

It has been demonstrated that bimodal drug release may also be necessary when a non-uniform drug release rate is desired (Streubel *et al*., 2000). The mechanism of release typically involves an initial rapid release, followed by a slower constant release, which is then followed by another rapid release period. Bimodal drug release may be advantageous in that the initial rapid release phase which is followed by a slow release phase is able to compensate for the slow absorption of drug from the stomach and small intestine. More uniform delivery of drug into the systemic circulation can be achieved because bimodal release systems increase the rate of drug release when the ability of the body to absorb the drug decreases. Streubel and co-workers (2000) developed multilayered matrix tablets that could achieve bimodal drug release rates. Hydroxypropylmethylcellulose acetate succinate (HPMCAS) was used to form the matrix due to the fact that its solubility varies with pH. It is in essence water soluble at high pH values and water-insoluble at low pH values. The study

aimed at determining the effect of HPMCAS on drug release from the different layers of the tablet.

The various geometries of triple-layered tablets may be quite useful for controlling the delivery of highly water soluble drugs. A study by Siahi and co-workers (2005) investigated the development of triple-layered tablets for the delivery of verapamil hydrochloride in a controlled manner. The tablets consisted of three layers that were prepared by compressing polymers which were either natural or semi-synthetic onto the sides of the drug core. HPMC, acacia and tragacanth were used as drug release delaying layers encompassing the core. Different formulations containing separate and combined amounts of these polymers were prepared. The results indicated that when tragacanth was used as a carrier, the release was better delayed than when acacia was used. Results also showed that the location of the polymers in the triple-layered tablets had a substantial effect on the release kinetics.

Triple-layer guar gum matrix tablet formulations were developed by Krishnaiah and co-workers (2002) in which the controlled delivery of aqueous soluble drugs using guar gum as a carrier was explored. The system was evaluated in terms of the release rate of trimetazidine dihydrochloride from the matrix. Different concentrations of guar (30%$^{w}/_{w}$, 40%$^{w}/_{w}$ and 50%$^{w}/_{w}$) were used to prepare the triple-layered tablets. The guar gum acted as a release retardant agent. The release rate from these formulations enabled a twice daily administration of the delivery system (Krishnaiah *et al.*, 2002).

2.6. Multilayered Osmotic Devices

An indented core tablet strategy for preparing monolithic osmotic pumps was developed by Longxiao and co-workers (2006). The tablet was compressed by a punch using a needle. The indented core was coated using EC as a semipermeable membrane coating and polyethylene glycol (PEG) was used as a plasticizer that controlled membrane permeability. The tablet was developed for the delivery of atenolol and sodium chloride and was used as an osmotic agent. Results showed that the tablet was capable of delivering the drug constantly over 24 hours and was not dependent on the agitation or release medium (Longxiao *et al.*, 2006). This system does not require specialised laser drills to form the orifices, thus reducing manufacturing costs. The study was useful in attempting to develop a system that functioned as efficiently as an osmotic pump however in a more feasible and cost-effective manner.

Longxiao and co-workers (2006) also prepared a bilayer osmotic pump tablet using the indented core strategy. The model drug used in the study was nifedipine. A modified tablet

punch was used to prepare the tablets whereby the punch formed an indentation in the centre of the drug surface layer. The indentation was sprayed with a coating solution with only the bottom of the indentation being sufficiently coated. The sides of the indentation were not completely coated, which left an aperture where drug release could occur (Longxiao *et al*., 2006). The tablet showed success in delivering nifedipine at a relatively constant rate for 24 hours (Longxiao *et al*., 2006).

The US patent RE 39069, by Faour and co-workers (1999), described a multilayered osmotic device that could deliver more than one pharmaceutical agent. The device was developed to deliver the first therapeutic agent by immediate release and the second in a controlled manner. Essentially, the device consisted of a core that contained a therapeutic agent, an osmotic agent and poly(vinylpyrrolidone) (PVP). The core was surrounded by a semipermeable membrane (as illustrated in Figure 2.7) that consisted of cellulose acetate esters and poly(ethylene glycol) (PEG) and contained a preformed passageway. The semipermeable membrane is essentially permeable to the dissolution environment and impermeable to the therapeutic agent in the core. The device was also coated with a poly(vinylpyrrolidone)-(vinyl acetate) copolymer that partially or completely surrounds the semipermeable membrane and covered the passageway like a plug. The final segment consisted of an external coat that was comprised of PVP and PEG and a second therapeutic agent that is immediately released. When the external coat releases the second agent, it erodes or dissolves thereby releasing the therapeutic agent that is contained in the core in a controlled manner.

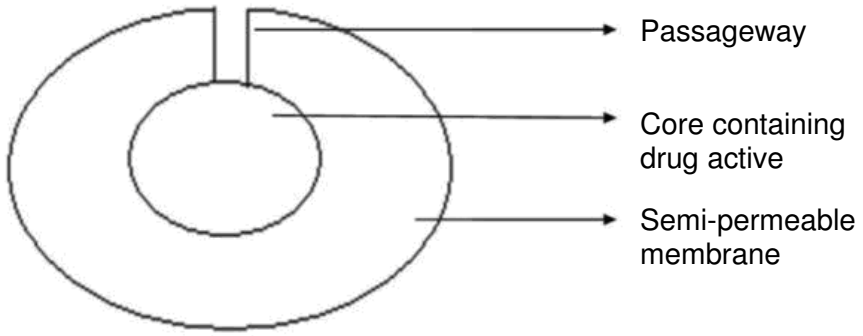

Figure 2.7: Schematic depiction of a multilayered osmotic device (Adapted from Fanner *et al*., 2005, US Patent 6838093).

2.7. Multilayered Floatable Drug Delivery Systems

A study that was conducted by Fassihi and co-workers (1995) looked at zero-order release kinetics from a self-correcting floatable asymmetric configuration drug delivery system. Theophylline was the model drug while PEO polymers of various molecular weights were employed as drug carriers. The various types of PEO polymers, drug and excipients were

directly compressed into a triple-layer asymmetric floatable device. The core layer contained theophylline while the outer layers were composed of polymers and excipients in order to delay the interaction of the core layer with water, thereby delaying and controlling the drug release. Dissolution studies over 16 hours showed that the entire amount of drug was released in a zero-order manner with no initial burst release (Fassihi *et al*., 1995). The release was dependent on the thickness of the layers and polymers used. Fassihi and co-workers (2007) also investigated zero-order delivery of alfuzolin hydrochloride via a gastroretentive system. Triple-layered and bilayered matrices were developed by compressing PEO, HPMC, sodium bicarbonate, citric acid and PVP. Dissolution studies demonstrated the ability of the matrices to achieve floatation in pH 2 and pH 6.8 as well as providing zero-order drug release (Fassihi *et al*., 2007). This system showed fine potential for providing enhanced bioavailability and targeted delivery to the small intestine.

A study by Yang and co-workers (1999) proposed a drug delivery system that would be able to treat *Helicobacter pylori*-associated gastric ulcers. The system was comprised of a swellable, asymmetric triple-layered tablet that was also floatable so as to increase the gastric retention time of the system. The employed rate-controlling polymers were HPMC and PEO. The core layer of the triple-layered tablet contained the drugs tetracycline and metronidazole. *In vitro* studies exhibited a sustained delivery of the two drugs over 6-8 hours, while the tablet was retained, showing the potential to achieve localized treatment, thereby improving therapeutic efficacy. This study poses great potential for the essential eradication of the *Helicobacter pylori* infection that often results in hospitalization of patients who develop serious ulcers.

A patent awarded to Doshi and co-workers (2007) described a floatable drug delivery system that is able to deliver multiple drugs. The system was bilayered and was able to deliver a drug from one layer immediately, followed by slow and controlled release of another drug from the other matrix-forming layer. The immediate release layer contained a disintegrating agent while the matrix-forming layer consisted of a gas generating component and a gelling agent (Doshi *et al*., 2007). The aim of this system was to attain a controlled delivery of fluoroquinolones and to maintain the plasma levels of the drugs within a therapeutic range with once daily administration.

2.8. Core-In-Cup Devices

Danckwerts (1994) developed a core-in-cup tablet system that was able to provide zero-order drug release of aqueous-soluble and aqueous-insoluble drugs. The system consisted of a disc-shaped matrix core that was compression-coated on one surface as well as at the

circumference in order to form a cup around the core. Drug was released in a sustained manner from one stable surface that had a constant surface area. By manipulating the grade, quantity and exposed surface area of any hydrophilic polymer or mixture of polymers that erode constantly over time, the core-in-cup compressed tablet is able to deliver a constant amount of drug over time (Danckwerts, 1994). Results showed that the system was able to provide zero-order drug release for time intervals between 8 and 23 hours, the time of linear release was approximately 8 hours when 5%$^{w}/_{w}$ HPMC K4M with caffeine core-in-cup tablets were produced and approximately 23 hours when 15%$^{w}/_{w}$ HPMC K15M in ibuprofen core-in-cup tablets were produced. The research that has been conducted on core-in-cup devices showed several interesting and useful techniques as well as beneficial application in terms of the solubility of drugs, the flexibility of delivering both aqueous soluble and aqueous insoluble drugs pose an advantage. Danckwerts and co-workers (1995) studied the effectiveness of cup tablets of different depths for use in core-in-cup tablets and the optimal formulation in terms of drug release behavior. They developed a specific punch that is able to change the depth of the cup tablet, thus allowing it to carry various cores in terms of hardness and mass. The efficiency of cup tablets with varying depths and the optimal formulation in terms of drug release were investigated in the study. The cup tablets were composed of 15%$^{w}/_{w}$ carnauba wax in EC while the core tablets were composed of 5%$^{w}/_{w}$ HPMC K4M in ibuprofen. The results indicated that Ibuprofen was released at a near zero-order rate for 18 hours for the cup tablets that had a final depth of 4mm (Danckwerts *et al*., 1995). Figure 2.8 shows the typical geometries of core-in-cup tablets.

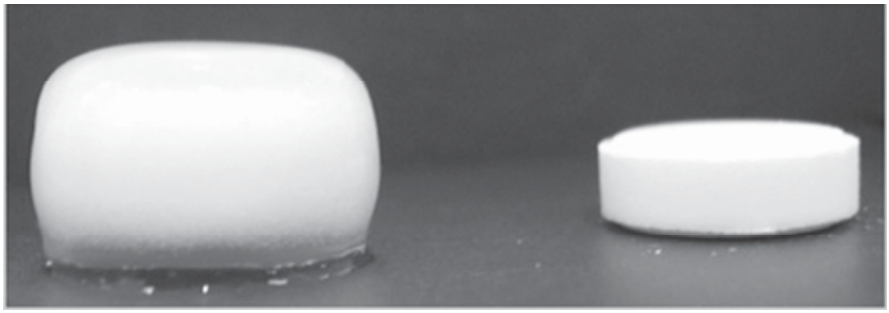

Figure 2.8: Typical geometries of core-in-cup tablets (Source: Guimarães *et al*., 2008).

2.9. Procise® Technology

The Procise® device has a specific geometric configuration (as depicted in Figure 2.5) that controls drug release behavior (Wise, 2000). It is composed of a core which contains uniformly dispersed drug with a core hole in the middle (Figure 2.9). It has been elucidated that altering the geometry of the core can vary the drug release kinetics to zero-order or even first order if desired (as indicated in Table 2.2) (Wise, 2000). The core's entire surface besides the surface of the cylindrical face is surrounded by a permeable inactive coat so that

drug release occurs solely from the cylindrical area. The device is also able to deliver up to two drugs simultaneously with varying release profiles (Wise, 2000). This technology further adds to the varied geometrical systems for flexible and simplified drug delivery.

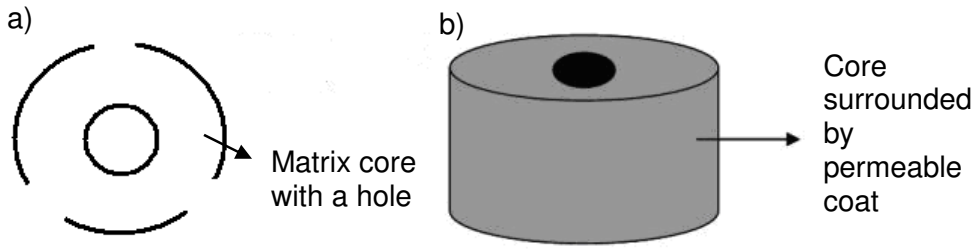

Figure 2.9: a) Aerial schematic of Procise® technology and b) Two-dimensional schematic of Procise® technology (adapted from Porter, 2009).

2.10. Donut-Shaped Devices for Controlled Drug Delivery

There are various publications dating rather far back that established that zero-order release kinetics could be achieved from a hemispherical device containing a hole (Cleave, 1966; Rhine *et al*., 1980; Hsieh, 1983; Kim, 1995; Kim, 1999; Cheng, 1999; Sundy *et al*., 2004). A study by Kim (1995) investigated drug release from uncoated compressed tablets that contained a single central hole. The impact of the hole size and drug solubility on drug release was also investigated. The tablets were composed of PEO and had a diameter of 12mm. Theophylline was used as the model drug. The tablets provided zero-order drug release for approximately 80-90% of the drug followed by a decreased drug release rate (Kim, 1995). The results also indicated that as the size of the hole increased, the rate of drug release also increased. Drug solubility proved to be inversely proportional to duration of linear drug release (Kim, 1995). It was concluded that the donut-shaped PEO tablets with an aperture were capable of providing zero-order drug release as the effect of surface area on release kinetics is reduced. The geometric factors that influence the drug delivery of donut-shaped tablets are presented in Table 2.3.

The hydrophilic polymer-based donut-shaped tablets developed by Kim (1995), exhibited a disadvantage as they adhered to biological tissues and solids causing dose dumping of the drug (Kim, 1999). It was due to this reason that Kim (1999), decided to undertake a study on coated donut-shaped tablets for parabolic and linear drug release. Two types of polymers namely rapidly erodible and slowly erodible polymers were investigated. Zero-order release was achieved when the slowly erodible polymers were used and parabolic drug release was achieved when rapidly erodible polymers were used when diltiazem hydrochloride was incorporated as a model drug. It was also found that the drug release characteristics depended on the stirring rate and hole size (Kim, 1999). These tablets did not adhere to

either biological tissues or solids (Kim, 1999), thus proving to be more effective than the uncoated systems (Kim, 1999). Furthermore, HPMC donut-shaped tablets were developed and investigated by Cheng and co-workers (1999). Theophylline and diltiazem hydrochloride were employed as model drugs. Results depicted that zero-order kinetics was achieved for approximately 90% of the duration of the study (Cheng *et al*., 1999). An increase in the size of the centre hole caused an increase in the rate of drug release and a longer duration of zero-order release (Cheng *et al*., 1999). A further study was conducted by Kim (2005) on triple-layered donut-shaped tablets (Figure 2.10) with enteric polymers to evaluate their controlled release ability. The tablets were prepared by layering three powders and compressing them with a punch. HPMCAS was the fundamental polymer of the core while the outer layers were composed of EC. The results showed that the solubility of the drugs had an effect on release kinetics. The hydrochloride salts of weakly basic drugs had a slower release rate than neutral drugs (Kim, 2005). Thus, this system is capable of providing zero-order drug release for drugs with varying solubilities.

A study completed by Sundy and co-workers (2004) developed a novel compression-coated doughnut-shaped tablet for zero-order sustained release. The tablets were also assessed for their reproducibility. The tablets were prepared using a uniquely designed punch set. Hydrophilic and hydrophobic polymers were employed and evaluated as the coating layers. Caffeine and ibuprofen were used as model drugs as they have different solubilities and allowed for a comparison of the drug release profiles. Results showed that a coating layer of HPMC K15M and a core layer of HPMC K4M provided zero-order release of both caffeine and ibuprofen (Sundy *et al*., 2004). The tablets also proved to be feasible to manufacture on a larger scale.

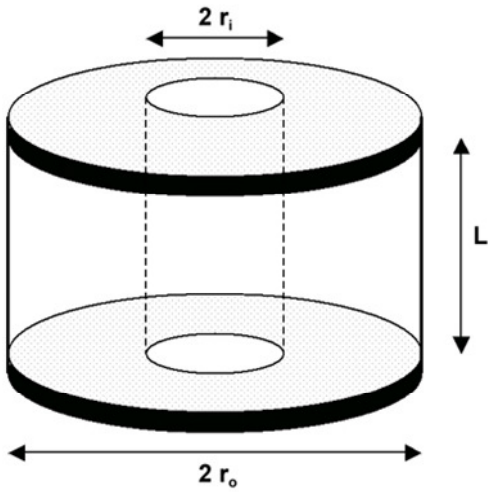

Figure 2.10: A schematic of a triple-layered, donut-shaped tablet (adapted from Kim *et al*., 2005).

2.11. Dome Matrix® and "Release Modules Assemblage" Technology

The dome matrix technology (described in Table 2.3) was developed by Losi and co-workers (2006). The elementary module (Figure 2.11a) is a swellable matrix device comprising of a concave base on one end and a convex base on the other end. Losi and co-workers (2006) also developed the "release modules assemblage" technology which implies the creation of different drug delivery systems, having various functions by the assemblage of two or more of the elementary/release modules. Figure 2.11 illustrates the dome matrix modules and examples of the possible assemblages that may be achieved. The drug release patterns from these assemblages depended on the manner in which the modules were placed or attached to each other (Losi *et al*., 2006). For example, multi-kinetics can be achieved and the delivery of two drugs in a single unit at a specific time and at a specific rate is also possible. Two types of assemblages were mentioned in this study; the first was called "piled configuration" (Figure 2.11c) where the convex base of one module is inserted into the concave base of another module and the second was called "void configuration" (Figure 2.11b) where the concave base of one module is fixed onto the concave base of another module creating a space/void between the two modules (Losi *et al*., 2006). The modules were compared to flat base matrices in terms of drug release behavior. Buflomedyl pyridoxal phosphate (BPP) was the model drug used in the study. The results depicted that the modules did not completely alter the kinetics compared to flat base matrices having the same weight and composition. However, the dome matrix® had a higher initial release rate.

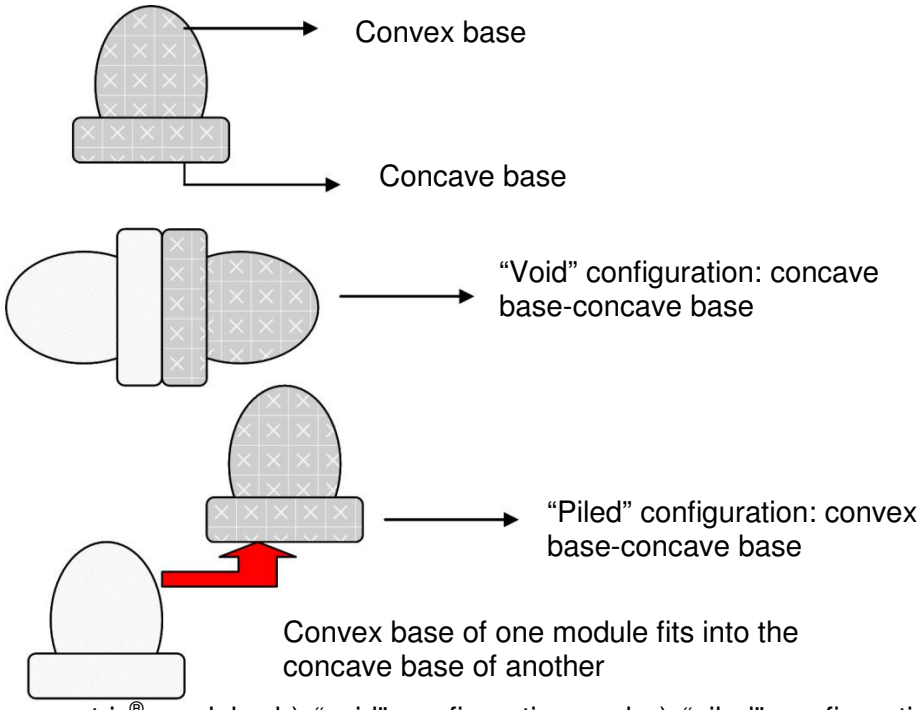

Figure 2.11: a) Dome matrix® module, b) "void" configuration and c) "piled" configuration (Adapted from Losi *et al*., 2006).

The concave and convex bases themselves exhibited different release patterns, with the convex base releasing drug faster (Losi *et al*., 2006). The technology proved to have potential benefits in terms of providing flexible drug release by increasing the amount of modules in an arrangement. This technology has various advantages although the complexity of the systems may be a shortcoming of the system in terms of administration of the devices to patients. A summary of various technologies that utilize geometric factors in drug delivery is provided in Table 2.3.

Table 2.3: Summary of various technologies that utilize geometric factors in drug delivery.

Technology	Design	Factors affecting drug release	Type of drug release
Geomatrix®	Triple/bi-layered tablet.	Type of polymer, thickness of layers.	Zero-order
Smartrix®	Triple-layered tablet with altered shape core layer	Shape of core layer.	Zero-order
Procise®	Uniformly dispersed drug core containing a hole.	Geometry of core	Zero-order
Dome Matrix®/"Release modules assemblage"	Various arrangements of elementary module containing a concave base and a convex base	Arrangement of modules, type of polymer.	Various according to arrangement of modules
Core-in-cup devices	Disc-shaped core compression coated on one surface and circumference to form a cup around it.	Type of polymer, dimensions of core and cup.	Zero-order
Doughnut-shaped tablets	Single/triple-layered tablets with a central hole/holes	Size and number of holes, type of polymer	Zero-order
Sodas®	Multilayered tablet	Type of polymer, thickness of layers. Shape of core layer	Pulsatile release
VersaTab®	Bilayered tablet	Core drug, polymer layers	Immediate or controlled release
Geolock™	Triple-layered tablet	Polymer layers, single or combination of drugs in the inner core	Immediate or modified release

2.12. Concluding Remarks

It has been elucidated that geometrically altered drug delivery systems especially multilayered tablets have provided various advantages to drug delivery technology. The ease of manufacture of these systems adds further benefit in terms of cost effectiveness. These systems therefore show promise for therapeutic use in the future. The technology that these systems encapsulate, offers valuable knowledge and insight for the inspiration of more intricate and constructive drug delivery systems for wider applications. Future research may thus focus further on modifying these systems and using the basic technological principles to develop novel systems that could be applied in broader and more complicated drug delivery

such as in the treatment of more complex diseases with a larger drug regimen that requires more individualised types of drug release. With the appropriate selection of polymer matrices and specialised geometries, these systems could be used to deliver more drugs in a more controlled manner for adequate time periods. The fact that drug delivery systems with altered geometric configurations (particularly tablets) have shown promising results in drug delivery technology and the ease of manufacturing is an added advantage to the pharmaceutical industry.

CHAPTER 3

FORMULATION, DEVELOPMENT AND CHARACTERIZATION OF NOVEL TRIPLE-LAYERED TABLETS MATRICES FOR ZERO-ORDER DRUG RELEASE

3.1. Introduction

Essential to the construction of a Triple-Layered Tablet (TLT) is the consideration of factors necessary for achieving zero-order drug release from the outer layers. Studies that have been performed give testimony that it is possible to obtain zero order drug release from the middle layer of a multilayered tablet due to the uniform area of the exposed surfaces of the layer allowing for a constant release of drug (Efentakis *et al*., 2006), it is however difficult to achieve zero order drug release from the outer layers as the surface area per unit volume changes therefore causing changes in the diffusion resistances causing changes in the diffusion path length which changes the diffusion coefficient which changes the flux ultimately preventing constant amounts of drug to be released. The focus will therefore be on developing these outer layers to achieve the desired release kinetics.

The basis for overcoming the challenges associated with the outer layer is the intimate selection of polymers based on their ability to control the rate of drug release by modifying the physicomechanical and physicochemical properties of the constituents and the geometry of the outer layers altering the diffusion and erosion kinetics which compensates for changes in surface area per unit volume resulting in uniform diffusion path lengths and uniform flux and hence, constant drug release. Polymers such as polyethylene oxide (PEO), PLGA and other specialised polymers will be assessed for use in the device.

The novelty of the system lies in its potential ability to dramatically increase patient compliance by markedly simplifying treatment regimens and reducing side effects. The cost to produce such a system is reduced as the equipment required is cost effective and easy to acquire. This system will potentially have a beneficial outcome in treatment efficacy.

The use of the Nylons in drug delivery has not been widely investigated. The Polyamides (Nylons) are materials that are mainly hydrophilic (Barringer *et al*., 1993) and erodible in nature (Kydonieus, 1999). These polymers are also hygroscopic (Bronzino, 2000); water attacks the amorphous regions affecting physical strength.

A study by Torres *et al*. (1995) formulated microcapsules of a synthetic polyamide that contained ion-exchange resins employing the interfacial polymerization procedure. Sodium fluoresceinate was used as a resinate. *In vitro* release studies showed that the polymeric

coat of the polyamide delayed drug release. García-Encina *et al*. (1993) investigated polyamide-coated ion exchange resins containing sodium diclofenac. Drug release results indicated that this formulation provided a more controlled and sustained release of sodium diclofenac than from the commercial sustained release product of sodium diclofenac. Theophylline loaded gelispheres that were coated with an aliphatic polyamide was prepared by Vyas *et al*. (2000). Results showed that the coating was able to reduce the rate of drug release and control the rate of release in a pseudo zero-order pattern.

Polyamide 6, 10 variants have been investigated for use in controlled drug delivery (Kolawole *et al*., 2007). Monolithic matrices comprising various variants of polyamide 6,10 were developed and evaluated in terms of drug release behaviour from the matrices. Three optimized variants were identified, namely the slow release, intermediate release and controlled release. The controlled release variant showed capability in providing zero-order release kinetics from a monolithic matrix.

Poly (lactic-*co*-glycolic acid) (PLGA) has proven in several studies to be suitable for providing controlled drug release (Song *et al*., 1997; Pillay *et al*., 1999; Mittal *et al*., 2007; Corrigan *et al*., 2009) These polymers have a great advantage of being biodegradable (Peppas, 1997). Pillay *et al*. (1999) investigated electrolyte- induced heterogeneity as a novel approach to rate-controlled drug delivery. Swellable polymers, for example, hydroxypropylmethyllcellulose (HPMC) were used in conjunction with specific electrolytes such as sodium bicarbonate and pentasodium tripolyphosphate and formulated into monolithic drug delivery matrices. The results showed that zero-order drug release from these matrices was achievable. The electrolytes compete with the polymers for water hydration.

Sibambo *et al*. (2008) performed a study on the development of salted-out PLGA scaffolds as monolithic drug delivery devices. The results showed that salting-out and crosslinking of PLGA modified the physicochemical properties of the original PLGA polymer thereby improving the potential for controlled drug release. The scaffolds showed excellent integrity in terms of structure and resilience. The bond formation in the PLGA backbone gives the scaffolds potential for providing zero-order release kinetics.

This chapter investigates the use of these polymers as outer layer drug matrices for achieving zero-order release kinetics. According to the literature reviewed in Chapter 2, PEO has been shown to provide controlled drug release as a swellable hydrophilic matrix and was therefore employed as the middle drug matrix of the TLT.

Furthermore, it was decided that the model drug to be employed in the study was one that possessed a high aqueous solubility. The ability to provide controlled release of a highly aqueous soluble drug active from the outer layers would certainly be a beneficial achievement. This is due to the difficulty that this challenge poses (Sandile *et al*., 2006; Rao *et al*., 2010). This may be advantageous for treatment regimens containing three drugs, minimizing effort in the administration of medication and multiple doses to be compacted into one dose for maximal therapeutic efficacy. Hence, diphenhydramine (DPH) was the model drug selected for the study. DPH inherently possesses a high aqueous solubility (100mg/mL).

Experimental studies involved the preparation of various TLT formulations, with either of the two novel aforementioned polymers employed as outer layer drug matrices. Drug release from these matrices was assessed. The effect of matrix hardness, swelling and erosion of the matrices on drug release behavior was also assessed. Differential scanning calorimetry was performed to determine the presence of chemical interactions between the various polymers as well as between the polymers and drug, the presence of drug may sometimes alter the thermal properties of polymers such as glass transition temperature which may have an effect on the mechanical properties of the polymer, thus affecting the functioning of the polymer in terms of drug release (Okhamafe *et al*., 1989; Wu *et al*., 1999; Nair *et al*., 2001). Fourier Transform Infrared Spectroscopy analysis was also carried out to determine any molecular variations of the polymers after compression and hydration.

3.2. Materials and Methods

3.2.1. Materials

Hexamethylenediamine (HMD, M_w=116.2g/mol) was purchased from Merck Schuchardt (Hohenbrunn, Germany). Sebacoyl chloride (SC, 98%, Mw=239.1g/mol) was purchased from Sigma-Aldrich Co. (Aldrich, Steinheim, Germany), ethylcellulose (EC), diphenhydramine hydrochloride (DPH) was purchased from Sigma Chemical Company (St Louis, MO, USA). Polyethylene oxide (Polyox™ WSR 303) (PEO) was purchased from The Dow Chemical Company (Midland, MI, USA) and poly(lactic-*co*-glycolic acid) (PLGA, Resomer RG504 50:50; M_w 48,000; i.v. 0.48-0.60dl/g) was purchased from Boehringer Ingelheim Pharma (Ingelheim, Germany). Sodium chloride, sodium sulphate, calcium chloride and zinc sulphate were purchased from Rochelle Chemicals (Johannesburg, South Africa). All other reagents used are of analytical grade and are used as purchased.

3.2.2. Methods

3.2.2.1. Synthesis of modified polyamide 6,10 using a modified interfacial polymerization reaction

The synthesis of polyamide 6,10 (PA6,10), involved the preparation of two solutions namely the aqueous phase and non-aqueous phase. HMD and sodium hydroxide (NaOH) were dissolved in de-ionised water (DW) to form the aqueous phase while the non-aqueous phase was composed of cyclohexane (C-HXN), hexane (HEX) and SC. Table 3.1 contains the quantities of constituents used in the two phases. The first solution was gradually added to the second to form two immiscible phases which resulted in a polymeric film being formed at the interface (i.e. by an interfacial polymerization process). The polymeric film was collected as a mass by slowly rotating a glass rod at the interface.

Table 3.1: Quantities of constituents used in the synthesis of PA6,10 for controlled drug release.

HMD(g)	SC(mL)	HEX(mL)	DW(mL)	C-HXN(mL)	NaOH(g)
1.75	0.20	40	10	10	0.4

Upon collection of the polymeric mass, it was thoroughly washed with HXN to remove any un-reacted SC and then with DW (3×300mL) to remove any un-reacted NaOH. The polymeric mass was then lightly rolled on filter paper (diameter 110mm, pore size 20µm) to remove excess solvent and dried to a constant weight at 40℃ over 48 hours.

3.2.2.2. Synthesis of salted-out PLGA

Synthesis involved the preparation of a polymeric solution and a salt solution. The polymeric solution was prepared by dissolving 400mg of PLGA 504 in 15mL of acetone and the salt solution was prepared by dissolving 1.15g of sodium chloride in 10mL de-ionized water. The polymeric solution was slowly added to 75mL of the salt solution while constantly stirring. The mixture was agitated on a magnetic stirrer for half an hour until a white mass of salted-out PLGA (s-PLGA) was formed.

3.2.2.3. Fourier Transform Infrared Spectroscopy analysis of components of the Triple-Layered Tablet formulations for the determination of molecular variations after compression and hydration

The native polymers, compressed polymers, compressed combinations of polymers and salts as well as hydrated samples were subjected to Fourier Transform Infrared (FTIR) analysis using a Perkin Elmer Spectrum 100 FT-IR Spectrophotometer (Massachusetts,

USA) in order to determine the presence of molecular structural variations that may have occurred after: i) compression of the polymers, ii) the combination of polymeric materials and iii) after hydration upon exposure to the dissolution medium. The consequences of the possible interactions on drug release from the matrices as well as possible interactions on drug release from the matrices were also evaluated.

3.2.2.4. Differential Scanning Calorimetry and Alternating Differential Scanning Calorimetry analysis of polymeric material to characterize thermal behavior and determine the presence of polymer-polymer molecular interactions

Differential Scanning Calorimetry (DSC) was carried out on native polymers, compressed polymers and compressed polymer combinations using a differential scanning calorimeter (Mettler Toledo, DSC1, STAR^e System, Swchwerzenback, Switzerland). Samples were weighed into aluminium pans and sealed. DSC thermograms were generated over wide temperature ranges at a rate of 10℃/min. Alternating differential scanning calorimetry (ADSC) was carried out on the samples at small temperature ranges depending on where thermal events occurred on the DSC thermograms at a rate of 1℃/min. Samples were assessed for potential chemical interactions that may have occurred at various temperatures by assessing changes in glass transition temperature (T_g) and melting points (T_m) of the polymers and the ultimate effect of these changes on drug release from the TLT.

3.2.2.5. Preparation of TLT formulations

TLT formulations as depicted in Figure 3.1 were prepared by direct compression using a Carver hydraulic press (Wabash, USA). PA6,10, s-PLGA and PEO were employed to comprise the three layers. Only one layer was loaded with drug at a time for the purpose of UV analysis. The effect of the addition of different salts namely sodium sulphate ($NaSO_4$), calcium chloride ($CaCl_2$) and zinc sulphate ($ZnSO_4$) on the physicomechanical properties of the matrices and on drug release behavior from the matrices were evaluated. DPH was directly combined with PA6,10 in the outer layer. The two subsequent layers were not loaded with drug.

Table 3.2 contains the quantities of constituents used in the various formulations prepared for comparative analysis of matrix hardness and drug release behavior of the PA6,10 layer. The same procedure was carried out for the preparation of tablets for assessment of drug release from the s- PLGA layer where the outer layer was composed of various quantities of s-PLGA and PEO, Table 3.3 contains the quantities used for these formulations.

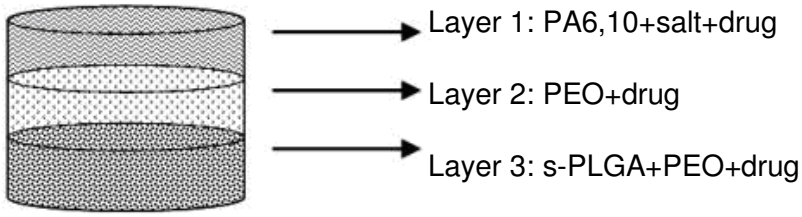

Figure 3.1: Schematic diagram of the TLT.

Table 3.2: Quantities of constituents used in preparation of TLT formulations – assessment of drug release from PA6,10 layer*.

Experiment	PA6,10 (mg)	Additives (Salts)
1	200	-
2	300	-
3	350	-
4	250	50mg sodium sulphate
5	250	50mg calcium chloride
6	250	50mg zinc sulphate
7	250	75mg sodium sulphate
8	100	250mg sodium sulphate
9	200	150mg sodium sulphate
10	300	50mg sodium sulphate

** All formulations contained 50mg DPH in outer layer. The middle and third layers of every formulation consisted of 350mg PEO and 350mg PA6, 10/salted-out PLGA respectively.*

Table 3.3: Quantities of constituents used in preparation of TLT formulations – assessment of drug release from s-PLGA layer*

Experiment	Salted-out PLGA (mg)	PEO (mg)
1	300	-
2	250	50
3	200	100
4	300	50
5	50	300
6	150	200
7	225	125

** All formulations contained 50mg DPH in outer layer. The middle and third layers of every formulation consisted of 350mg PEO and 350mg PA6, 10/salted-out PLGA respectively.*

3.2.2.6. Computational modeling to determine the nature of formation and dissolution behavior of the TLT

Computational and molecular modeling was employed to characterize the potential interactions that may occur between the polymeric layers of the matrices at a molecular level due to compression and to characterize the possible formation, layering and dissolution behavior of the TLT matrices. Schematic models depicting the compressed layers and matrix formation and drug/matrix bonding were generated on ACD/I-Lab, V5.11 (Add-on) software (Advanced Chemistry Development Inc., Toronto, Canado, 2000).

3.2.2.7. In vitro dissolution studies for DPH release analysis

In vitro drug release studies were performed on the different formulations using a USP 25 rotating paddle method in a dissolution apparatus (Caleva Dissolution Apparatus, model

7ST; G.B. Caleva Ltd., Dorset, UK) at 50 rpm with 900mL simulated gastric fluid (SGF) (pH 1.2, 37℃) and 900mL phosphate-buffer solution (PBS) (pH 6.8; 37℃). A stainless steel mesh was used in the dissolution vessels in order to prevent the formulations from floating. Samples of 5 mL were drawn at predetermined time intervals over a 24 hour period.

3.2.2.8. Determination of matrix swelling and gel strength using textural analysis

The outer s-PLGA-PEO layer was assessed in terms of axial and radial swelling, under conditions identical to those described for *in vitro* dissolution testing i.e. tablets were subjected to analysis in 900mL SGF (pH 1.2, 37℃) and 900 mL PBS (pH 6.8, 37℃) using a USP 25 rotating paddle method in a dissolution apparatus (Caleva Dissolution Apparatus, model 7ST; G.B. Caleva Ltd., Dorset, UK) at 50 rpm. The other two layers were coated with a 10% EC coating which was 5g in 50mL of acetone to prevent them from swelling/eroding in the dissolution medium.

3.2.2.9. Assessment of erosion of the modified PA6,10 layer

The outer PA6,10 layer was assessed for erosion in terms of percentage mass loss under the same conditions; the tablets were weighed before testing and dried and re-weighed after testing. Equation 3.1 was used to calculate percentage mass loss (*%ML*).

At each time interval the matrices were removed from the apparatus, measured in terms of swelling size, the gel was subjected to textural analysis in order to determine gel strength and FTIR analysis in order to determine changes in molecular structure upon hydration and swelling.

$$\%ML = \frac{(M_I - M_F)}{M_I} \times 100$$

Equation 3.1

Where M_I is the initial mass of the matrix, and M_F is the final mass of the same dried and partly eroded matrix.

3.2.2.10. Determination of matrix hardness

Formulations were assessed for matrix hardness using a calibrated TA.XT*plus* Texture Analyzer (Stable Microsystems, UK). The analyzer was fitted with a steel probe (3.125mm diameter). The probe was lowered such that the ball made an indentation of predetermined distance (0.5mm) on the matrix layer. Force-distance profiles were generated for the various

formulations and along with the Brinell hardness equation was used to calculate matrix hardness and Brinell hardness numbers (BHN) (N/mm^2). Brinell hardness numbers for various formulations were obtained using the maximum force of resistance as a variable. Specific parameters were set for the assessments which are depicted in Table 3.4

$$BHN = \frac{2F}{\pi D\left(D - \sqrt{D^2 - d^2}\right)}$$

Equation 3.2

Where P is the load/applied force (kg), D is the steel ball diameter (mm) and d is the depression diameter (mm).

Table 3.4: Textural analysis parameters for the assessment of BHN

Parameter	Settings
Pre-Test speed	1mm/s
Test speed	0.5mm/s
Post-test speed	1mm/s
Compression force	40N
Trigger type	Auto
Load cell	50kg

3.2.2.11. Molecular mechanics simulations

All modeling procedures and calculations, including energy minimizations in molecular mechanics, were performed using the HyperChem™ 8.0.8 Molecular Modeling System (Hypercube Inc., Gainesville, Florida, USA) and ChemBio3D Ultra 11.0 (CambridgeSoft Corporation, Cambridge, UK). The octamers of s-PLGA and PEO and dimer of PA6,10 were generated from standard bond lengths and angles employing polymer builder tools using ChemBio3D Ultra in their syndiotactic stereochemistry as 3D models and were saved in .skc file format readable to HyperChem 8.0.8.

The models were initially energy-minimized using a MM+ Force Field and the resulting structures were again energy-minimized using the Amber 3 (Assisted Model Building and Energy Refinements) Force Field. The conformer having the lowest energy was used to create the polymer-cation and polymer-polymer complexes. A complex of one polymer molecule with another was assembled by disposing the molecules in a parallel way, and the same procedure of energy-minimization was repeated to generate the final models: PA6,10-Na^{2+}, PA6,10-Ca^{2+}, PA6,10-Zn^{2+} and s-PLGA-PEO.

Full geometry optimization was carried out in vacuum employing the Polak–Ribiere conjugate gradient algorithm until an RMS gradient of 0.001kcal/mol was reached. Force field options in

the AMBER (with all hydrogen atoms explicitly included) and MM+ (extended to incorporate non-bonded cut-offs and restraints) methods were the HyperChem 8.0.8 defaults. For molecular mechanics calculations, the force fields were utilized with a distance-dependent dielectric constant scaled by a factor of 1. The 1-4 scale factors were electrostatic 0.5 and van der Waals 0.5.

3.3. Results and Discussion

3.3.1. Molecular variations after compression of matrices employing Fourier Transform Infrared Spectroscopy

The analysis on compressed and plain PA6,10 showed no significant differences in terms of the spectra generated indicating that little/no structural variations occur after compression. Figure 3.2a exhibits a typical FTIR spectrum of the comparison between non-compressed and compressed PA6,10. The spectra showed very similar prominent peaks indicating no significant difference in chemical composition in the different dissolution mediums. The peaks show: NH stretching (at 3300-3305cm^{-1}); trisubstituted CH stretching (at 3072-3077cm^{-1}); alkyl CH stretching (at 2852-2922cm^{-1}); strong: pyridyl C-C and C-N stretching (at 1633-1634cm^{-1}); NH bending (at 1535-1536cm^{-1}); CH_2 deformation (at 1465-1467cm^{-1}); CH out-of-plane deformation (at 679-682cm^{-1}); H – C=O bend in aliphatic aldehydes (at 1418cm^{-1}). A peak at 1102 is indicative of C-OH stretching possibly due to H-bonding. No structural interaction was noted between PA 6,10 and sodium sulphate after compression. The same was noted for s-PLGA. The spectra showed very similar prominent peaks which include: C-H stretching (at 2920-2952cm^{-1}); C=O stretching (at 1745-1750cm^{-1}); C=C stretching (at 1635-1636cm^{-1}); – CH_3 (at 1452,1465 and 1384cm^{-1}); H-C=O bend in aliphatic aldehydes (at 1341cm^{-1}); C-N stretching (at 1162cm^{-1}); Si-O-C stretching or C-OH stretching (at 1076-1080cm^{-1},1084-1095cm^{-1}); C-C stretching (at 948-960cm^{-1}); C-C stretching/C-H bending/C-N stretching (at 847-869cm^{-1}); out of plane CH deformation (at 840-841cm^{-1}). 1600-1900cm^{-1} (C=O) bands were noted, which confirm the cross-linking bonds between the salt (sodium chloride) and oxygen molecules in PLGA, hydrogen bonds, ether bonds (Sibambo *et al.*, 2008). No molecular interaction was found between PEO and s-PLGA after compression (Figure 3.2b). This proved that compression and hydration did not affect the inherent nature of the polymers and drug release from the polymer matrices is attributed to the nature and characteristics of the polymers.

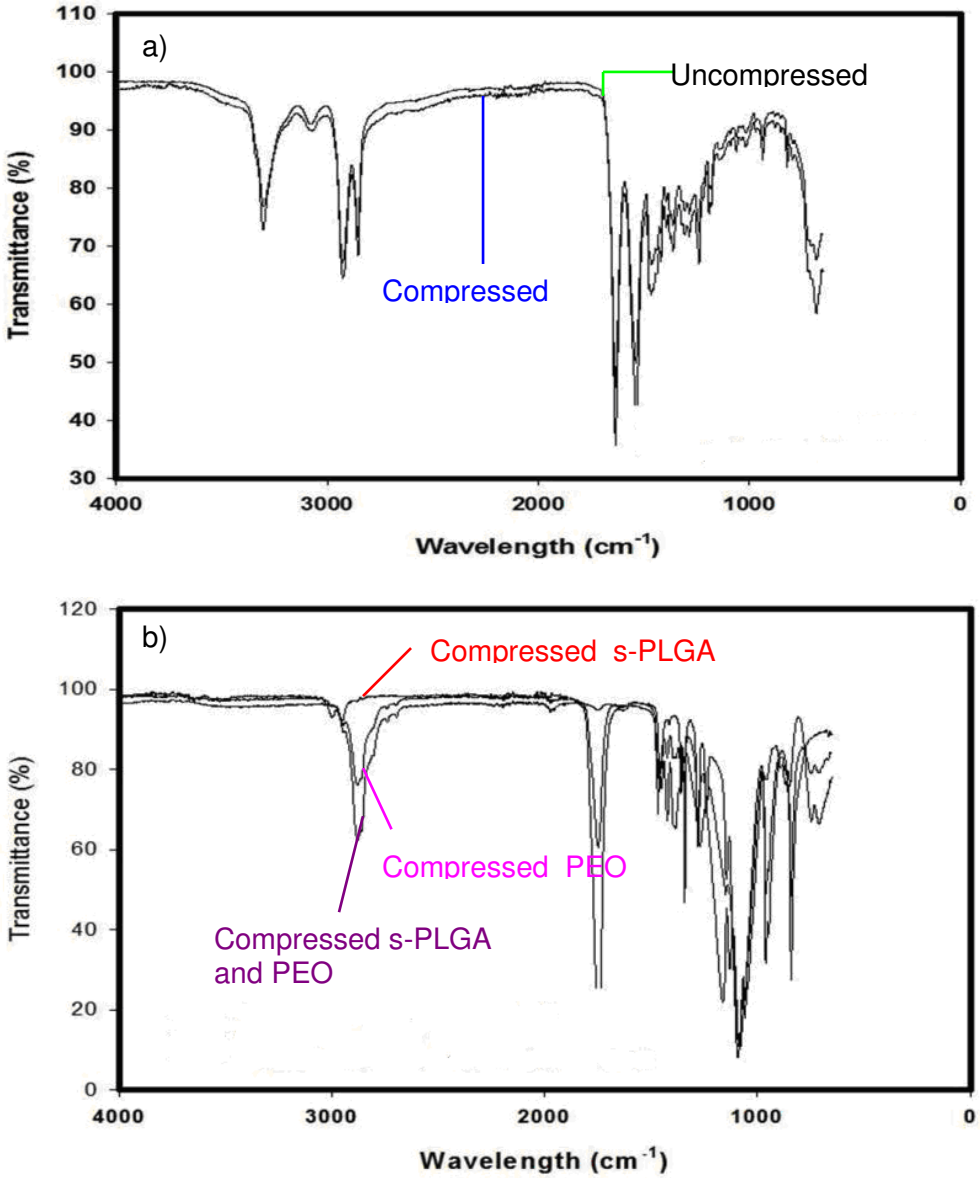

Figure 3.2: a) FTIR Spectrum of compressed and non-compressed PA6, 10, b) FTIR spectra of compressed s-PLGA, compressed PEO and combined compressed s- PLGA and PEO.

Analysis on hydrated PA6,10 samples also revealed no significant structural changes upon hydration of the matrices. Characteristic bands and peaks remained noticeable. FTIR performed on the hydrated swelled s-PLGA-PEO layer showed that no significant structural changes occurred with each polymer, there was no merging of peaks or the formation of new peaks which indicates no interaction or molecular variations. Broad bands at 3370-3384cm^{-1} represent water due to hydration of the formulation. This lack of interaction is visible to the eye upon removal of the formulations from the dissolution medium.

3.3.2. DSC and ADSC analysis for the determination of thermal variations and molecular interactions

DSC was carried out on samples in order to determine changes in thermal behavior after compression as well as after combination with other materials. The thermograms obtained from the polymers are shown in Figure 3.3. Plain PA6,10 exhibited a thermal transition at ~50℃, which relates to its glass transition temperature which suggests that it is crystalline at room temperature (25℃). Another transition occurred between 200-220℃ which might be rationalized as the melting point. This was confirmed by the investigations of Kohan (1999). The thermogram displayed by the compressed PA6,10 displayed the same thermal transitions occurring as the pure polymer indicating that there is minimal or no variation to PA6,10 after compression. Compressed PA6,10 also remained crystalline.

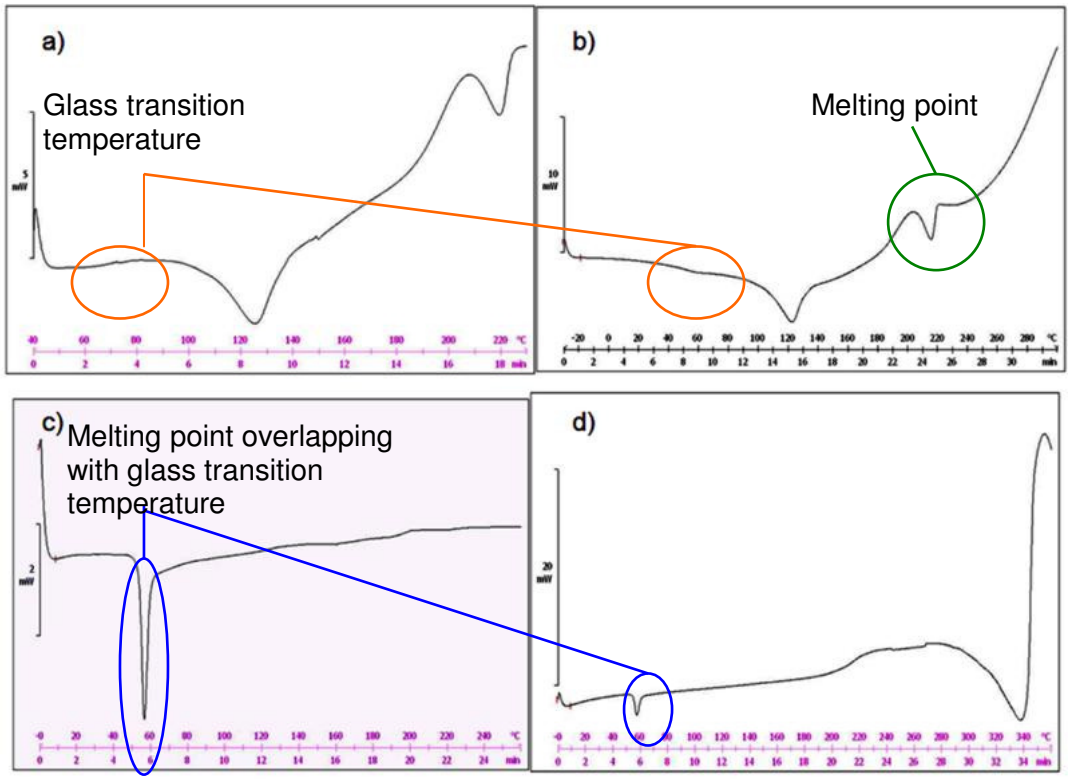

Figure 3.3: DSC thermograms of a) uncompressed PA6,10, b) compressed PA6,10; c) uncompressed s-PLGA and d) compressed s-PLGA.

These results establish that no thermal interactions occur which may affect the release of drug from the matrices which further confirms the FTIR characterization of the polymer. The presence of interactions may have untowardly affected the release of drug from the matrices. The compressed combination of PA6,10 and sodium sulphate showed no significant changes in the thermal behavior of PA6,10 indicating that no chemical interaction occurred between them.

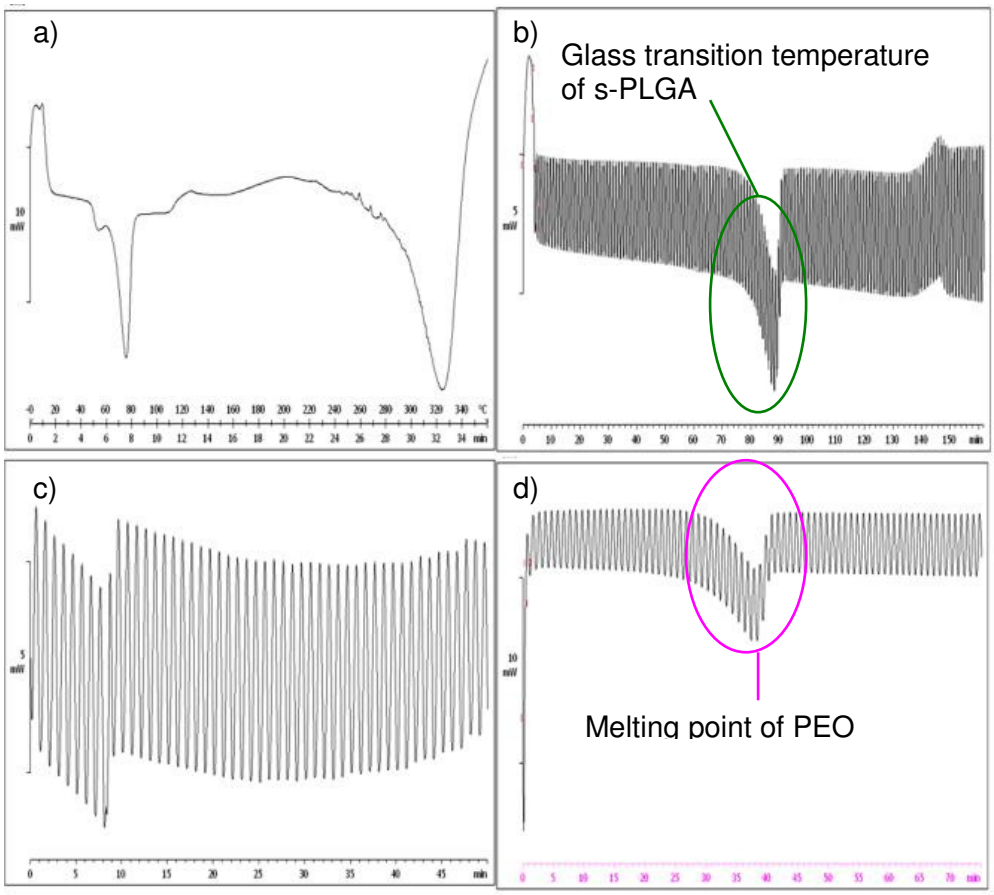

Figure 3.4: DSC and ADSC thermograms of compressed salted-out PLGA and PEO at a) 0-360℃, b) 0-130℃ c) 240-280℃, and d) 40-100℃.

Native s-PLGA exhibited a thermal transition between 50-60℃ indicating its T_g. A broad T_m peak was observed at 320-340℃. Native PEO showed a thermal transition between 70-80℃ which is attributed to its melting temperature. The compressed combination of s-PLGA and PEO revealed separate T_g and T_m peaks which can be explained by a lack of interaction between the two polymers. Alternating differential scanning calorimetry (ADSC) was employed to provide a more accurate and comprehensive confirmation of the results. While DSC may overlook minute variations, ADSC analysis is a more sensitive analysis of the variations that may occur with temperature fluctuations. Thermograms from ADSC analysis are provided in Figure 3.4b and c.

3.3.3. Computational modelling of the formation and dissolution of the Triple-Layered Tablet

The compressibility of a polymer may have an effect on the interaction of drug in the polymer matrix i.e. a higher compressibility will hold the drug; a chemical interaction may occur which may be ionic or covalent leading to changes in structure of the drug or an inter-play may occur between the drug and matrix where the drug is in a free floating embedded state but is tightly surrounded by the polymer matrix. This occurrence may be likened to submerged or

embedded balls in ice cubes where there is no interaction between the ball and ice matrix. The additional energy that is supplied due to compression energy is absorbed onto the drug molecules as well as the polymer matrix may partake in stabilization of the free floating system. The energy will be released making dissolution faster on contact with the dissolution medium. The TLT as depicted in Figure 3.5a displays layers of polymers loaded with drug molecules (circular entities). Intermixed or combined layers that are depicted may occur with occasional drug entrapments due to heavy compressions applied for the different polymer layers. Figure 3.5b demonstrates the actual formation of the layers. The first polymer with drug loaded is compressed followed by the second drug-loaded polymer and finally the third polymer and drug layering sequentially on one another. The intermixed polymer layers are also shown which are expected to intermingle due to adhesion. Drug molecules may also seep into other polymer layers due to high compression forces.

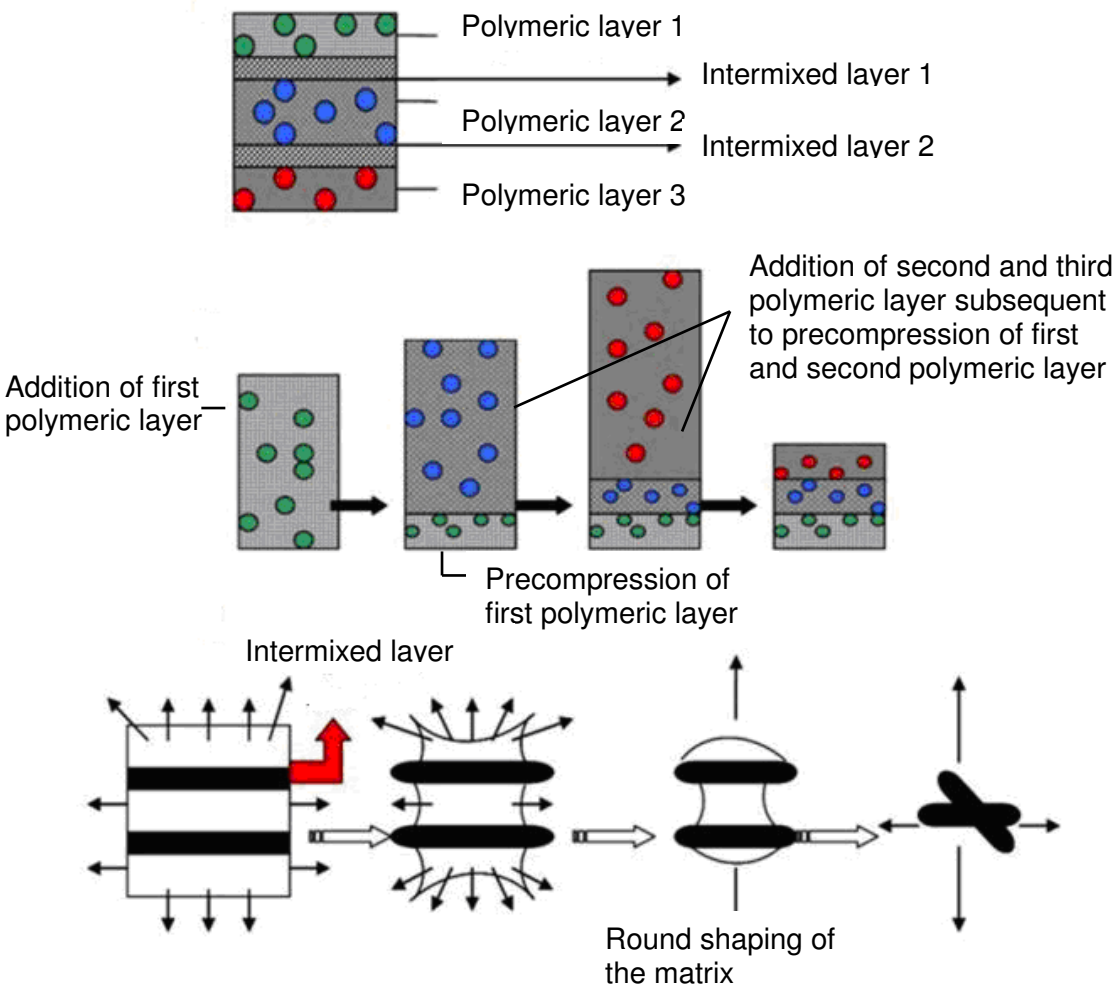

Figure 3.5: a) Compressed TLT containing layers of polymer matrices and drug with intermixed layers; b) different layering in the compressed tablet formation; c) disintegration of the compressed TLT in the dissolution medium.

A predictable approach to the dissolution of the TLT was adopted. There is a high possibility of the polymer becoming solvated because the compressed polymer will not immediately

dissolve out. However, the dissolution medium may interact with the portions of the compressed polymer strands and the polymer may swell in the case of it being hydrophilic. In the case of the polymer not being hydrophilic, the dissolution medium may then relax the compression of the matrix. The relaxation occurs akin to the slow melting of the ice cube embedded ball model to release the drug from the embedded matrix.

The rate of solvation of the matrix is higher than the rate of disintegration that would be the slowest to occur. There is initially a slow dissolution of the polymer layer in the dissolution medium with extremely slow dissolution occurring at the outer curve of the layers and the intermixed layers. The inner areas of the layer are more prone to dissolution resulting in a round shaping of the matrix as depicted in Figure 3.5c. The arrows indicate the areas that are disintegrating in the dissolution medium. This is where the matrix loses a major part of the polymer matrix and solvated, polymer embedded or chemically conjugated drug. It is predicted that the less compressible polymer will disintegrate more rapidly thereby releasing drug faster. The multidirectional dissolution that occurs, leaving the outer edges and intermixed layers most intact, balances out the release and the cumulative drug release appears to be linear or near linear.

3.3.4. *In vitro* drug release from the TLT formulations

3.3.4.1 Assessment of DPH release from the PA6,10 layer

Figure 3.6a and b display the calibration curves constructed for DPH. It was discovered that using a quantity of 300mg PA6,10 depicted the most desirable, near linear release profile that could be explained by a more compact matrix, due to the higher packing density making the matrix more resistant to penetration by the dissolution medium, resulting in more adequate retardation of drug release as depicted in Figure 3.7a, than with a smaller quantity of PA6,10. However there was an occurrence of an undesirable initial burst release of drug. The addition of various salts to the layer was investigated in an attempt to eliminate the initial burst release. The formulations containing SS (as an additional salt to PA6,10 layer) demonstrated the highest capability in reducing the burst release and exhibited a linear release profile with no burst release as shown in Figure 3.7b. Various ratios of PA6,10 to SS were prepared and the most linear release over 24 hours was achieved with 300mg: 50mg (Figure 3.7b).

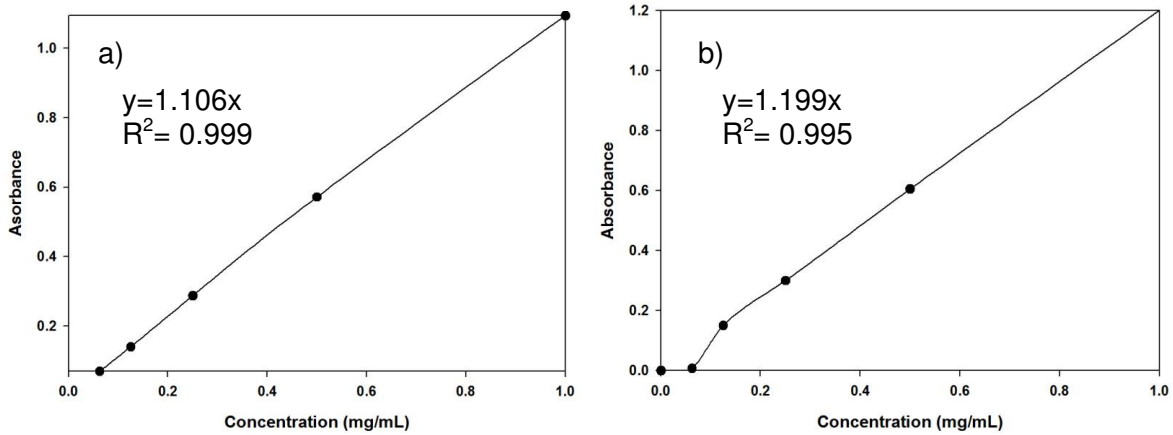

Figure 3.6: Calibration curve for the determination of DPH in a) SGF (pH 1.2, 37℃) and b) PBS (pH 6.8, 37℃).

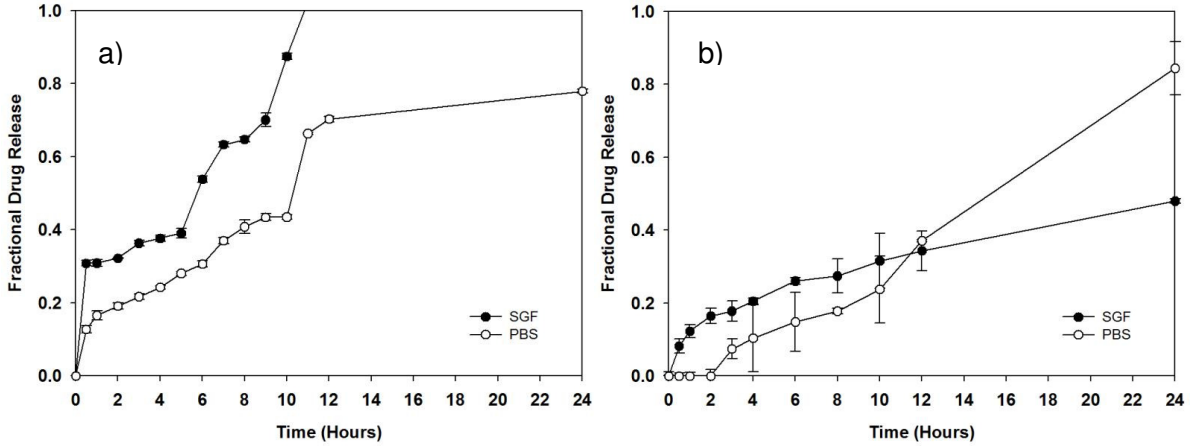

Figure 3.7: DPH release profiles from a) 300mg PA6,10 layer; b) 300mg PA6,10 and 50mg SS (N=2).

3.3.4.3. DPH release from the s-PLGA layer

Direct combination of s-PLGA with DPH exhibited a significant burst release of 6% and total drug release within 4 hours in SGF (pH 1.2, 37℃) with a 28% burst release in PBS (pH 6.8, 37℃) (Figure 3.8a) and total drug release before 24 hours. This may be due to the possibility that s-PLGA utilized unaccompanied as a matrix may not be adequate to retard drug release due to the inability to form a sufficiently compact matrix that may be explained by the crystalline nature of the polymer. Another contributing factor is that s-PLGA is hydrophobic (Sibambo *et al.*, 2007) and therefore does not swell. The formulations containing the addition of PEO to the s-PLGA layer showed more desirable results in terms of a reduced burst release and a more linear release profile. The proposed rationale for the addition of PEO is that it increases the elasticity of the layer which allows for a more constant diffusion path length and a more constant release of drug over time. From the various ratios of s-PLGA to PEO the results showed that the 50mg: 300mg ratio showed the most desirable release profile in SGF (pH 1.2, 37℃) and PBS (pH 6.8, 37℃) as can be seen in Figure 3.8b.

3.3.4.4. Drug release from the middle PEO layer

The release profile of DPH from the middle PEO layer proved to be near linear (as displayed in Figure 3.9) this may be due to the uniform swelling of the polymer as only two of the surfaces are exposed to the dissolution medium. The release extended over 24 hours in SGF (pH 1.2, 37℃) and only approximately 30% was released after 24 hours in PBS (pH 6.8, 37℃). A constant quantity of 350mg of PEO was selected as a drug matrix.

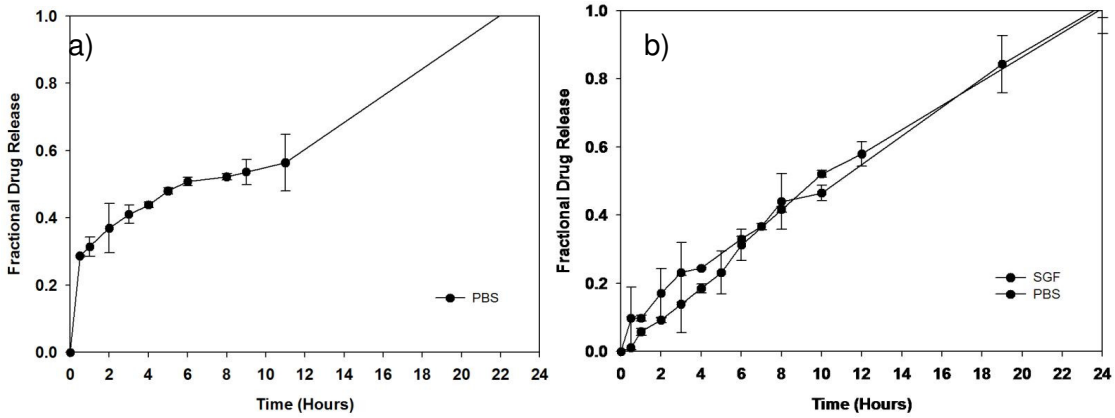

Figure 3.8: Drug release profiles from a) 300mg s-PLGA; b) 50mg s-PLGA: 300mg PEO (N=2).

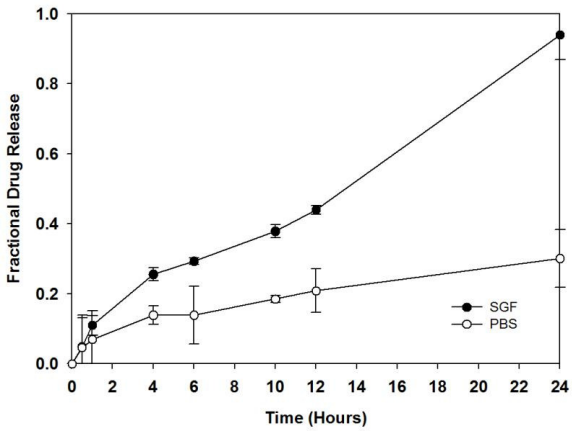

Figure 3.9: DPH release profiles from 350mg PEO (N=2).

3.3.5. Determination of axial and radial swelling and gel strength upon hydration of the TLT formulations

The two formulations that were analysed showed small increases in diameter and thickness of the swollen layer over 24 hours. The changes in diameter and thickness are noted in Table 3.5. The matrices were found to swell to a slightly greater extent in PBS (pH 6.8, 37℃) as compared to SGF (pH 1.2, 37℃). Figures 3.10a, b and c display force-distance profiles of the 150:200 s-PLGA-PEO layer after 2, 12 and 24 hours of hydration in SGF (pH 1.2, 37℃). It has been observed that the force of resistance that the probe experiences as it penetrates the swollen layer is dependent on the distance that the probe travels into the gel layer (Yang *et al*., 1998).

The profiles obtained show that there is an initial low resistance to penetration at the surface of the layer and an increased resistance to penetration deeper into the layer indicating an increase in the gel strength advancing into the swollen layer. The results also indicate that at a higher degree of hydration, the gel strength decreases with a lower resistance to penetration by the probe. The formulations did not show a great increase in swelling especially between 12 and 24 hours therefore in some cases the force of resistance to penetration did not increase after 24 hours of hydration. Evidently, the formulation with a higher amount of PEO showed a greater extent of swelling and a higher force of resistance indicating greater gel strength of that layer.

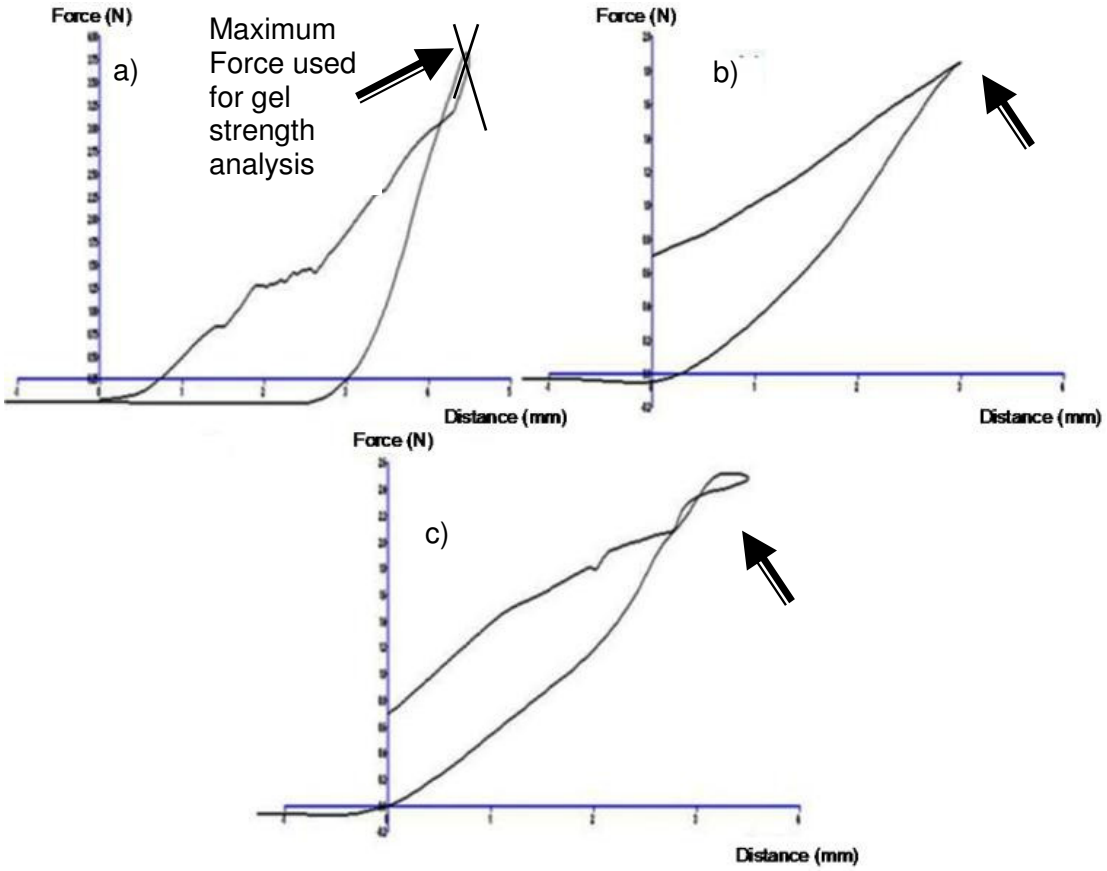

Figure 3.10: a) Force-distance profile for the s-PLGA layer after 2 hours of hydration in SGF (pH 1.2, 37℃), b) Force-distance profile generated for s-PLGA layer after 12 hours of hydration in SGF (pH 1.2, 37℃) and c) Force-distance profile generated for s-PLGA layer after 24 hours of hydration in SGF (pH 1.2, 37℃).

Table 3.5: Changes in thickness and diameter of the gel layer after 2, 12 and 24 hours of hydration of the s-PLGA-PEO formulations

Ratio (mg)	Dissolution Medium	Diameter (mm)			Thickness (mm)		
		2hrs	12 hrs	24 hrs	2hrs	12 hrs	24hrs
50 : 300	SGF	16	20	23	5	6	7
150 : 200	SGF	13	18	20	4	5	5.5
50 : 300	PBS	14	22	25	5	7	8
150 : 300	PBS	13	20	21	4	6	7

3.3.6. Determination of degree of erosion of the PA 6, 10 layer upon hydration over 24 hours in correlation with drug release behavior

Polymer erosion can be defined as the process by which a polymer hydrolyzes and disappears into its environment (Yu *et al*., 2008). Nylon is an erodible polymer (Kydonieus, 1999), which can be observed from the results. Results from erosion studies performed on formulations containing 300mg PA6,10 and 300mg PA6,10:50mg sodium sulphate demonstrated an approximate 3% mass loss of the matrices over 24 hours. Table 3.6 displays the changes in weight and percentage mass loss of the formulations after 2, 12 and 24 hours. As the time of exposure to the dissolution medium increased, percentage mass loss also increased for all formulations.

The formulation with sodium sulphate showed a greater percentage mass loss which is due to the quicker dissolution of sodium sulphate in the dissolution medium. It is logical that an increase in erosion of PA6,10 will allow for greater drug surface exposure to the dissolution medium (Danckwerts, 1994), however the rate at which this occurs contributes towards controlling drug release i.e. a slower rate of erosion allows for slower drug release. Thus the maintenance of a constant surface area for drug diffusion during dissolution is critical for zero-order drug delivery (Sundy *et al*., 2004; Liu *et al*., 2008).

Table 3.6: Percentage mass loss of PA 6,10 formulations after 2, 12 and 24 hours of hydration.

Formulation	Dissolution medium	Percentage Mass Loss (%)		
		2hours, mean ± S.D.	12 hours, mean ± S.D.	24 hours, mean ± S.D.
300mg PA6,10	SGF	1.00% ± 0.14	0.70% ± 0.10	17.4% ± 2.42
300:50mg SS	SGF	1.32% ± 0.56	2.35% ± 0.84	40.4% ± 1.98
300mg PA6,10	PBS	0.79% ± 0.14	1.25% ± 0.14	19.4% ± 0.14
300:50mg SS	PBS	1.17% ± 0.35	1.88% ± 0.00	1.95% ± 0.00

3.3.7. Effect of matrix hardness on drug release behavior

Table 3.7 exhibits the BHN values for various TLT formulations. The BHN analysis revealed that the formulations comprising higher quantities of PA6,10 and s-PLGA possessed higher BHN values which may be attributed to the formation of a more compact matrix at higher polymer quantities. It has been proven that matrix hardness can noticeably influence drug release behavior (Apu *et al*., 2009). This can be correlated to the drug release from these matrices, DPH release from the formulations containing higher quantities of PA6,10 were the most sustained and linear over 24 hours. This is explained by a more compact, hard matrix that is able to retard drug release more efficiently. The addition of SS may also have a role to play in the compactness of the matrices due to the crystalline nature that it possesses.

Table 3.7: BHN for PA 6,10 formulations.

Formulation	BHN (N/mm^2) ± S.D.
300mg PA6,10:50mg SS	17.31 ± 1.13
200mg PA6,10: 150mg SS	13.74 ± 0.17
50mg s-PLGA:300mg PEO	11.98 ± 0.47
150mg s-PLGA: 200mg PEO	14.32 ± 0.64

The formulations containing higher quantities of s-PLGA however, did not provide desirable release of DPH. The higher quantity of PEO was found to be necessary for the uniform release of DPH. Figure 3.11 shows a typical force-distance profile generated from the Texture Exponent 32 software (StableMicroSystems, Surrey, UK).

In general, the TLT formulations do not have high BHN values that could be explained by the low compression force of 3 tons that they are subjected to, although the effect that compression force had on hardness was found to be modest.

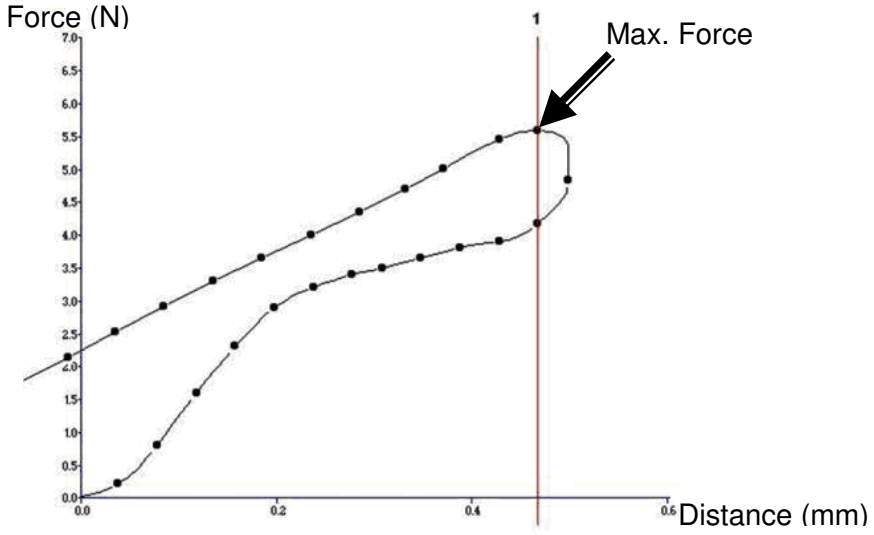

Figure 3.11: Typical force-distance profile for 50mg s-PLGA: 300mg PEO.

3.3.8. Molecular mechanics assisted model building and energy refinements, influence of addition of salts on the performance of PA6,10 layer

The polyamides display a wide range of physicomechanical properties when complexed physically, chemically or physicochemically with metal cation in form of metal salts which mainly rest on their ability to form Lewis acid-base complexes (Mit-uppatham *et al*., 2004; Gupta *et al*., 2009). A generalized molecular mechanics program was used in this study to compute the energy attributes of PA6,10 and PA6,10-cation conformations. PA6,10 interactions were screened for the three metal cations (Na^+, Ca^{2+} and Zn^{2+}) in an attempt to corroborate and elucidate the experimentally observed drug release profiles. The cation probe was moved around the van der Waals surface of the amide chain and the energy minimized structures following molecular mechanics simulations are depicted in Figure 3.12

and the possible component binding energies, and the intrinsic molecular attributes to which they will be responsive, are listed in Table 3.8. The polyamide chain assumed a intramolecular, tail-head, bonded, ordered structure (Figure 3.12a and b) after geometry optimization. The cation binding was evident from the presence of binding sites distributed in ordered arrays and formed between chains (Figure 3.12c, d and e). It is evident from the energy attributes that PA6,10-Na^{+} (ΔE=-92.02kcal/mol) and PA6,10-Ca^{2+} (ΔE=-62.72kal/mol) were forming more thermodynamically stable conformers than that of Zn^{2+} (ΔE=-2.29kal/mol). These energy minimizations were supported both by bonding interactions (angle energy) and non-bonding interactions (van Der Waals forces). These two energies seem to be complementary to each other in this case. The bond angle contributions, reference values assigned to all of the bond angles for the structure may arise from the force between two instantaneously induced dipoles (London dispersion force) and the resulting steric adjustment caused due to inclusion of metal ions in the polymer matrix.

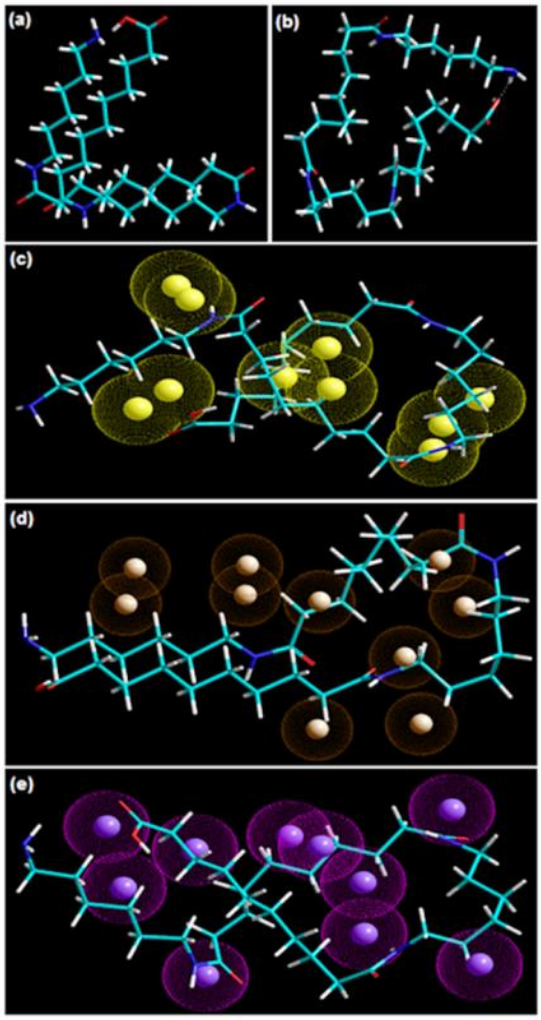

Figure 3.12: Geometrically constrained models of the polyamide-metal ion complexes derived from molecular mechanics calculations: (a) PA6,10-non energy-minimized; (b) PA6,10-energy minimized; (c) PA6,10-Ca^{2+}; (d) PA6,10-Zn^{2+}; and (e) PA6,10-Na^{+}. Color codes for elements are: Carbon (cyan), Nitrogen (blue) and Oxygen (red), Calcium (yellow), Zinc (brown) and Sodium (purple).

The significant lowering of angle energy [PA6,10-Na^+ (ΔE~-52kcal/mol) and PA6,10-Ca^{2+} (ΔE~-50kal/mol)] and vdW energy [PA6,10-Na^+ (ΔE~-40kcal/mol) and PA6,10-Ca^{2+} (ΔE~-13kal/mol)] demonstrate the efficient fitting of metal ions with aliphatic groups of the polymer chain. The complexation of these metal ions with polyamide chain may be governed by the values of the surface coordination number, ionization potential and ionic radius of the metal cations as described by (Frolov *et al*., 1999). The metal ion with largest ionic radius may form a close packed geometry conformation maximally filling the available lattice space (Figure 3.13e). The results obtained demonstrated the importance of the structural features of the oligosaccharide chains and the steric arrangement of the active groups where the cation-interaction displays considerable stereospecificity, proper spacing and geometry of the coordination shell.

Table 3.8: Calculated energy parameters for the molecular assemblies involving PA6,10, s-PLGA and PEO.

Structure	Energy (kcal/mol)							
	Total	**$\Delta E_{binding}$**	**Bond**	**Angle**	**Dihedral**	**VDW**	**ΔE_{vdw}**	**H bond**
PA6,10	64.425	--	1.153	54.931	4.771	3.963	--	-0.391
PA6,10-Zn^{2+}	62.135	-2.29	1.076	52.586	8.739	-0.267	-4.23	-0.0003
PA6,10-Ca^{2+}	1.709	-62.72	0.619	4.256	6.361	-9.434	-13.397	-0.093
PA6,10-Na^+	-27.595	-92.02	0.266	2.400	5.439	-35.701	-39.664	0
s-PLGA	2.638	--	0.288	2.534	0.885	-1.062	--	-0.007
PEO	12.635	--	0.216	0.985	7.003	4.431	--	-0.001
s-PLGA-PEO	2.571	-25.343	0.639	4.612	18.112	-19.896	-27.696	-0.902

$\Delta E_{binding} = E_{(Host.Guest)} - E_{(Host)} - E_{(Guest)}$
$\Delta E_{vdw} = Vdw_{(HostGuest)} - VdW_{(Host)} - VdW_{(Guest)}$

This complexation between surface electron-donor groups of the PA6,10 fibre and metal cations may be responsible for the altered physicomechanical (breaking load) and physicochemical properties of the fibre (by decreasing or increasing the effective pore size). It may be too difficult for the drug to be entrapped into the polyamide matrix because of very high intermolecular bonding between the polymer filaments as shown in Figure 3.13. In this way, drug may remain outside the matrix and be released as soon as it comes in contact with dissolution media (high initial burst release). However, addition of metal salts (monovalent or divalent) may cause breaking of these intermolecular bonds, thereby creating space for the drug molecules to be embedded into the polymer matrix (Gupta *et al*., 2009) (Figure 3.13). Additionally, water being a stronger Lewis base than nylon may cause leaching of salt molecules creating a porous matrix architecture.

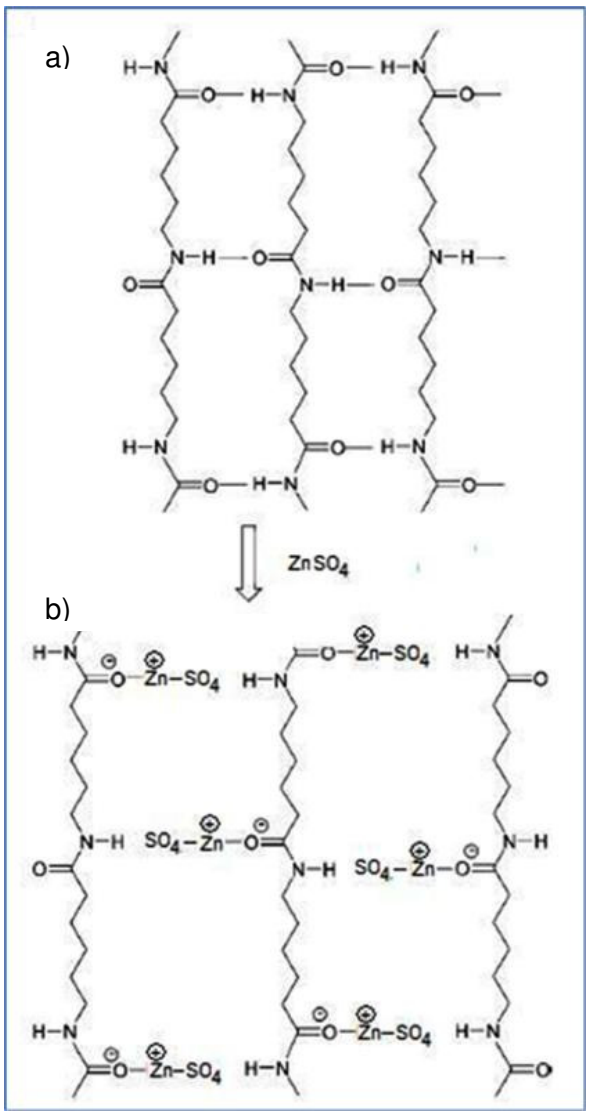

Figure 3.13: Schematic of reference polyamide with a) intermolecular hydrogen bonds and b) polyamide complexed with $ZnSO_4$.

Sodium ions, having larger binding energy and more stabilized complex, may delay the release culminating in the release of drug to a lesser extent (lowered initial burst release). This is also evident from the geometrical preferences shown in the polymer salt complexes, (Figures 3.12c, d and e), where sodium ions are forming a dense matrix structure than calcium and zinc. Additionally, Mit-uppatham and co-workers described that the viscosity value of polyamide solutions increases with the addition of monovalent ions such as Na^+ and Li^+ (as compared to divalent ions such as Mg^{2+}) due to an increase in the viscoelastic force (Mit-uppatham *et al.*, 2004). This increase in viscosity may be a determining factor for the zero-order controlled release profile due to inclusion of Na_2SO_4. These results in conjunction with the comparable FTIR spectra of the non-compressed and compressed matrices indicates that the introduction and removal of salts is a reversible process and does not alter the final properties of PA6,10.

3.3.9. Influence of the incorporation of PEO on the performance of the s-PLGA layer

The energy minimized structures of the s-PLGA-PEO, before and after molecular mechanics simulations, are depicted in Figure 3.14 and the corresponding connolly molecular surface structures are demonstrated in Figure 3.15. The possible component binding energies and the intrinsic molecular attributes to which they will be responsive, are listed in Table 3.8.

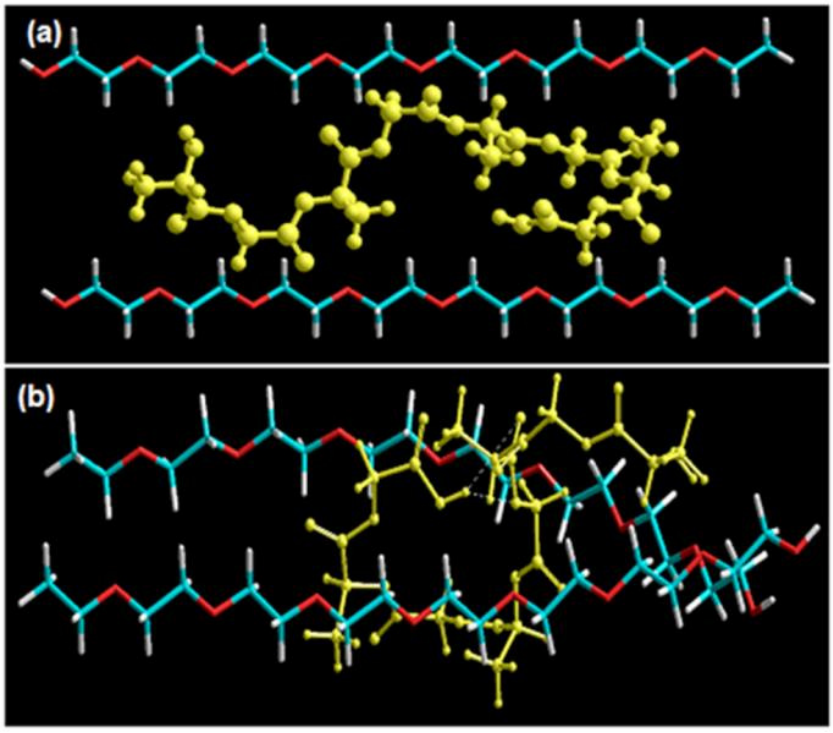

Figure 3.14: Visualization of optimized geometrical preferences showcasing the s-PLGA-PEO complex systems: (a) before and (b) after molecular mechanics' energy refinements. Color codes: s-PLGA (yellow) and PEO (standard element colors: Carbon (cyan), Nitrogen (blue) and Oxygen (red).

Invariant factors common to mathematical description of binding energy and substituent characteristics have been ignored. It is evident from the energy values that the s-PLGA-PEO complex is stabilized by a binding energy ΔE≈-25kcal/mol. The global energy minimum was supported mainly by the van der Waals interactions between the polymer molecules (ΔE_{vdw}=-27.696) due to the presence of aliphatic groups in the polymers. These underlying weak chemical interactions may not cause a structural change in the polymers but may initiate aggregation of the aliphatic chains, as both the polymers synthesized are long chain aliphatic polymers, resulting in localized regions with a density and refractive index different from that of the bulk polymers. Figures 3.15a and b visualize the comparative molecular surface preferences of the two polymers before and after the computational refinement. Additionally, the PEO induced intramolecular hydrogen bonding in s-PLGA (≈100 times more than the individual polymers) (Figure 3.14b) may influence the hydration process of the PLGA polymer matrix. The stratified zero-order drug release along with reduced burst release from

the s-PLGA-PEO blend layer of TLT formulations is in line with the earlier reported results involving s-PLGA–PEO polymeric blend films and microparticles by Santander-Ortega *et al*. (2010).

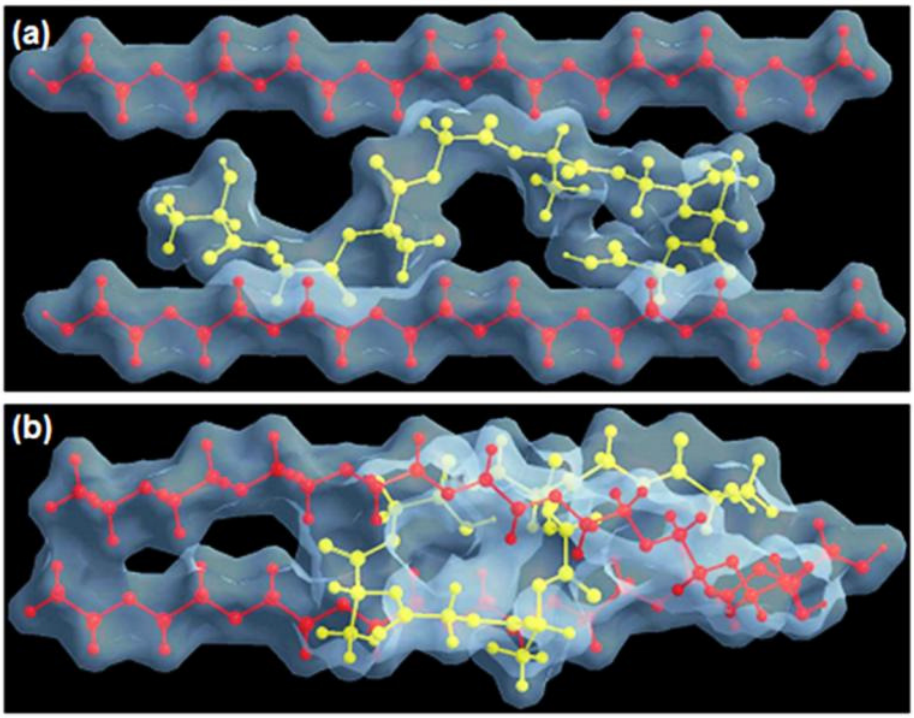

Figure 3.15: Connolly molecular electrostatic potential surfaces in translucent display mode showcasing the PLGA-PEO complex systems: (a) before and (b) after molecular mechanics' energy refinements. Color codes: PLGA (yellow) and PEO (red).

3.4. Concluding Remarks

It was elucidated that the employed novel polymers have shown significant potential as outer layer drug matrices in the TLT formulations for potential zero-order drug release. Linear profiles were observed from all three layers of specific formulations. It was determined that each layer should have a weight of 400mg including 50mg of drug for optimum results. The ratio of polymers to salt and other polymers were proven to have an effect on the physicomechanical properties of the matrices and had an influence on drug release behavior. It is logical that the intimate selection of appropriate polymer and excipient ratios are critical in achieving the desired drug release outcomes. The Molecular Mechanics simulations demonstrated that the obtained release pattern may be attributed to the modified matrix hydration process of PLGA (hydrogen bonding induced by the presence of the PEO) and continued retarded release of the PEO derivative due to its entanglement with the polyester chains as was shown in connolly molecular surface architecture. The matrices exhibited much promise for the controlled delivery of various drugs including those with high water-solubility. Further research will focus on the optimization of the TLT formulations. It is apparent that the proposed system potentially offers a significant positive impact on patient compliance and therefore therapeutic efficacy.

CHAPTER 4

EXPERIMENTAL DESIGN AND STATISTICAL OPTIMIZATION OF THE TRIPLE-LAYERED TABLET MATRICES

4.1. Introduction

The preformulation studies summarized in the previous chapter were essential for identifying formulation factors (independent variables) used in the optimization of the triple-layered tablet (TLT) matrices. The independent variables previously mentioned are outlined in this chapter. It is known that in modern years, chemometric approaches are commonly applied to the optimization of scientific systems (Ferreira *et al*., 2007). This approach carries various advantages such as condensing the amount of experiments and therefore laboratory work that is required and subsequently a reduction in the amount of chemicals that are used.

Multivariate design of experiments allow for the determination of important interactions between the different experimental variables that may occur permitting a more accurate optimization of the systems. An experimental design was employed in the study whereby the aforementioned variables were varied accordingly in order to evaluate measured responses of the TLT formulations.

Response surface methodology was opted for while the experimental design was being executed. This was selected in order to determine the optimal combination of the formulation constituents. This methodology along with a Box-Behnken design was employed to optimize the TLT. Hence, the process of optimization that was utilized involved a number of steps that were conducted in a specific manner which includes developing a design of experiments utilizing the formulation independent variables, conducting *in vitro* tests on the formulations generated in the design of experiments, employing regression analysis to determine the coefficients of a mathematical model and the forecasting of the dependent variables or measured responses.

Two new model drugs were introduced to the TLT in order to generate more in depth *in vitro* drug release results for ultimate optimization of the TLT. Hence, the aim of this chapter was to outline the comprehensive in vitro analysis of the Box-Behnken design formulations with specific focus on the two valid experimental responses that were selected. The results obtained were aided by specific contour plots and diagnostic plots to assess the relationships between constituents that may have been established and to assess the efficiency of the Box-Behnken design.

4.2. Materials and Methods

4.2.1. Materials

Ranitidine hydrochloride (RDH), promethazine (PMZ) and chlorpromazine (CP) were purchased from Sigma Chemical Company (St Louis, MO, USA). HPLC grade Acetonitrile (ACN) was purchased from Microsep (Johannesburg, South Africa). Potassium dihydrogen phosphate and methyl paraben (MP) was purchased from Rochelle Chemicals (Johannesburg, South Africa). All other reagents used are of analytical grade.

4.2.2. Methods

4.2.2.1. Determination of appropriate independent formulation variables to explicate desired responses for the TLT matrices

Separate factors were chosen for each constituent of the TLT matrices in order to be capable of generating specific mathematical models per constituent. The most fundamental variables to be considered were the quantities of PA6,10 and SS in the first layer and s-PLGA and PEO in the third layer. Thus the independent variables were quantitative in nature.

Patterns were observed with regards to the amount of PA6,10 utilized in the formulation and the effect of this on drug release behavior from the preformulation studies. These patterns were quantified and used as upper and lower limit variables for drug release. Further patterns were noted with the amount of s-PLGA and PEO utilized in the third layer. Thus the quantities of each individual polymer were allocated upper and lower limits and used as variables for the optimization of the TLT matrices. For the purposes of this study the responses selected for optimization were rate constants (*k*) and correlation coefficients (R^2 values). Rate constants were to be obtained corresponding to those of zero-order drug release kinetics while correlation coefficients were to be maximized in order to obtain an optimal formulation. Table 4.1 displays the formulation variables and responses with the goal of TLT optimization. These values were selected according to the desired drug release profiles from the TLT matrices. The drug release profiles from all the layers would be required to be linear or near linear (zero-order) for the desired outcome of this study.

Each of the three drugs incorporated into the formulations would need to be released at a constant rate per a predetermined time interval over 24 hours. This was to be attempted in the anticipation that as drug is released it is being absorbed in the same ratio and quantity that it was released. During the preliminary studies, the formulations that essentially

displayed similar release profiles to the desired release profiles were selected for further studies and variable development.

Table 4.1: Formulation variables and responses for TLT optimization.

Independent variables	Upper limits	Lower limits
PA6,10 (mg)	300	100
SS (mg)	150	50
s-PLGA (mg)	300	50
PEO (mg)	300	50
Response	**Upper limits**	**Lower limits**
Rate constant (*k*)	0.06	0.039
Correlation coefficient (R^2)	1	0.7

It was noted that the quantity of PA6,10 added to the formulation had a significant impact on the retardation of drug release from the TLT matrices. It was elucidated that a more substantial quantity of PA6,10 was required for adequate retardation and control of drug release from the first layer. The same was noted for the ratio of s-PLGA to PEO in the third layer. A lower ratio displayed a more desired control of drug release from the third layer. Thus specific numerical values for the independent variables were selected according to influence they had on the drug release profiles.

4.2.2.2. Box-Behnken Experimental Design for the evaluation of drug release from the TLT matrices

A Box-Behnken Experimental Design was generated with experimental runs, essentially, being the basic backbone of the design. The rationale behind this was fundamentally to minimize the quantity of experimental runs that would be necessary to collect the optimal amount of data required for adequate interpretation (Karnachi and Khan, 1996; Chopra *et al*., 2007). This was also due to the complex nature of data that would be generated from the TLT formulations. The design software employed (Minitab® V15, Minitab®, PA, USA) was used to generate seventeen (17) formulations that would undergo experimental runs. The variable factors for the experimental runs of the TLT matrices are displayed in Table 4.2. The experimental (measured) responses that result from the design of experiment stage are utilized to establish an adequate mathematical model that may explain the relationship of the variables with the measured outcomes (responses).

Table 4.2: The Box-Behnken design experimental runs employed to optimize TLT formulations displaying the possible combinations of polymers and excipients that were utilized.

Experiment	Layer 1 (outer)		Layer 2 (middle)	Layer 3 (outer)	
	s- PLGA (mg)	PEO (mg)	PEO (mg)	PA 6,10 (mg)	SS (mg)
1	300	50	350	300	50
2	50	300	350	200	150
3	238	113	350	275	75
4	175	175	350	250	100
5	207	142	350	263	87
6	131	219	350	241	109
7	50	300	350	300	50
8	117	233	350	280	70
9	113	238	350	275	75
10	219	131	350	241	109
11	300	50	350	200	150
12	238	113	350	225	125
13	142	208	350	263	87
14	113	238	350	225	125
15	70	280	350	233	117
16	233	117	350	280	70
17	280	70	350	233	117

4.2.2.3. Selection of measured formulation responses for the experimental optimization of TLT formulations

The selected measured responses employed for optimization of the TLT formulations were rate constants (*k* values) and correlation coefficients (R^2 values). The Peppas model (Equation 4.1.) was utilized to generate rate constants by fitting in the individual values per design formulation. *In vitro* drug release data from each of the design formulations were fitted to the Peppas model (Equation 4.1). It is known that if the value of the exponent (n) is one, zero-order drug release kinetics is followed. It is due to this that the value of n was fixed at 1 and the ideal rate constant value was obtained. The rate constants for each of the design formulations were calculated in the same manner.

$$\frac{Mt}{M\infty} = kt^n$$

Equation 4.1

Where, *Mt* is the quantity of drug released at time t; *M*∞ is the drug loading; *k* is an experimentally determined kinetic constant and *n* is an exponent that depends on the geometry of system and indicates the release mechanism (Davidson III and Peppas, 1986; Colombo, 1993).

The *k* and R^2 values were computed for each layer of the TLT formulations i.e. three *k* and R^2 values were calculated per formulation. Table 4.5 lists the *k* values for each of the design formulations.

4.2.2.4. Preparation of the design formulations

Due to the fact that each layer of the TLT would have to be analyzed separately per design formulation, a decision was made to incorporate three drugs simultaneously to increase the efficiency of the study. Upon investigation it was found that ranitidine HCl (RDH) and promethazine (PMZ) possessed the same aqueous solubility as DPH (100mg/mL). This proved to be beneficial in further proving the controlled release of highly aqueous soluble drug actives. Therefore it was decided that a logical simultaneous incorporation of the two drugs into the TLT was favorable. PMZ was incorporated into the middle PEO layer and RDH was incorporated into the outer s-PLGA layer. The formulations were prepared by direct compression as described in Chapter 3, Section 3.2.2.5.

4.2.2.5. In vitro dissolution testing on the Box-Behnken Experimental Design formulations

In vitro drug release studies were performed on the different formulations using a USP 25 rotating paddle method in a dissolution apparatus (Caleva Dissolution Apparatus, model 7ST; G.B. Caleva Ltd., Dorset, UK) at 50 rpm with 900mL simulated gastric fluid (SGF) (pH 1.2, 37℃) and 900mL phosphate-buffer solution (PBS) (pH 6.8; 37℃). A stainless steel mesh was used in the dissolution vessels in order to prevent the formulations from floating. Samples of 5 mL were drawn at pre-determined time intervals over a 24 hour period.

4.2.2.6. High Performance Liquid Chromatographic analysis of in vitro dissolution samples

Analysis of dissolution samples were carried out on a Waters High Performance Liquid Chromatography (HPLC) machine (Waters Acquity, Microsep, JHB, South Africa). Adequate HPLC method conditions were determined and utilized to analyze dissolution samples from the Box-Behnken design formulations. Various methods were attempted in order to obtain a chromatographic separation method for the simultaneous determination of all three drugs. This was necessary as DPH, PMZ and RDH were loaded into the TLT formulations simultaneously in order to perform dissolution testing. Phosphate buffer solution (PBS) (pH 3, 30℃) and Acetonitrile (ACN) were selected as the mobile phases for the separation method. A substantial amount of time was utilized in attempting to develop a suitable method. Finally, an isocratic method (as shown in Table 4.3) for the chromatographic quantification of DPH was obtained as the determination of all three was not easily achievable. Methylparaben (MP) was employed as the internal standard (IS) for calibration and analysis. Figure 4.1 is a chromatogram displaying the separation peaks of DPH and MP. Once the chromatographic

method was optimized, calibration curves were prepared by running the standards through the HPLC column.

Table 4.3: HPLC conditions for the chromatographic analysis of DPH.

Parameter	Condition
Column	Xterra™ RP_{18}, 5µm, 4.6×150mm
Mobile phase	Acetonitrile/20mM potassium dihydrogen phosphate pH=3, 35:65
Flow rate	1mL/min
Injection volume	20µl
Detection	UV 210nm
Column Temperature	30℃

The AUC of DPH and MP were noted for each concentration. The ratio between the AUC of DPH and MP was plotted against concentration. Figure 4.2a and Figure 4.2b display the calibration curves for DPH quantification in PBS (pH 6.8, 37℃) and SGF (pH 1.2, 37℃) respectively.

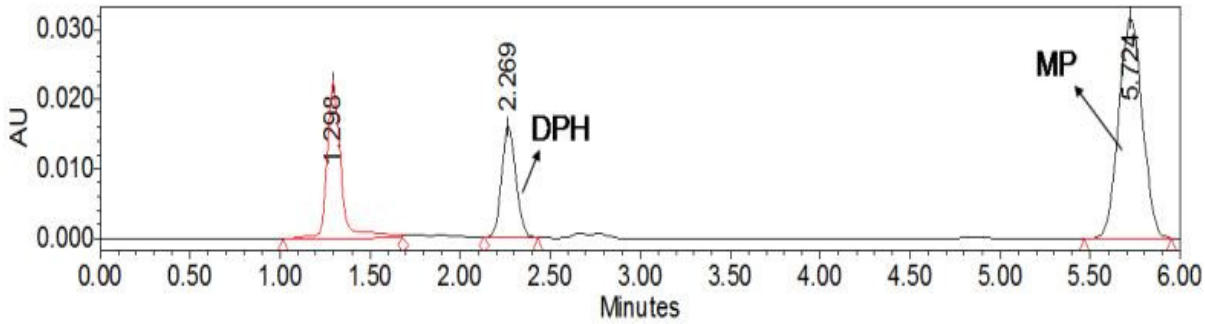

Figure 4.1: Chromatogram depicting the separation peaks of DPH and MP.

Standard stock solutions ranging between 0-0.1mg/mL of DPH, PMZ and RDH were prepared both in PBS (pH 6.8, 37℃) and SGF (pH 1.2, 37℃) for the calibration analysis. The ratio between the area under the curve (AUC) of the three drugs and the IS was plotted against concentration to produce each calibration curve.

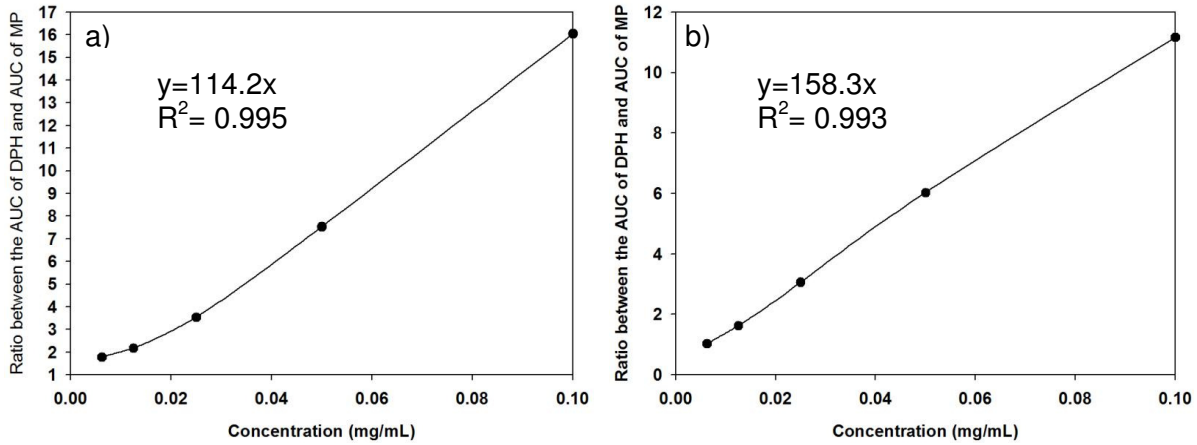

Figure 4.2: Calibration curves for DPH quantification in a) PBS (pH 6.8, 37℃) and b) SGF (pH 1.2, 37℃).

Table 4.4 displays the method conditions for the simultaneous determination of PMZ and RDH.

Table 4.4: HPLC conditions for the chromatographic analysis of PMZ and RDH.

Parameter	Condition
Column	Xterra™ RP_{18}, 5µm, 4.6×150mm
Mobile phase	Acetonitrile/20mM potassium dihydrogen phosphate pH=5, gradient method
Flow rate	1mL/min
Injection volume	20µl
Detection	UV 254nm
Column Temperature	30℃

The mobile phases employed were PBS (pH 5) and ACN using a gradient method as shown in Table 4.4. Chlorpromazine (CP) was employed as the IS for calibration and analysis. Figure 4.3 is a chromatogram displaying the separation peaks of PMZ, RDH and CP. After method optimization, calibration curves were prepared. Figures 4.4a and b depict the calibration curves computed for PMZ in PBS (pH 6.8, 37℃) and SGF (pH 1.2, 37℃) respectively. Similarly, Figures 4.5a and b depict the calibration curves computed for RDH in PBS and SGF (pH 1.2, 37℃).

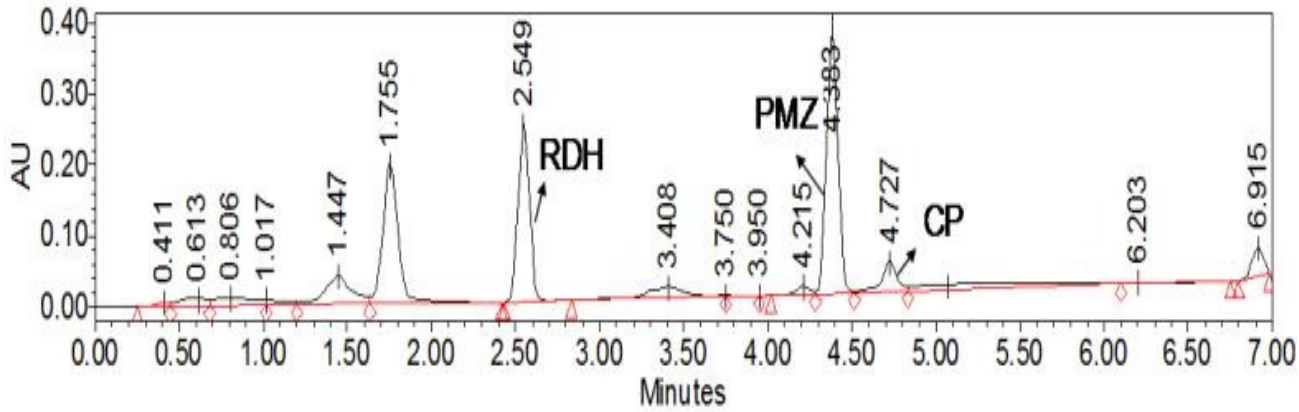

Figure 4.3: Chromatogram depicting the separation peaks of RDH, PMZ and CP.

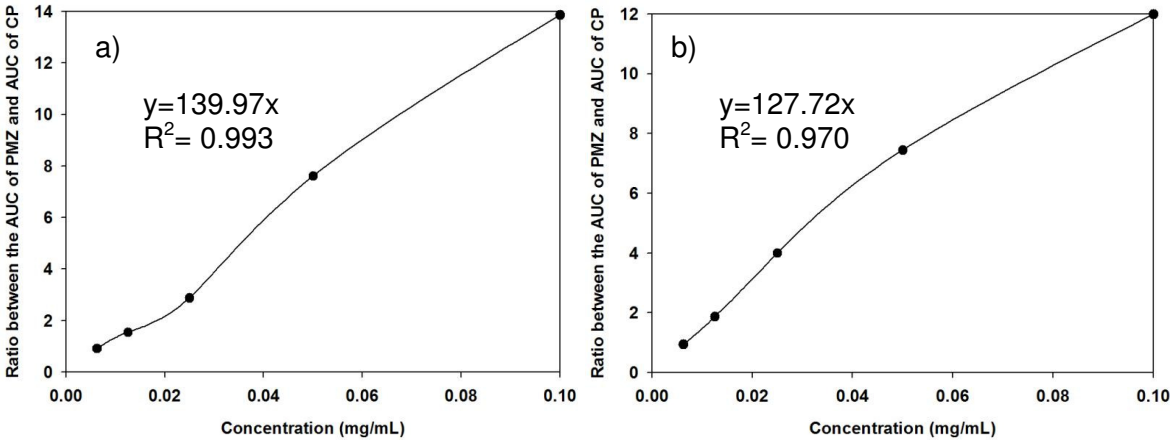

Figure 4.4: Calibration curves for PMZ quantification in a) PBS (pH 6.8, 37℃) and b) SGF (pH 1.2, 37℃).

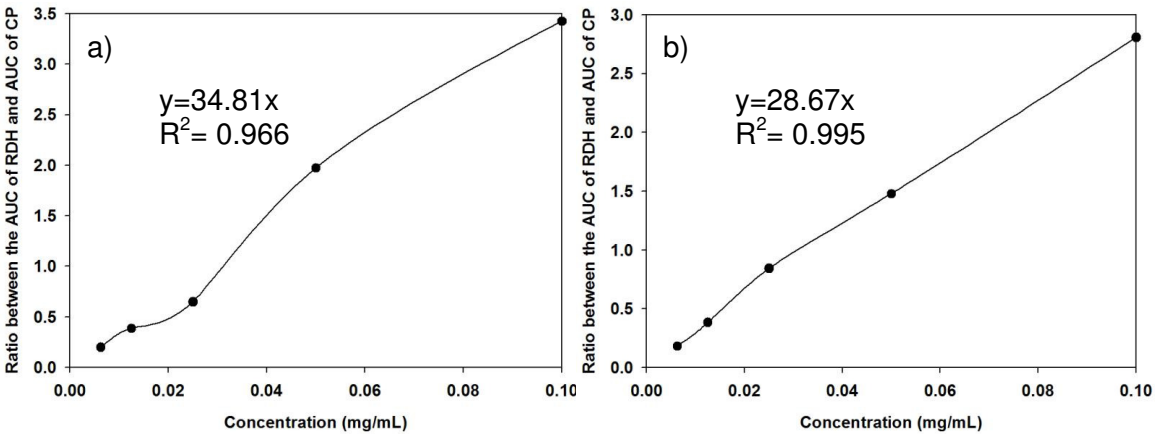

Figure 4.5: Calibration curves for RDH quantification in a) PBS (pH 6.8, 37℃) and b) SGF (pH 1.2, 37℃).

4.3. Results and Discussion

4.3.1. *In vitro* drug release analysis of the Box-Behnken Experimental Design formulations

Figure 4.6a exhibits the release profiles of DPH from all the design formulations in PBS (pH 6.8, 37℃). Drug release results of DPH from the design formulations essentially confirmed those of the preliminary results where the formulations containing a higher quantity of PA 6,10 provided more linear release profiles of DPH. This trend was noted for most of the formulations. F1 and F7 displayed the most linear release profiles. Release from PBS (pH 6.8, 37℃) was more desirable than the release from SGF (pH 1.2, 37℃).

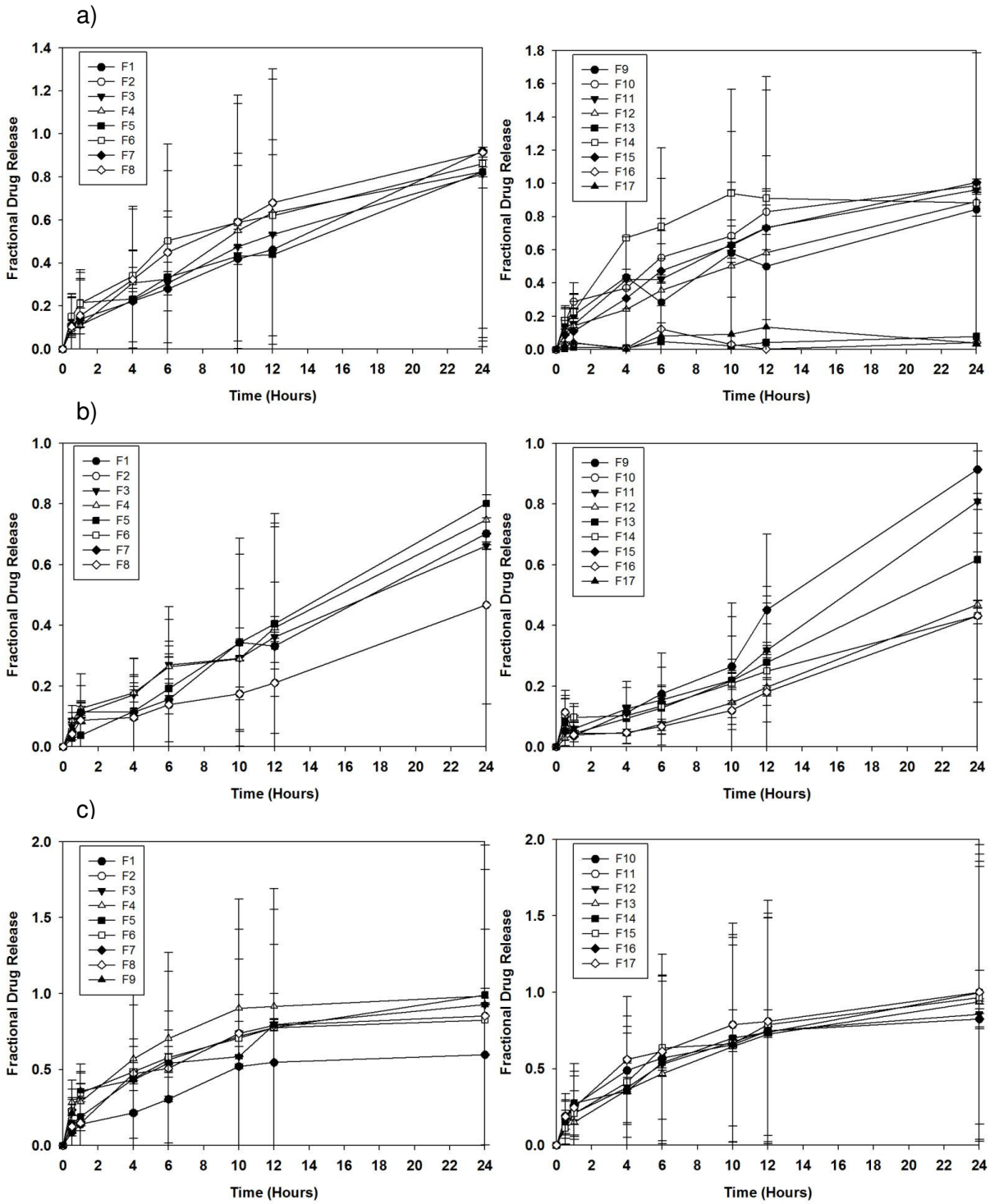

Figure 4.6: Drug release profiles of a) DPH, b) PMZ and c) RDH from the Box-Behnken design formulations in PBS (pH 6.8, 37℃).

PMZ release from the middle layer was linear in most of the formulations as was noted in the preliminary studies. This was due to the uniform area of the surfaces that are exposed to the dissolution medium which allows for a constant diffusion path length. Hence, this is conducive to a uniform flux and thus a constant release of the drug over a time interval (Yang and Fassihi, 1997; Abdul and Poddar, 2004). Figure 4.6b displays the drug release profiles of PMZ from the design formulations. Release from the outer s-PLGA layer proved to be the most challenging in providing linear release of RDH (Figure 4.6c), F7 showed the most linear

release profile of RDH that confirms the results from the preliminary drug release results; a lower s-PLGA to PEO ratio evidently appeared to have generated more favorable results. A possible mechanism for this may be that the s-PLGA functioned as a controlling mechanism by retarding the swelling of PEO in a more uniform manner.

4.3.2. Evaluation of rate constants computed from the design formulations

4.3.4.1. DPH rate constants

The average rate constants for each formulation are exhibited in Table 4.5. Following the scrutiny of *k* values computed for the design formulations it was discovered that F1 and F3 displayed the most desirable rate constants relative to the ideal while F10, F13 and F16 displayed the least desirable rate constants in PBS (pH 6.8, 37℃). F1, F7 and F16 were observed to have more desirable rate constants in SGF (pH 1.2, 37℃).

Table 4.5: Rate constants (k values) for the experimental optimization of TLT formulations.

	***k* (SGF)±S.D.**		***k* (PBS) ±S.D.**	
Formulation	**Layer 1 (DPH)**	**Layer 3(RDH)**	**Layer 1 (DPH)**	**Layer 3 (RDH)**
1	0.037 ± 0.0020	0.049 ± 0.0013	0.041 ± 0.0020	0.033 ± 0.0004
2	0.046 ± 0.0002	0.040 ± 0.0010	0.043 ± 0.0040	0.051 ± 0.0026
3	0.052 ± 0.0070	0.039 ± 0.0065	0.041 ± 0.0030	0.049 ± 0.0011
4	0.052 ± 0.0080	0.039 ± 0.0020	0.042 ± 0.0003	0.055 ± 0.0042
5	0.035 ± 0.0030	0.057 ± 0.0016	0.032 ± 0.0030	0.050 ± 0.0030
6	0.043 ± 0.0070	0.058 ± 0.0018	0.046 ± 0.0030	0.052 ± 0.0059
7	0.039 ± 0.0074	0.054 ± 0.0025	0.029 ± 0.0005	0.051 ± 0.0006
8	0.031 ± 0.0050	0.051 ± 0.0019	0.029 ± 0.0003	0.047 ± 0.0035
9	0.045 ± 0.0034	0.038 ± 0.0133	0.040 ± 0.0012	0.054 ± 0.0028
10	0.047 ± 0.0006	0.050 ± 0.0003	0.051 ± 0.0025	0.045 ± 0.0028
11	0.052 ± 0.0062	0.034 ± 0.0205	0.047 ± 0.0030	0.051 ± 0.0061
12	0.053 ± 0.0025	0.024 ± 0.0029	0.040 ± 0.0035	0.049 ± 0.0021
13	0.037 ± 0.0002	0.058 ± 0.0037	0.054 ± 0.0026	0.048 ± 0.0011
14	0.030 ± 0.0016	0.052 ± 0.0021	0.047 ± 0.0042	0.051 ± 0.0006
15	0.025 ± 0.0005	0.073 ± 0.0128	0.039 0.0010	0.050 ± 0.0021
16	0.041 ± 0.0001	0.052 ± 0.0071	0.052 ± 0.0026	0.061 ± 0.0013
17	0.048 ± 0.0148	0.046 ± 0.0018	0.042 ± 0.0028	0.055 ± 0.0003

The analysis of *k* values obtained in accordance with DPH release from the TLT formulations revealed that an increase in PA6,10 concentration in the TLT correlated with a *k* value that was inclined towards the ideal value of 0.0417. However, the increase in PA6,10 was limited essentially to 300mg within the layer which allows for a more reasonable tablet size and therefore uncomplicated patient administration. Also, with regards to the ratio of PA6,10 to SS it was important to note that the polymer (PA6,10) ideally should comprise the bulk of the layer as the function of SS was to inhibit the initial burst release of drug. Hence, it was noted that formulations that were comprised of a large PA6,10 to SS ratio resulted in a more desirable *k* value for drug release. This may be attributed to the PA6,10 being capable of forming a more compact drug matrix which may be able to retard and control the release of

DPH in a more superior manner as mentioned in Chapter 3 during preformulation studies. Figure 4.7 contains typical contour plots depicting the relationship between the rate constants and polymer concentrations in the TLT matrix for the release of DPH in SGF (pH 1.2, 37℃).

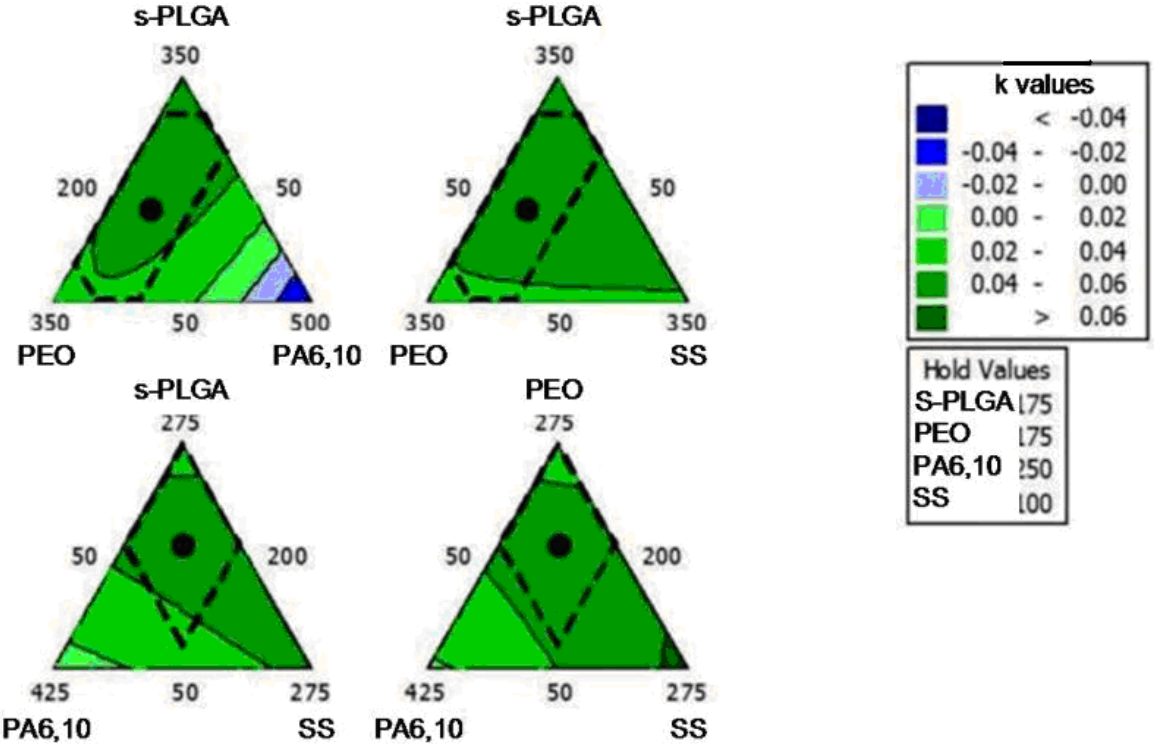

Figure 4.7: Contour plots of the relationship between rate constant and polymer concentration for DPH release in SGF (pH 1.2, 37℃).

4.3.4.2. RDH rate constants

The average *k* values for each of the design formulation constants are displayed in Table 4.5. Subsequent to analysis it was noted that F8 and F10 displayed the most desirable *k* values in comparison to the ideal while F1, F4 and F17 displayed the least desirable k values in PBS (pH 6.8, 37℃). F2, F3 and F4 displayed the most desirable *k* values while F6, F13 and F15 displayed the least desirable rate constants in SGF (pH 1.2, 37℃). The analysis of rate constants obtained according to RDH release from the TLT formulations uncovered observations revealing that decreased concentrations of s-PLGA in the TLT were associated with a more desirable rate constant and a lower s-PLGA to PEO ratio exhibited a similar result. The reason for this detected behavior may be explained by the swelling of PEO which may provide a constant diffusion path length for RDH to be released as observed during preformulation in Chapter 3. The s-PLGA was rationalized to facilitate uniform swelling of PEO. Figure 4.8 contains typical contour plots illustrating the relationship between polymer concentration and rate constants for RDH release in SGF (pH 1.2, 37℃). The plots illustrate the significant relationship between PEO and s-PLGA which result in desirable *k* values in

the range of 0.03-0.06 occurring with PEO quantities between 200mg to 350mg and s-PLGA quantities between 40mg and 50mg.

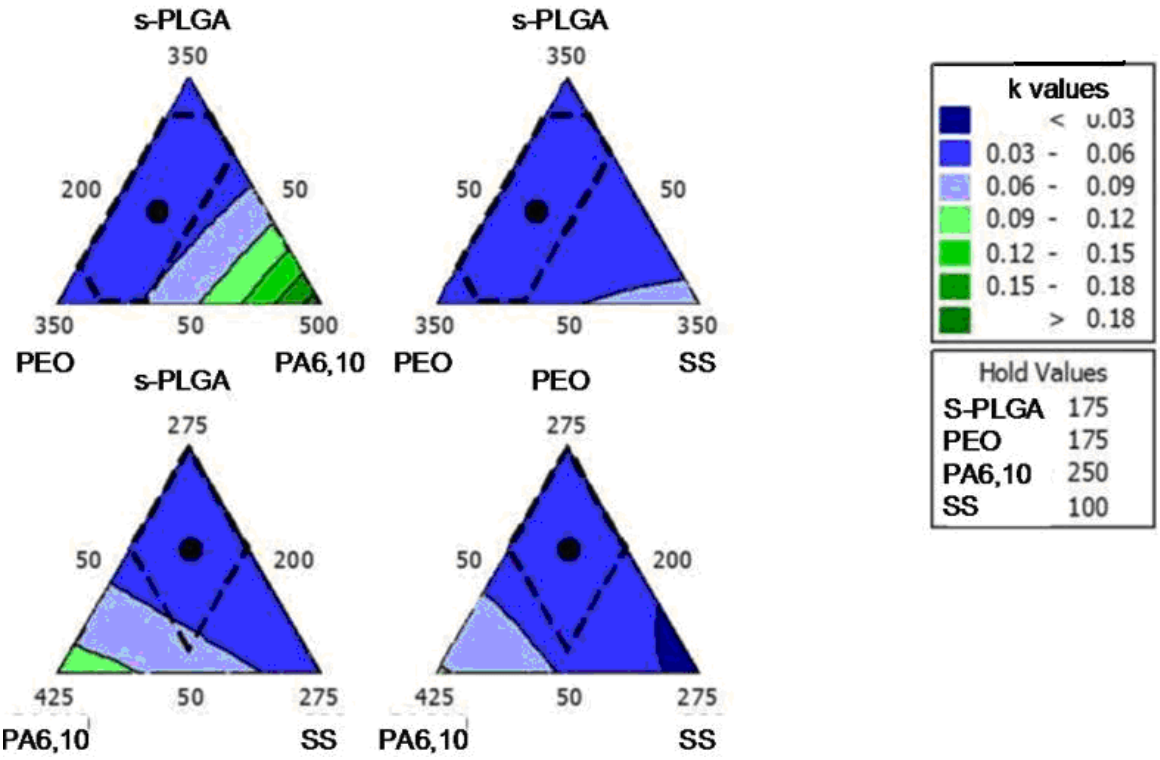

Figure 4.8: Contour plots of the relationship between *k* values and polymer concentration for RDH release in SGF (pH 1.2, 37℃).

4.3.5. Evaluation of correlation coefficients obtained from experimental design formulations

4.3.5.1. DPH correlation coefficients

The average R^2 values for each of the design formulations accompanied by standard deviations are displayed in Table 4.6. In all cases N=2. With the essential aim of establishing the optimal inclination to linearity, the analysis of R^2 values computed from the design formulations was indeed necessary. It was revealed that F1 and F9 displayed the most favorable R^2 values while F5, F15 and F16 exhibited the least favorable R^2 values in SGF (pH 1.2, 37℃). F1, F3 and F7 displayed the most favorable R^2 values while F13 and F16 exhibited the least favorable R^2 values in PBS (pH 6.8, 37℃).

Upon analysis, a similar pattern as with the rate constants was noted, that is a greater quantity of PA6,10 resulting in more linear profiles which is fundamentally in accordance the most desirable R^2 values. The certain instances where a high PA6,10 quantity correlated with an unfavorable R^2 value may be due to experimental or observational error. Figure 4.9 displays vertical bar charts depicting the average R^2 values of the experimental design

formulations for DPH release a) PBS (pH 6.8, 37℃) and b) SGF (pH 1.2, 37℃). The favorable behavior of the formulations in PBS (pH 6.8, 37℃) is clearly noticeable in the bar graphs. A greater tendency towards an R^2 value of 1 was evident in PBS (pH 6.8, 37℃) as opposed to SGF (pH 1.2, 37℃). Figure 4.10 is comprised of contour plots depicting the relationship between polymer quantities and R^2 values. It was observed that the desirable R^2 value range of 0.5-1 was achieved with PA6,10 quantities between 250 and 400mg and SS quantities between 50-150mg.

Table 4.6: Correlation coefficients (R^2 values) for the experimental optimization of TLT formulations.

Formulation	R^2 (SGF))±S.D.		R^2 (PBS))±S.D.	
	Layer 1 (DPH)	Layer 3 (RDH)	Layer 1 (DPH)	Layer 3 (RDH)
1	0.984 ± 0.0132	0.704 ± 0.0172	0.938 ± 0.0313	0.606± 0.0527
2	0.606 ± 0.0990	0.816 ± 0.0341	0.782 ± 0.0416	0.607± 0.0811
3	0.622 ± 0.1430	-0.424 ± 0.0930	0.900 ± 0.0132	0.400± 0.0341
4	0.388 ± 0.0220	-0.424 ± 0.0513	0.876 ± 0.0465	0.284± 0.0496
5	-0.512 ± 0.3470	0.298 ± 0.0099	0.687 ± 0.0057	0.733± 0.0863
6	0.384 ± 0.0370	0.631 ± 0.0254	0.629 ± 0.0331	0.438± 0.3385
7	0.410 ± 0.0410	0.414 ± 0.1034	0.908 ± 0.0662	0.725± 0.0100
8	0.808 ± 0.0540	0.057± 0.0084	0.849 ± 0.0522	0.679± 0.0672
9	0.819 ± 0.0142	0.959± 0.2893	0.610 ± 0.0228	0.641± 0.0921
10	0.326 ± 0.0104	0.681± 0.0054	0.690 ± 0.0706	0.275± 0.0577
11	0.275 ± 0.0586	0.576± 0.0552	0.798 ± 0.0153	0.368± 0.1963
12	0.659 ± 0.1380	0.565± 0.1613	0.896 ± 0.0129	0.653± 0.1009
13	0.505 ± 0.0303	0.588± 0.0496	0.024 ± 0.1980	0.739± 0.0494
14	-1.000 ± 0.0087	0.436± 0.1573	0.904 ± 0.0482	0.695± 0.0054
15	-1.144 ± 0.0513	0.818± 0.2563	0.938 ± 0.0317	0.782± 0.1742
16	0.599 ± 0.0419	0.670± 0.1786	-0.403 ± 0.0422	0.594± 0.0578
17	-0.481 ± 0.007	0.247± 0.0392	0.528 ± 0.1564	0.433± 0.0912

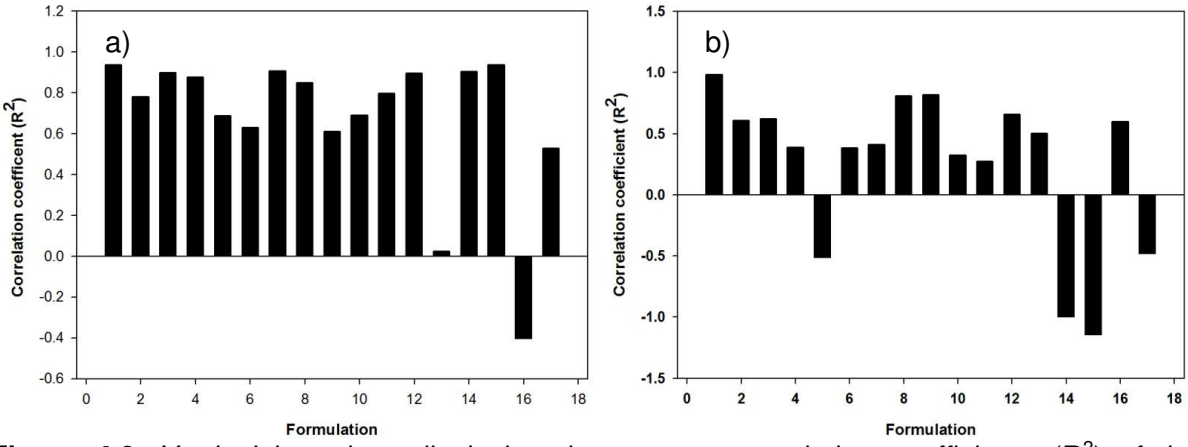

Figure 4.9: Vertical bar chart displaying the average correlation coefficients (R^2) of the design formulations in a) PBS (pH 6.8, 37℃) and b) SGF (pH 1.2, 37℃), (N=2).

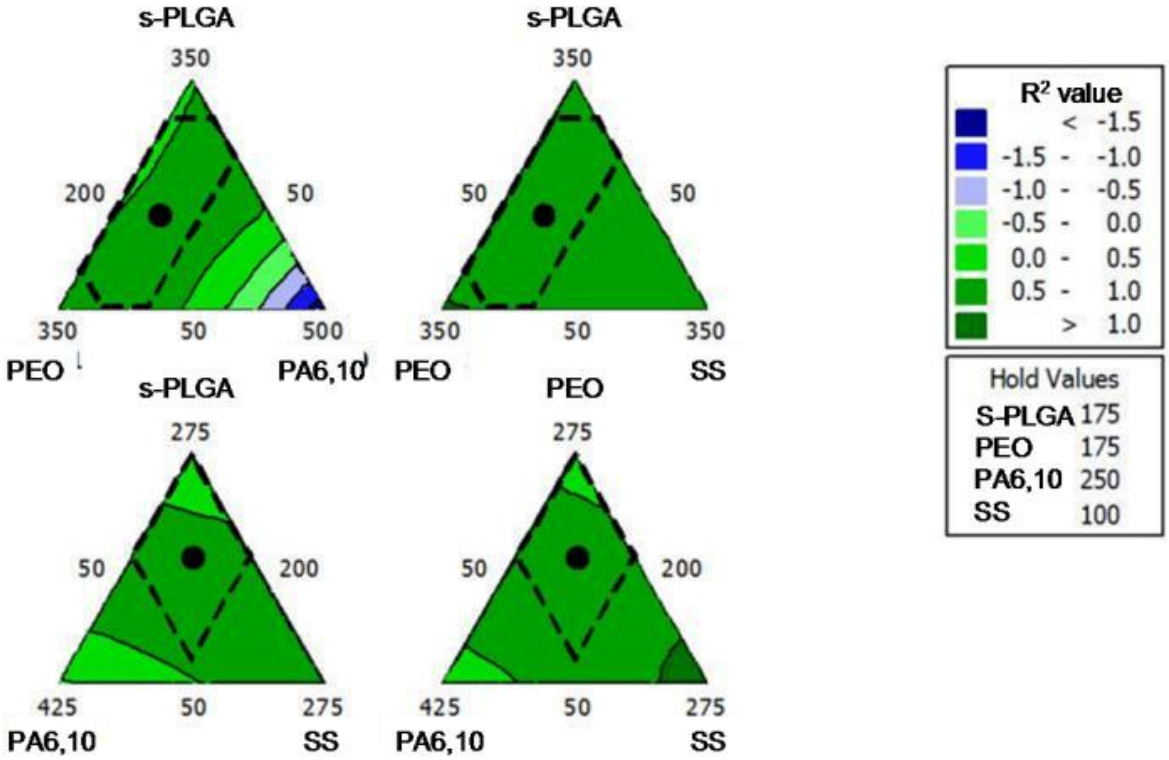

Figure 4.10: Contour plots depicting the relationship between the polymer mixtures and the R^2 values of DPH release from the design formulations in PBS (pH 6.8, 37℃).

4.3.5.2. RDH correlation coefficients

F5, F7 and F13 displayed the most favorable R^2 values while F4 and F10 displayed the least favorable R^2 values in PBS (pH 6.8, 37℃). F2 and F9 exhibited the most desirable R^2 values while F3 and F4 exhibited the least desirable R^2 values in SGF (pH 1.2, 37℃). As previously mentioned, this fits in with the pattern observed for the rate constants. A higher PEO to s-PLGA ratio resulted in more desirable R^2 values. The opposite was noted for lower PEO to s-PLGA. This is owed to the resulting R^2 values being very distant to the ideal. Figure 4.11 includes the contour plots illustrating the relationship between polymer concentrations and R^2 values for RDH release in PBS (pH 6.8, 37℃) which further substantiates the optimal R^2 values in the range of 0.8-1 being achieved within the polymer mixtures containing 300-350mg PEO and 0-50mg s-PLGA.

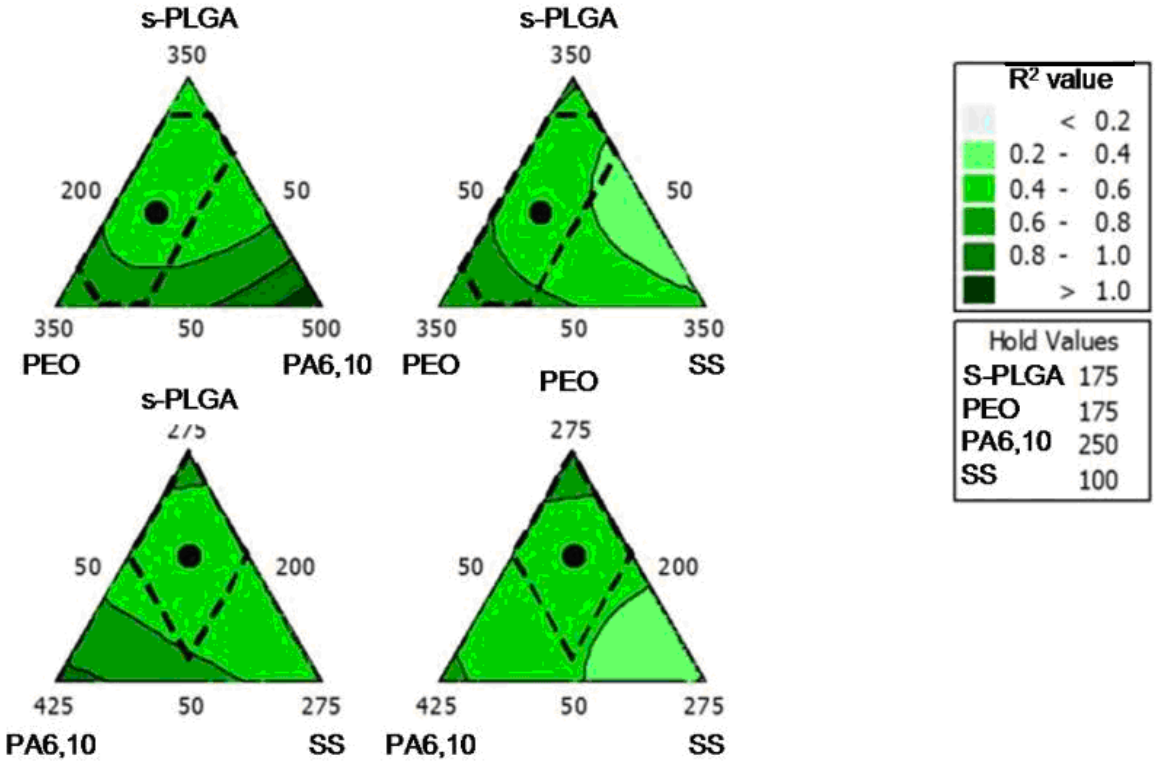

Figure 4.11: Contour plots depicting the relationship between the polymer mixture and the R^2 values of the release of RDH from the design formulations in PBS (pH 6.8, 37℃).

4.3.6. Assessment of the experimental and fitted response values calculated for the experimental optimization of TLT formulations

The measured responses obtained from the design of experiments were plotted relatively against the fitted responses obtained. The experimental versus fitted k values plots for DPH in PBS (pH 6.8, 37℃) and SGF (pH 1.2, 37℃) are displayed in Figures 4.12a and b respectively. R^2 values for the comparative responses were computed to be 0.696 and 0.593 in SGF (pH 1.2, 37℃) and PBS, respectively. The experimental versus fitted *k* values plots for RDH in SGF (pH 1.2, 37℃) and PBS are displayed in Figures 4.12c and d. R^2 values for the comparative responses were calculated to be 0.772 and 0.715 in SGF (pH 1.2, 37℃) and PBS (pH 6.8, 37℃), respectively.

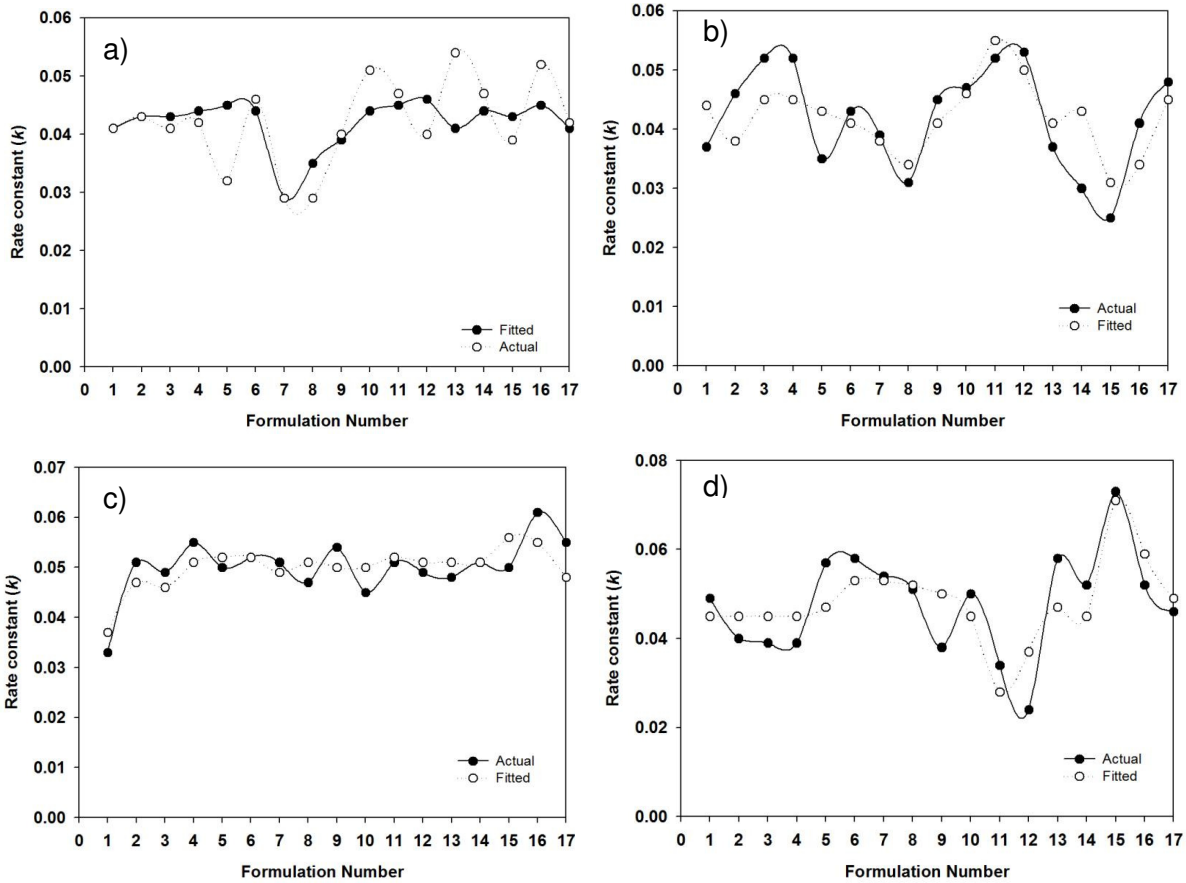

Figure 4.12: Regression plots for rate constants (*k*) for a) DPH in SGF (pH 1.2, 37℃), b) DPH in PBS (pH 6.8, 37℃), c) RDH in SGF and d) RDH in PBS.

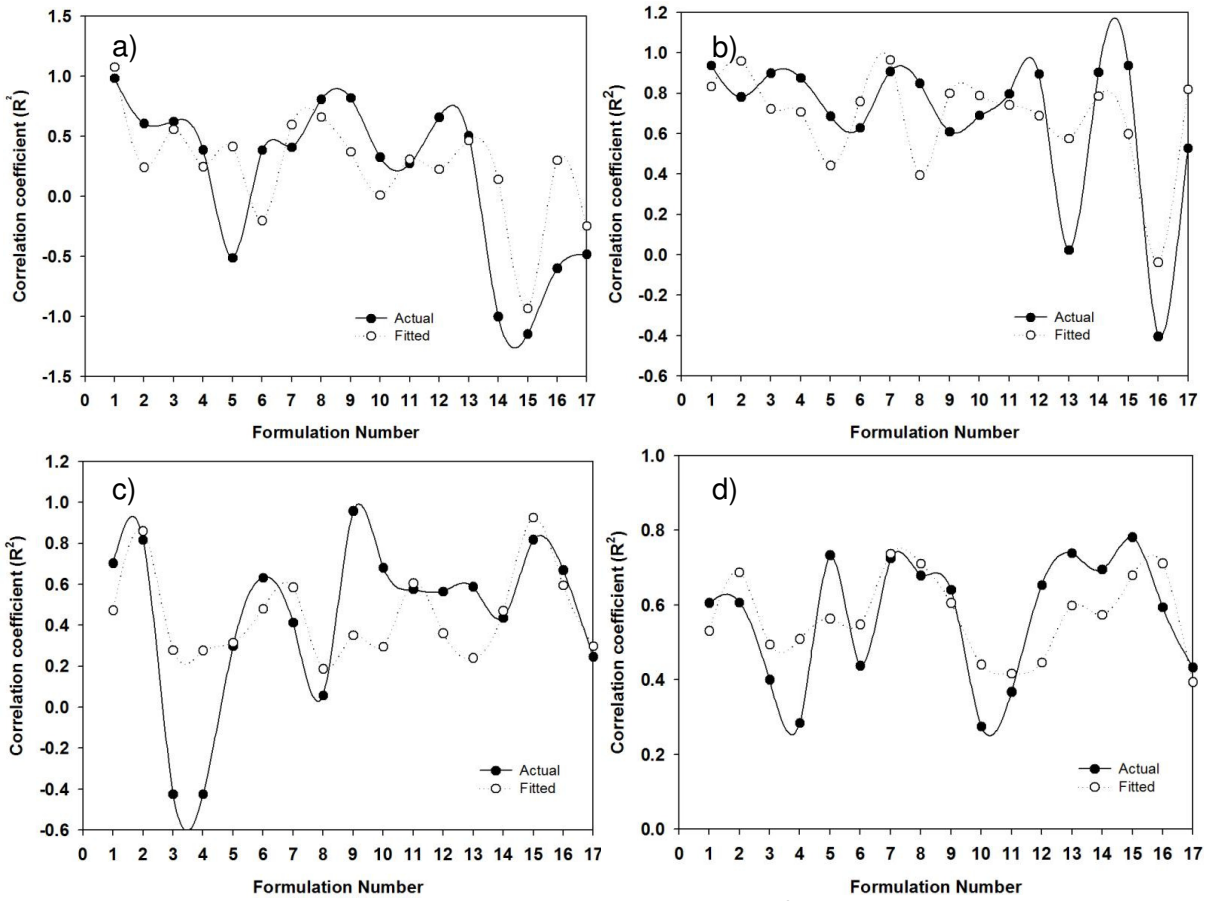

Figure 4.13: Regression plots for correlation coefficients (R^2 values) for a) DPH in SGF (pH 1.2, 37℃) b) DPH in PBS (pH 6.8, 37℃), c) RDH in SGF (pH 1.2, 37℃) and d) RDH in PBS (pH 6.8, 37℃).

The plots for experimental versus fitted R^2 values for DPH in SGF (pH 1.2, 37℃) and PBS (pH 6.8, 37℃) are displayed in Figures 4.13a and b. Correlation coefficients of 0.719 and 0.670 were demonstrated for SGF (pH 1.2, 37℃) and PBS (pH 6.8, 37℃) respectively. Figures 4.13c and d illustrate the experimental versus fitted plots for R^2 values of RDH in SGF (pH 1.2, 37℃) and PBS (pH 6.8, 37℃) with correlation coefficients of 0.532 and 0.597 being obtained for SGF (pH 1.2, 37℃) and PBS (pH 6.8, 37℃) respectively.

4.3.7. Evaluation of residual plots for optimization and subsequent response optimization of the TLT matrices

Residuals plots may be employed to analyze the fit of regression models in a Box-Behnken design. These plots can be defined as measuring the variation between the actual observed responses and the predicted responses. Figures 4.14, 4.15, 4.16, 4.17, 4.18, 4.19, 4.20 and 4.21 display the residual plots for the analysis of the Box-Behnken Experimental Design.

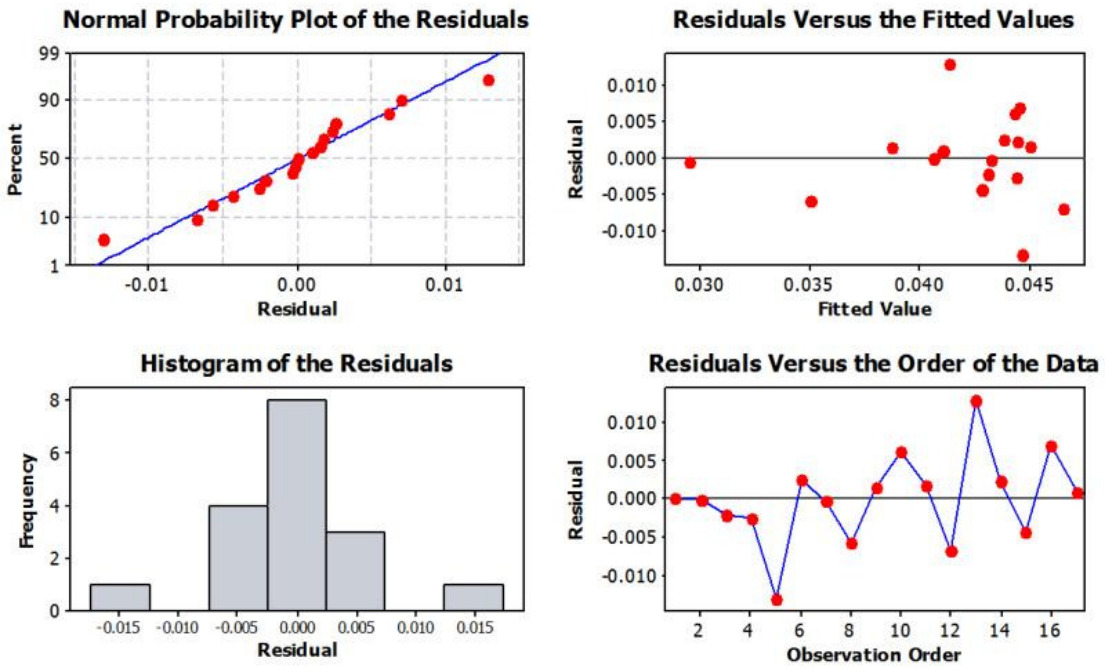

Figure 4.14: Diagnostic plots showing residual plots for rate constant (*k*) of DPH in PBS (pH 6.8, 37℃).

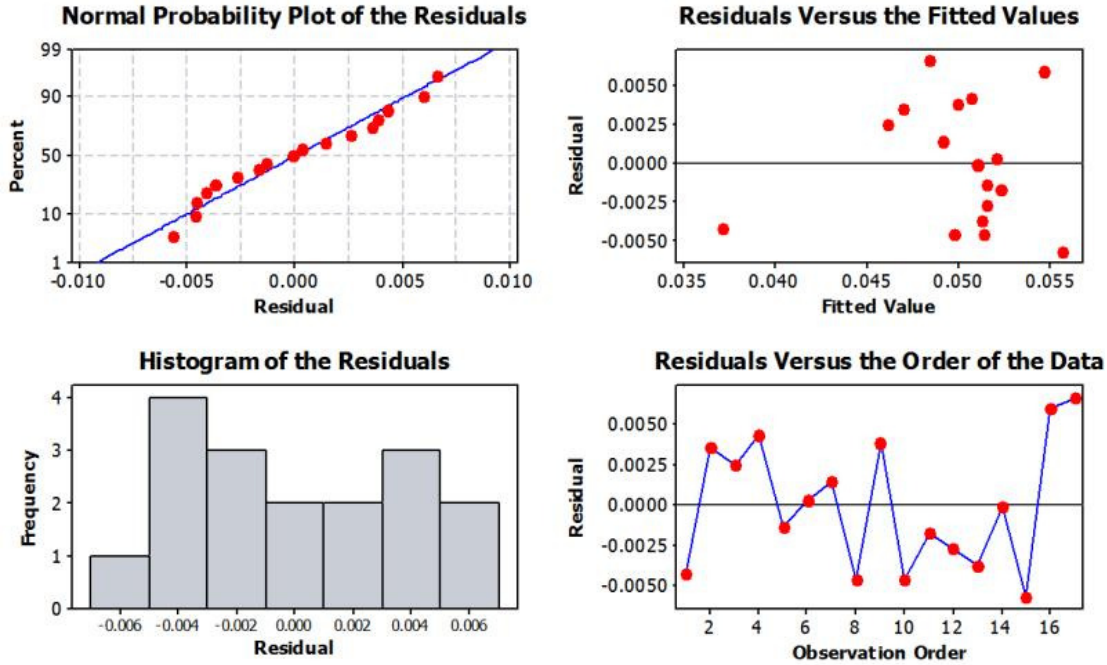

Figure 4.15: Diagnostic plots indicating the residual plots for rate constant (*k*) of RDH in PBS (pH 6.8, 37℃).

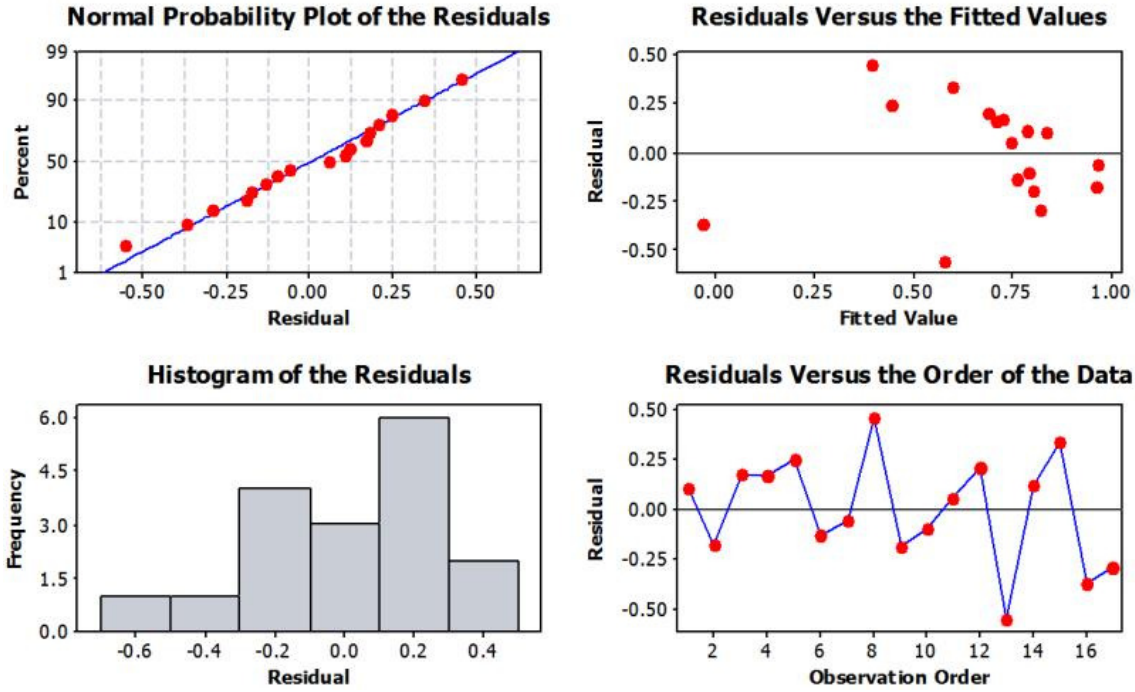

Figure 4.16: Diagnostic plots indicating the residual plots for correlation coefficients (R^2 values) for DPH in PBS (pH 6.8, 37℃).

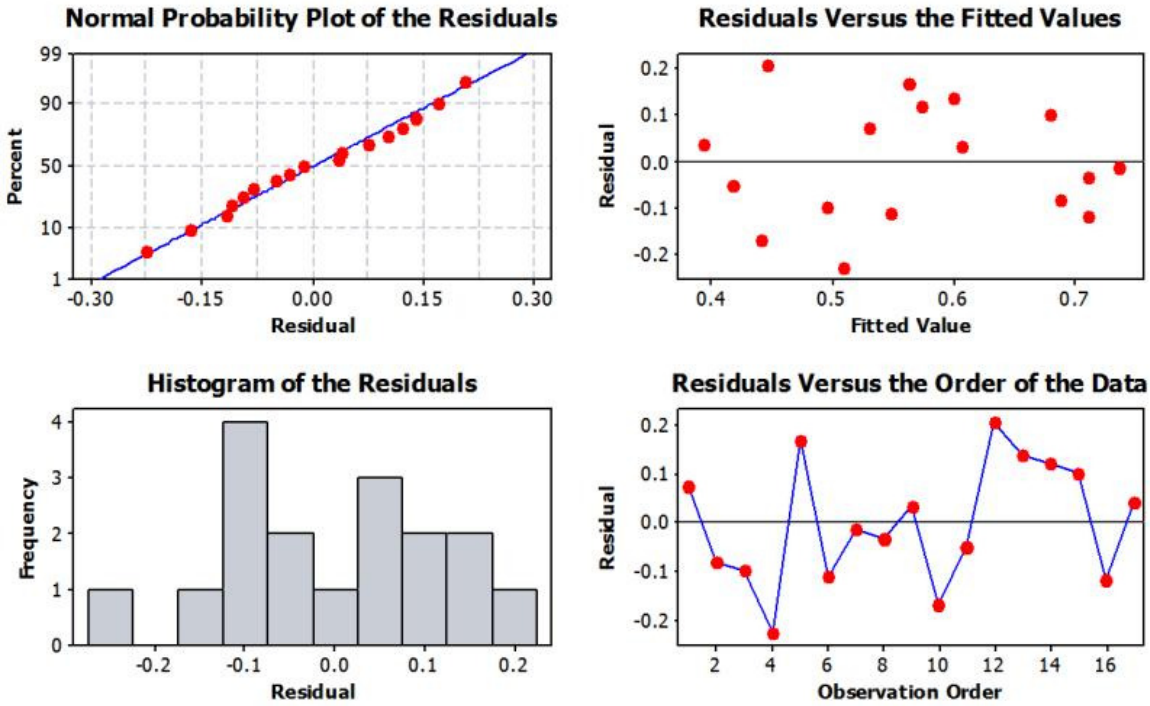

Figure 4.17: Diagnostic plots indicating the residual plots for correlation coefficients (R^2 values) for RDH in PBS (pH 6.8, 37℃).

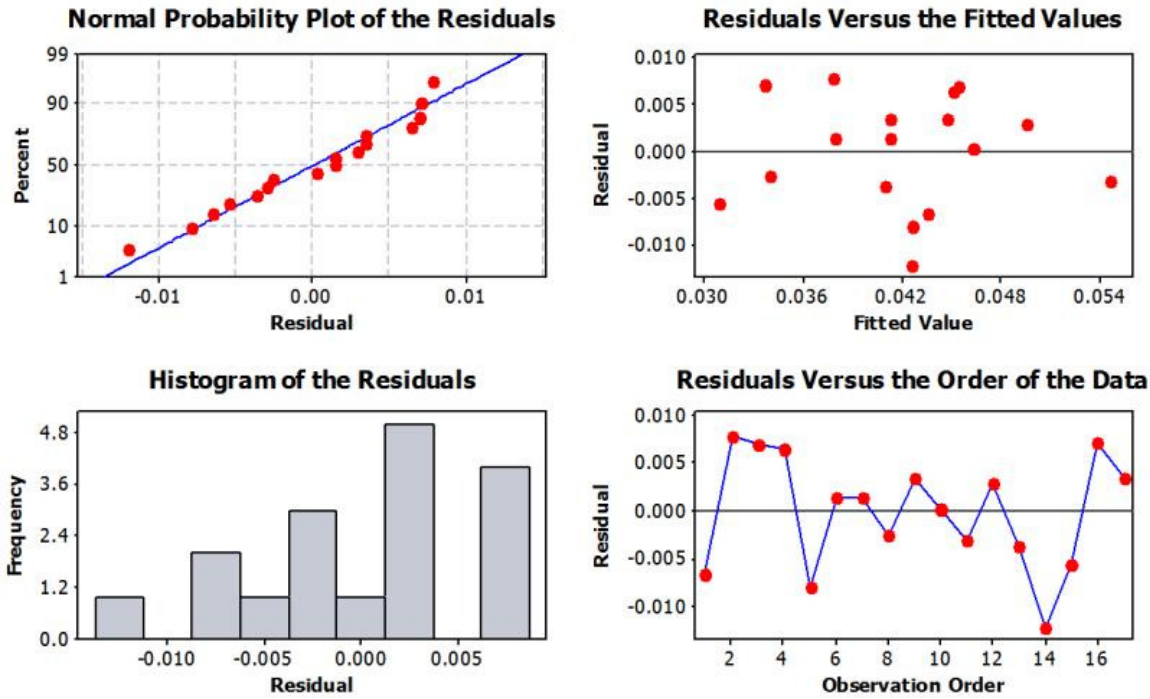

Figure 4.18: Diagnostic plots indicating the residual plots for rate constants (*k*) for DPH in SGF (pH 1.2, 37℃).

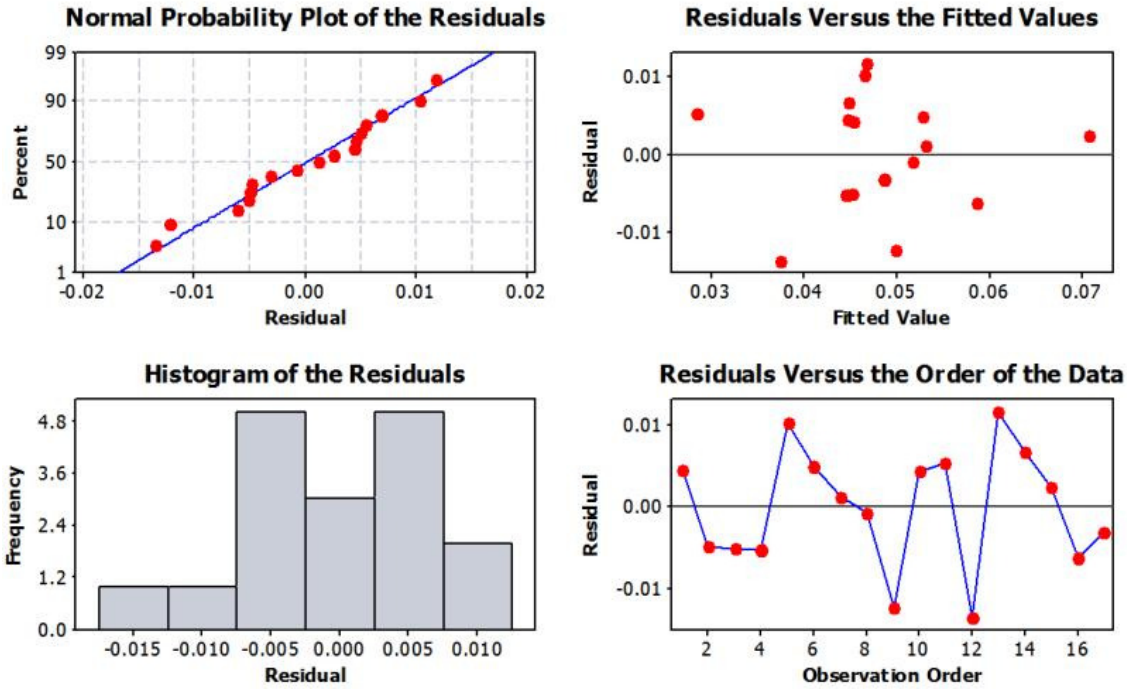

Figure 4.19: Diagnostic plots indicating the residual plots for rate constants (*k*) for RDH in SGF (pH 1.2, 37℃).

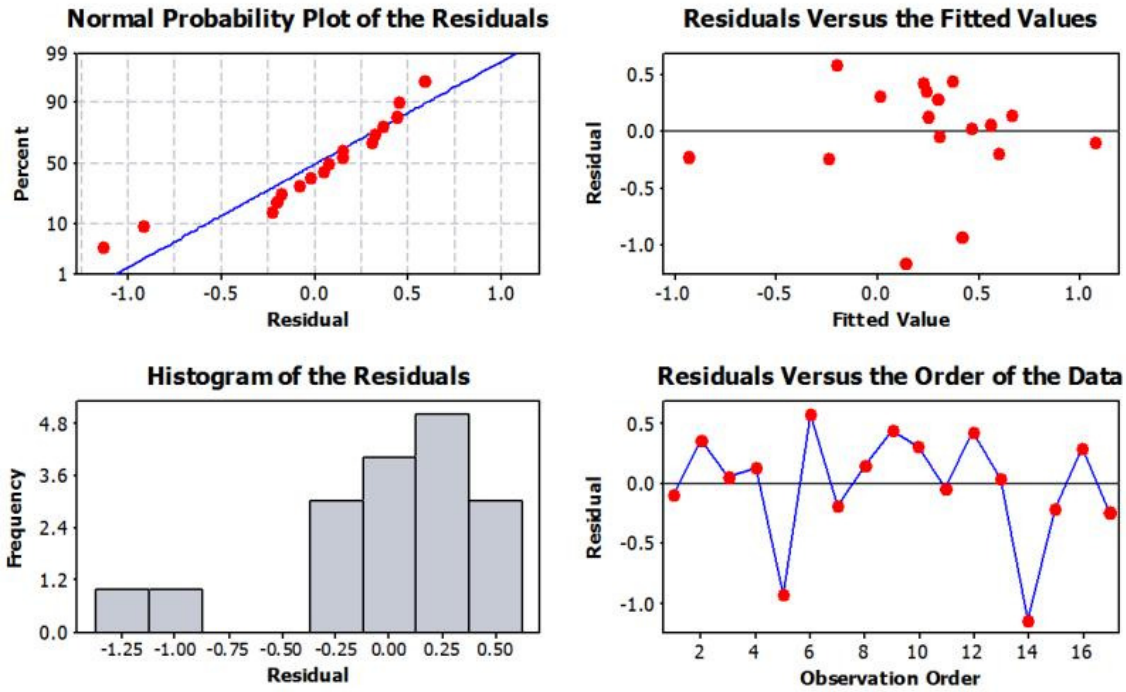

Figure 4.20: Diagnostic plots indicating the residual plots for correlation coefficients (R^2 values) for DPH in SGF (pH 1.2, 37℃).

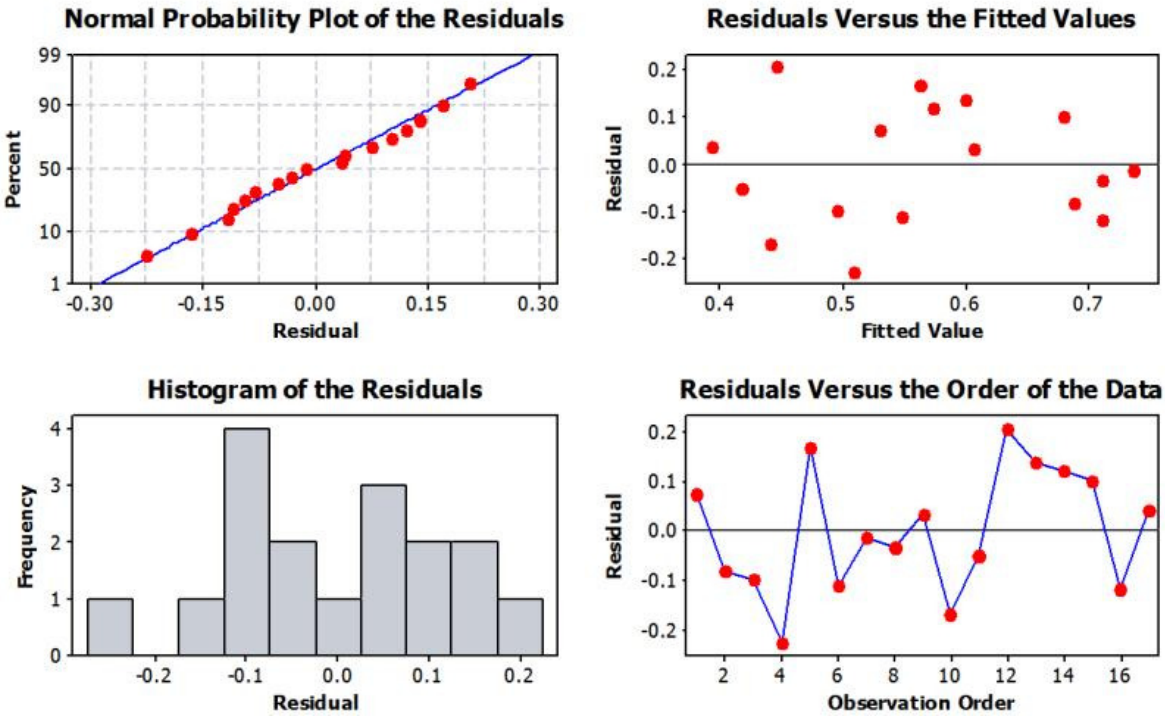

Figure 4.21: Diagnostic plots indicating the residual plots for correlation coefficients (R^2 values) for RDH in SGF (pH 1.2, 37℃).

On analysis of *k* (Figures 4.14, 4.15, 4.16 and 4.17) and R^2 values (Figures 4.18, 4.19, 4.20 and 4.21) for drug release from the two outer layers, it was found that there was an indiscriminate distribution of data. The scatter of data observed in the residual versus fitted value plots showed a random arrangement of data indicating that the fit of the data to the linear regression model was of a satisfactory nature. The residual histograms exhibited

nearly bell-shaped curves with the exception of a few. The presence of a bell-shaped curve indicates a relatively normal distribution of data. If this shape is not observed, it is indicative of an aspect of the data that is not accounted for in the model which needs to be identified for a better outcome. The residual versus observation order plots showed indiscriminate fluctuations in relation to the centre line which suggests that the error terms did not correlate amongst one another. The regression equations generated for the two responses for each layer in both PBS (pH 6.8, 37°C) and SGF (pH 1.2, 37°C) are demonstrated below for *k* value (DPH, PBS (pH 6.8, 37°C), Equation 4.2), *k* value (DPH, SGF (pH 1.2, 37°C), Equation 4.4), *k* value (RDH, PBS (pH 6.8, 37°C), Equation 4.3), *k* value (RDH, SGF (pH 1.2, 37°C), Equation 4.5), R^2 value (DPH, PBS (pH 6.8, 37°C), Equation 4.6), R^2 value (DPH, SGF (pH 1.2, 37°C), Equation 4.8), R^2 value (RDH, PBS (pH 6.8, 37°C), Equation 4.7) and R^2 value (RDH, SGF, Equation 4.9).

$$k = 0.0046[\text{s}-\text{PLGA}] - 0.0867[\text{PEO}] - 0.1035[\text{PA6,10}] + 0.2258[\text{SS}] + 0.1059[\text{s}-\text{PLGA}][\text{PEO}] - 0.3455[\text{s}-\text{PLGA}][\text{PA6,10}] - 0.2778[\text{s}-\text{PLGA}][\text{SS}] + 0.4398[\text{PEO}][\text{PA6,10}]$$

Equation 4.2

$$k = 0.1359[\text{s}-\text{PLGA}] + 0.0217[\text{PEO}] + 0.1236[\text{PA6,10}] + 0.0388[\text{SS}] + 0.1353[\text{s}-\text{PLGA}][\textit{PEO}] - 0.4343[\text{s}-\text{PLGA}][\text{PA6,10}] - 0.0024[\text{s}-\text{PLGA}][\text{SS}] - 0.0893[\text{PEO}][\text{PA6,10}]$$

Equation 4.3

$$k = -0.1364[\text{s}-\text{PLGA}] - 0.0762[\text{PEO}] - 0.1756[\text{PA6,10}] + 0.1327[\text{SS}] + 0.0526[\text{s}-\text{PLGA}][\textit{PEO}] + 0.7697[\text{s}-\text{PLGA}][\text{PA6,10}] + 0.3387[\text{s}-\text{PLGA}][\text{SS}] + 0.6487[\text{PEO}][\text{PA6,10}]$$

Equation 4.4

$$k = -0.311[\text{s}-\text{PLGA}] + 0.125[\text{PEO}] + 0.397[\text{PA6,10}] - 0.058[\text{SS}] + 0.058[\text{s}-\text{PLGA}][\textit{PEO}] - 1.216[\text{s}-\text{PLGA}][\text{PA6,10}] - 0.557[\text{s}-\text{PLGA}][\text{SS}] - 0.819[\text{PEO}][\text{PA6,10}]$$

Equation 4.5

$$R^2 = -6.927[\text{s}-\text{PLGA}] - 0.946[\text{PEO}] - 5.990[\text{PA6,10}] + 3.318[\text{SS}] - 5.280[\text{s}-\text{PLGA}][\textit{PEO}] + 29.922[\text{s}-\text{PLGA}][\text{PA6,10}] + 9.808[\text{s}-\text{PLGA}][\text{SS}] + 18.470[\text{PEO}][\text{PA6,10}]$$

Equation 4.6

$$R^2 = 3.448[s-PLGA] + 1.912[PEO] + 2.306[PA6,10] - 0.407[SS] - 2.637[s-PLGA][PEO] - 8.973[s-PLGA][PA6,10] - 5.318[s-PLGA][SS] - 4.930[PEO][PA6,10]$$

Equation 4.7

$$R^2 = -6.464[s-PLGA] + 2.186[PEO] - 9.553[PA6,10] - 2.220[SS] - 9.760[s-PLGA][PEO] + 39.610[s-PLGA][PA6,10] + 13.023[s-PLGA][SS] + 18.469[PEO][PA6,10]$$

Equation 4.8

$$R^2 = 7.66[s-PLGA] + 0.02[PEO] + 0.66[PA6,10] + 3.69[SS] - 11.12[s-PLGA][PEO] - 13.67[s-PLGA][PA6,10] - 18.30[s-PLGA][SS] + 1.83[PEO][PA6,10]$$

Equation 4.9

4.3.8. Response Optimization

Optimization was executed using Minitab®, V15 (Minitab® Inc, Pennsylvania, USA). The TLT was optimized in accordance with the dependent variables (measured responses) of k values and R^2 values. The values of the measured responses were targeted within the limits according to those of the ideal formulation outlined previously. Figures 4.22 and 4.23 exhibit the ultimate optimization plots for rate constants in SGF (pH 1.2, 37℃) and PBS (pH 6.8, 37℃) displaying a composite desirability of 88.23%.

Table 4.7: Targeted response values for TLT optimization in both SGF (pH 1.2, 37℃) and PBS (pH 6.8, 37℃).

Response	Lower	Target	Upper
k value	0.0350	0.0417	0.0500
R^2 value	0.7000	1.0000	1.0000

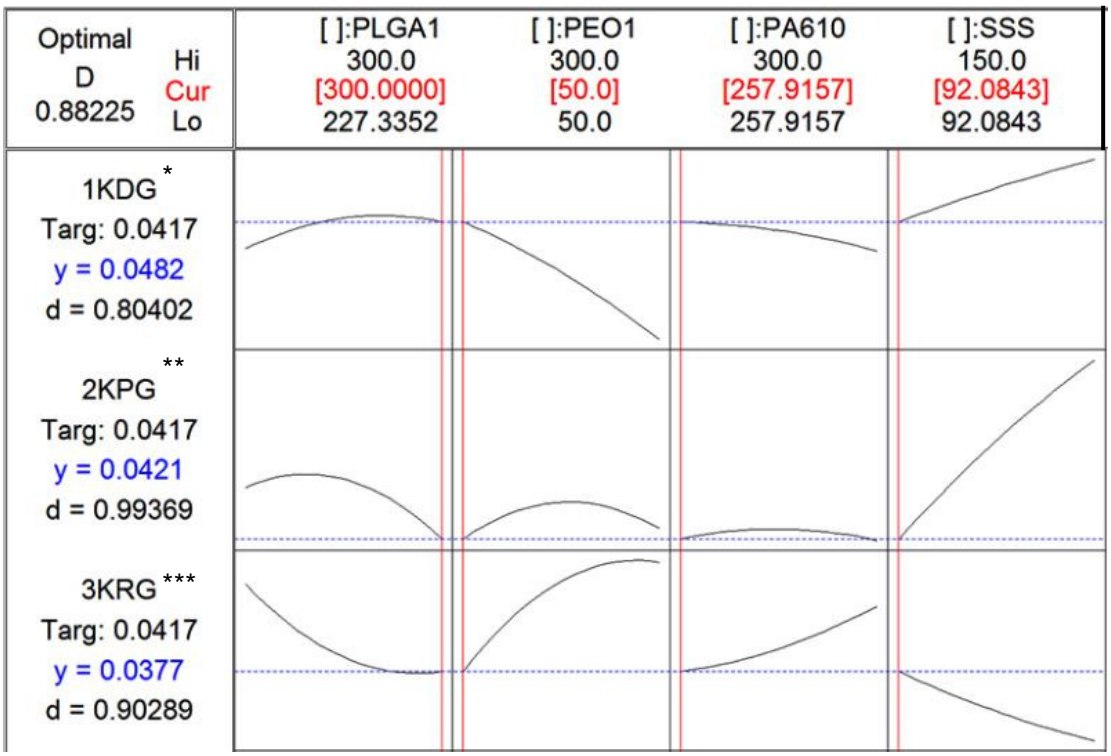

Figure 4.22: Optimization plots for rate constants in SGF (pH 1.2, 37℃), *1KDG refers to the rate constant for DPH in SGF (pH 1.2, 37℃), **2KPG refers to the rate constant for PMZ in SGF (pH 1.2, 37℃) and ***3KRG refers to the rate constant for RDH in SGF (pH 1.2, 37℃) .

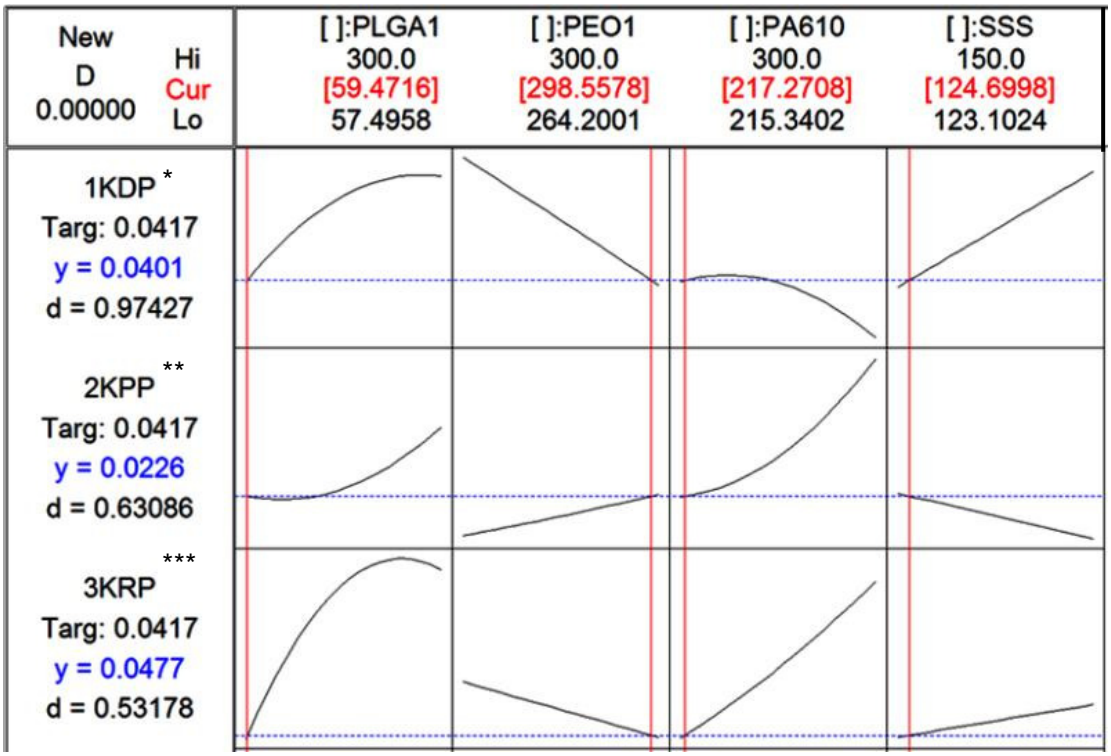

Figure 4.23: Optimization plots for rate constants in PBS (pH 6.8, 37℃), *1KDP refers to the rate constant for DPH in PBS, **2KPP refers to the rate constant for PMZ in PBS and ***3KRP refers to the rate constant for RDH in PBS.

4.3.9. *In vitro* assessment of the optimized TLT formulation

The two established optimized formulations which were 217.27mg PA6,10: 124.70mg SS and 59.47mg s-PLGA: 298.56g PEO in PBS (pH 6.8, 37℃)) and 257.92mg PA6,10: 92.98mg SS and 50mg s-PLGA: 300mg PEO in SGF (pH 1.2, 37℃) were subjected to the same *in vitro* dissolution conditions as those from the experimental design. Each optimized formulation was tested in both SGF (pH 1.2, 37℃) and PBS (pH 6.8, 37℃) once again for a comprehensive analysis.

After further analysis it was discovered that a combination of the two optimized formulations provided superior linear release in both SGF (pH 1.2, 37℃) and PBS (pH 6.8, 37℃) which was more desirable since having one formulation that is capable of providing linear release in both gastrointestinal environments would fundamentally be more feasible and simple.

The optimal formulation was found to be 257.92mg PA6,10: 92.08mg SS and 59.47g s-PLGA: 298.56mg PEO with the middle layer having a constant quantity of 350mg PEO. This was further confirmed by subjecting the formulation to dissolution in a USP 32 Apparatus 3 (Bio-Dis II Release Rate Tester, Vankel Industries). This allowed for automatic changes in pH environments essentially simulating the potential gastrointestinal transit of the TLT. Figures 4.24a, b and c demonstrate the drug release profiles achieved from the optimized formulation. Table 4.8 exhibits the experimental versus predicted responses computed for the optimized TLT formulation.

Table 4.8: The predicted versus experimental values of the measured responses after optimization.

Response	Predicted value	Experimental value	Desirability
k value DPH (SGF)	0.0482	0.0422 ± 0.005	80.40%
k value DPH (PBS)	0.0401	0.0454 ± 0.012	97.42%
R^2 value DPH (SGF)	0.7527	0.8309 ± 0.017	88.76%
R^2 value DPH (PBS)	0.9310	0.8354 ± 0.024	89.73%
k value RDH (SGF)	0.0377	0.0481 ± 0.020	90.29%
k value RDH (PBS)	0.0477	0.0601 ± 0.008	53.18%
R^2 value RDH (SGF)	0.5297	0.7407 ± 0.035	78.62%
R^2 value RDH (PBS)	0.6862	0.4046 ± 0.023	58.96%

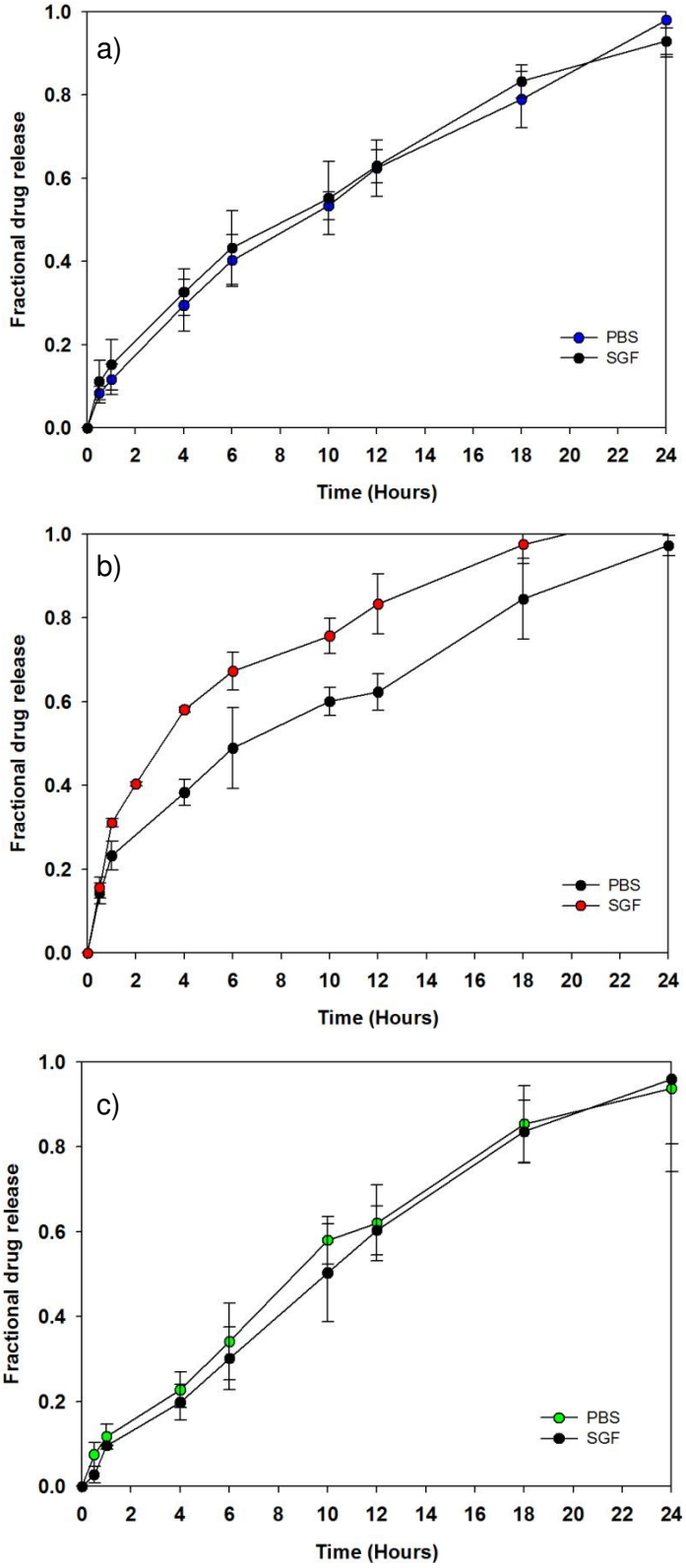

Figure 4.14: Drug release profiles of a) DPH; b) RDH and c) PMZ from the optimized TLT formulation (N=3).

4.4. Concluding Remarks

TLT matrices were prepared and optimized according to a Box-Behnken Experimental Design. The influence that the independent variables had on the measured responses was

analyzed, resulting in the statistical establishment of an optimized formulation. The optimized formulation displayed a satisfactory near linear release of the model drugs. The chosen experimental design proved to be satisfactory yet not optimal for the complex facets of the said TLT. Further research should focus on establishing a more fitting and comprehensive statistical analysis for the intricate nature of the TLT.

CHAPTER 5

CHARACTERIZATION AND FURTHER INTROSPECTIVE EVALUATION OF THE OPTIMIZED TRIPLE-LAYERED TABLET FORMULATION

5.1. Introduction

The physicomechanical properties of a drug delivery system may have a significant effect on drug release behavior. Therefore, it is necessary to assess the physicomechanical characteristics, and the effects of such characteristics on physicochemical and drug release performance (Tiwari and Rajabi-Siahboomi, 2008). By assessing the overall structural characteristics of a formulation, it is possible to gauge the effects of said characteristics on drug release potential and stability of the formulation.

The stability of the TLT upon storage and under *in vivo* conditions is extremely significant as it determines whether the TLT is a feasible system to develop. The presence of pores within the TLT structure may vastly affect the drug release potential and is therefore another important analysis that needs to be performed. The physical behavior of the drug delivery system in the gastrointestinal environment is also a factor that needs to be determined as it may affect the patient tolerability of the system. When developing such a drug delivery system, it is necessary to gauge the versatility of drug release capabilities. It would be ideal, in this instance, that the drug delivery system be capable of acting as a matrix to a variety of drugs with various structures.

Subsequent to the design and optimization of the TLT, the matters summarized in this Chapter were further characteristic studies performed to ascertain the flexibility and overall behavior of the optimized TLT formulation. To begin with, the most logical approach was established to be the determination of superiority in drug release of the TLT to the conventional (commercial) drug products in an *in vitro* setting. This comparison was performed along with various other investigations, namely, Brinell Hardness Number evaluation, Scanning Electron Microscopy (SEM) imaging, porosity analysis and Magnetic Resonance Imaging (MRI). Another fundamental investigation that was conducted was the application of a therapeutic drug treatment regimen to the optimized TLT formulation.

5.2. Materials and Methods

5.2.1. Materials

Atenolol (ATN) and acetylsalicylic acid (ASA) were purchased from Sigma Chemical Company (St Louis, MO, USA). Simvastatin (SMV) was received as a gift sample from Adcock-Ingram (Johannesburg, South Africa). SLEEPEZE-PM®, Ranihexal® and Phenergan® were purchased from Parklane Hospital Pharmacy (Johannesburg, South Africa). All other reagents used were of analytical grade.

5.2.2.1. Brinell Hardness Number evaluation of the optimized TLT formulation

Matrix hardness evaluation of the optimized TLT formulation was performed as a function of Brinell Hardness Number (BHN) as per the parameters described in Chapter 3, section 3.2.2.10. This was determined to assess the robustness of the TLT.

5.2.2.2. Morphological surface structure imaging of the optimized TLT formulation employing Scanning Electron Microscopy

Scanning Electron Microscopy (SEM) was carried out using a Phenom scanning electron microscope (FEI Company, Hillsboro, Oregon, USA) was employed to produce imaging of the PA 6,10 layer surface for a holistic characterization and investigation for the presence of pores.

5.2.2.3. Porosity analysis of the PA6,10 layer of the optimized TLT formulation

Porosity analysis was conducted as a supplementary investigation to determine the presence of pores and pore size within the PA6,10 layer of the optimized TLT formulation. The rationale for this analysis is the untoward unhomogenous pores that might develop after compression (Wu *et al*., 2005). Surface area and porosity studies were conducted using a micromeritics ASAP analyzer (Micromeritics ASAP 2020, GA, USA). The procedure involved the degassing of samples prior to analysis. Degassing functions as a preparation stage to condition the sample to the appropriate state for analysis. A dissected section of the PA6,10 layer was placed in the sample tube for analysis.

5.2.2.4. In vitro dissolution testing on SLEEPEZE-PM®, Ranihexal®and Phenergan®

In order to authenticate the results achieved by the optimized TLT formulation, it was necessary to draw a comparison in drug release behaviour between the TLT and the

conventional tablets available. The tablets selected were SLEEPEZE-PM® containing diphenhydramine (DPH), Ranihexal® containing ranitidine (RDH) and Phenergan® containing promethazine (PMZ). *In vitro* drug release studies were performed on the tablets using a USP 25 rotating paddle method in a dissolution apparatus (Caleva Dissolution Apparatus, model 7ST; G.B. Caleva Ltd., Dorset, UK) at 50rpm with 900mL simulated gastric fluid (SGF) (pH 1.2, 37℃) and 900mL phosphate-buffer solution (PBS) (pH 6.8; 37℃). A stainless steel mesh was used in the dissolution vessels in order to prevent the formulations from floating. Samples of 5 mL were drawn at pre-determined time intervals over a 24 hour period.

5.2.2.5. Application of a therapeutic drug regimen to the optimized TLT formulation

Three cardiovascular related drugs were selected for evaluating the flexibility of the optimized TLT formulation. Atenolol (ATN) which is a beta-blocker used to treat hypertension was selected for incorporation into the PA6,10 outer layer; aspirin (ASA) which is used as an anticoagulant in heart disease was selected for incorporation into the middle PEO layer and simvastatin (SMV) which is an antihyperlipidaemic drug was selected for incorporation into the s-PLGA outer layer. These drugs were chosen due to the high frequency with which they are used in conjunction with each other in cardiovascular related treatment regimens. Therefore a dosage form in which they all may be administered in a single dose would essentially be very beneficial in terms of patient compliance.

Table 5.1 indicates the therapeutic quantities incorporated in to the TLT formulation. *In vitro* drug release studies were performed as described in Chapter 5, section 5.2.2.4. Ultraviolet (UV) spectrophotometry was employed to analyze the dissolution samples.

Table 5.1: Quantities of drug actives incorporated in to TLT for the evaluation of drug release of therapeutic regimen.

Drug	Layer 1 (PA6,10)	Middle layer (PEO)	Layer 3 (s-PLGA)
ATN	50mg	-	-
ASA	-	100mg	-
SMV	-	-	40mg

5.2.2.6. Comparative in vitro dissolution analysis between the conventional therapeutic regimen formulations and the release of therapeutic regimen drugs from the optimized TLT formulation

In order to confirm the superior release of ATN, SMV and ASA from the optimized TLT formulation, conventional drug products Tenormin® 50; DISPRIN CV®100 and Adco-Simvastatin 40 were subjected to the equivalent *in vitro* dissolution studies as the optimized TLT formulation mentioned in Chapter 3, section 3.2.2.7. Calibration curves were constructed by preparing a stock solution which was serially diluted to prepare five standard solutions

employing grade A volumetric flasks. Linear curves were plotted as absorbance versus concentration (mg/mL).

5.2.2.7. Benchtop Magnetic Resonance Imaging (MRI) of TLT performance

A magnetic resonance system with digital MARAN-i System configured with a DRX2 HF Spectrometer console (Oxford Instruments Magnetic Resonance, Oxon, UK) equipped with a compact 0.5 Tesla permanent magnet stabilized at 37^{o}C and a dissolution flow through cell was employed for the viewing of the mechanical behaviors of the matrices. . The image acquisition parameters are depicted in Table 5.2.

Table 5.2: Image acquisition parameters applied during magnetic resonance imaging using MARAN-iP.

S. No.	Parameter	Value
1	Imaging protocol	FSHEF
2	Requested gain (%)	4.17
3	Signal strength	68.92
4	Average	2
5	Matrix size	128
6	Repetition time (ms)	1000.00
7	Spin Echo Tau (ms)	6.80
8	Image acquired after	60min
9	Total scans	64

After duly configuring, optimizing the shims and probe tuning, the cone-like lower part of the cell was filled with glass beads to provide laminar flow at 16mL/min of the solvents employed. The matrices were placed in position each time within the cell which in turn was positioned in a magnetic core of the system and magnetic resonance images were acquired every 30 minutes over 12 hours with MARAN-iP version 1.0 software. The image was acquired after setting the frequency offset and testing gain employing RINMR version 5.7 under continuous solvent flow conditions. MARAN-iP software comprises image acquisition software and image analysis software.

5.3. Results and Discussion

5.3.1. Assessment of BHN

The optimized TLT formulation was found to have a BHN of 13.63±0.009N/mm^2 which correlated well with the previous hardness patterns and drug release behavior. The mechanical strength of the TLT is significant in order to assess the stability of the TLT against fracture upon agitation. This also confirmed the robust nature of the TLT. Upon physical handling and observation of the TLT it was virtually impossible to crack the surface

of the compressed TLT structure which further supported the mechanical strength of the optimized TLT.

5.3.2. SEM images depicting the PA6,10 layer surface of the TLT

SEM images of the PA6,10 layer showed irregular surfaces with minimal pores. The lack of pores observed on a surface image was found to be desirable. This is due to the possibility that the presence of pores after compression may alter the release of drug from the layer. The irregular surface may be attributed to the crystalline nature of PA6,10 at room temperature (25℃) which may have resulted in uneven compression and irregular distribution of the layer. The presence of such irregularities did not appear to significantly affect the release of drug from the layer. The reason for the lack of interaction may be the unhindered and uniform erosion of the PA6,10 layer upon dissolution irrespective of irregular surface. Upon interaction of the dissolution medium, the relaxation of PA6,10 in the layer may cancel out the irregular surfaces thereby resulting in uniform erosion and drug release. Figures 5.1a and b are SEM images obtained on analysis of the surface of the PA6,10 layer.

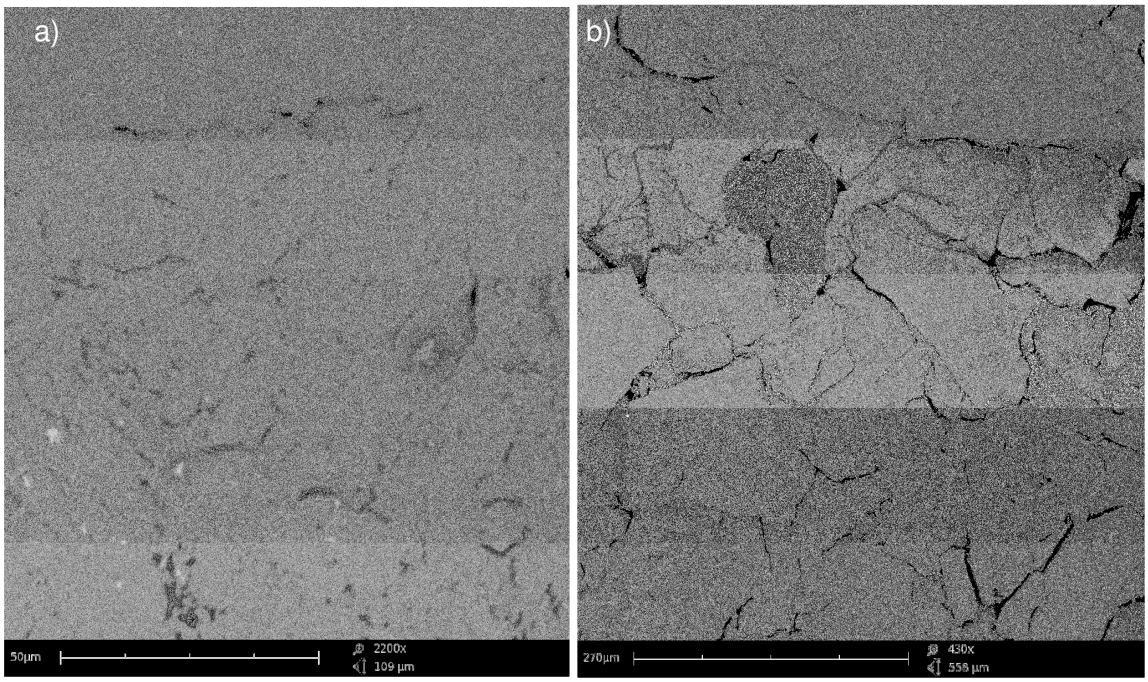

Figure 5.1: Typical SEM images of a) the PA6,10 layer of the TLT at a lower magnification depicting irregular surfaces and b) the PA6,10 layer of the TLT at a greater magnification.

5.3.3. Porosity analysis

Porosity analysis was conducted in order to determine the volume of distribution of pores if pores were found to be present in the optimized TLT. Pore size was also investigated. Table 5.3 shows the resultant values subsequent to analysis using the Barret, Joyner and Halenda Method (BJH).

Table 5.3: Assessment of pore volume and pore size of the TLT.

Parameter	Value
Pore Size	
Adsorption average pore width	99.7681Å
BJH adsorption average pore diameter	163.958Å
BJH desorption average pore diameter	141.604Å
Pore Volume	
BJH Adsorption cumulative volume of pores between 17.000Å and 3000.000Å diameter	0.013191cm^3/g
BJH Desorption cumulative volume of pores between 17.000Å and 3000.000Å diameter	0.013085cm^3/g

It was discovered that the pores contained in the TLT were chiefly mesoporic within the sizes of 99.7681Å and 163.958Å in diameter. No micropores were identified. The total pore volume ranged between 0.0065 and 0.0132cm^3/g indicating a decreased pore volume which was desirable. This is due to the variable influence on drug release behavior that may occur in the presence of large pores. Therefore the lack of large pores is advantageous so as to not hinder drug release behavior.

5.3.4. Comparative analysis of drug release behavior from conventional tablets SLEEPEZE-PM®, Ranihexal®and Phenergan® and optimized TLT formulation

In vitro dissolution results revealed that the optimized formulation profile depicted a significant superior release of DPH, PMZ and RDH as compared to the respective conventional tablets. The optimized TLT achieved extended controlled release of all three drugs over 24 hours while the disintegration times of SLEEPEZE-PM® tablets, Ranihexal® tablets and Phenergan® tablets were approximately 1 hour, 1 hour and 30 minutes respectively. Figures 5.2a, b and c illustrate the drug release profiles of the conventional tablets.

Furthermore, the erratic spiked concentrations due to an immediate burst release are also noted from the conventional products. This is exactly what the TLT aims to rectify wherever

applicable. By decreasing the initial rapid release of drug the TLT may thus decrease the potential of increased plasma drug levels that may lead to unwanted side-effects or toxicity.

The rate constant (*k)* values calculated from the release profiles of SLEEPEZE-PM® tablets, Ranihexal® tablets and Phenergan® tablets were 1.3824, 1.3693 and 1.4701 respectively. The correlation coefficients (R^2 values) generated from the release profiles were established to be 0.344, 0.366 and -0.340 respectively. The measured responses achieved by the conventional tablets further confirm the vast variance to controlled release patterns. This unmistakeable difference solidifies the controlled release capability of the TLT.

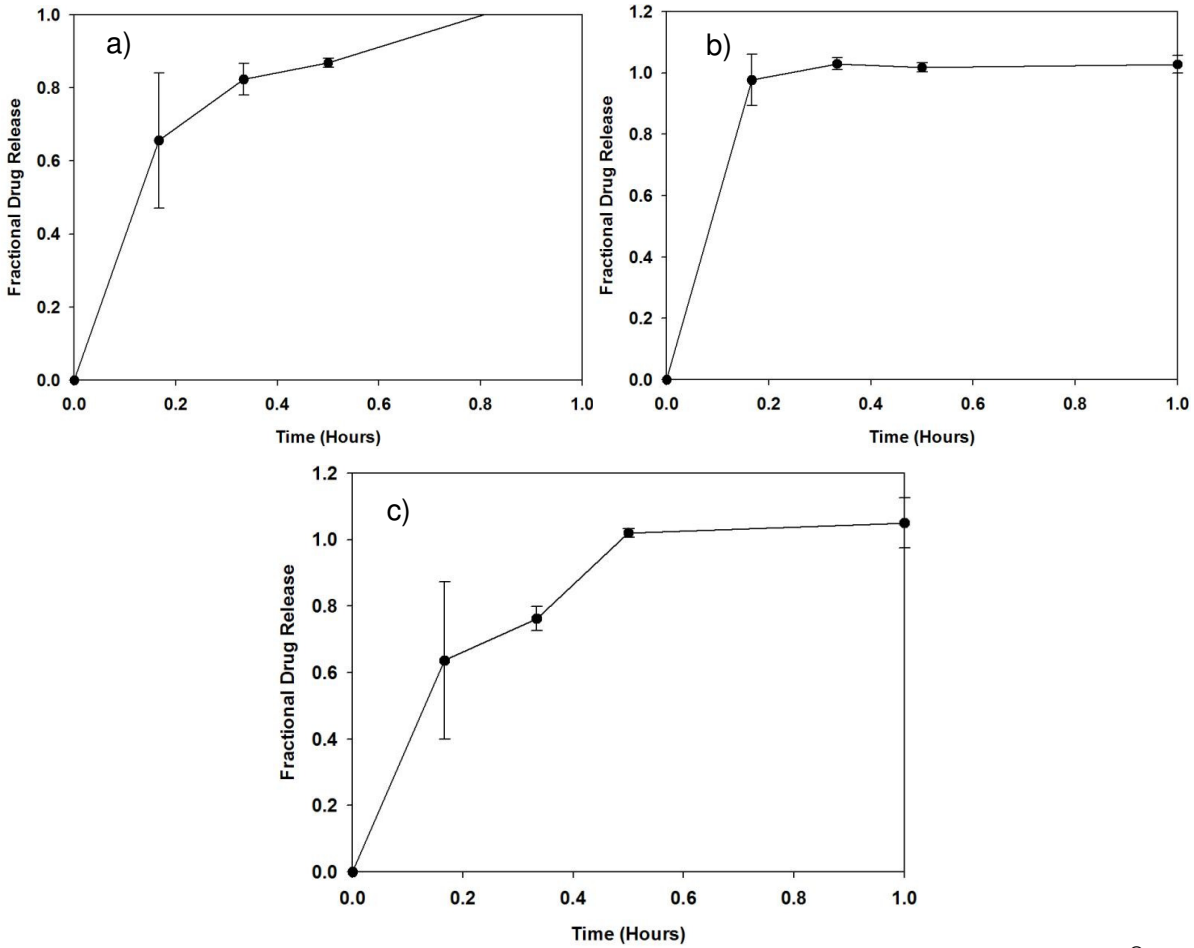

Figure 5.2: Drug release profiles from conventional tablets a) SLEEPEZE-PM®, b) Phenergan® and c) Ranihexal® in PBS (pH 6.8, 37℃).

5.3.5. Establishment of the efficacy of the TLT for the controlled delivery of a cardiovascular therapeutic drug regimen

5.3.5.1. Construction of calibration curves

Correlation coefficients (R^2 values) were calculated to be more than 0.96 for all plots. Figures 5.3, 5.4 and 5.5 display the calibration curves prepared for ATN, ASA and SMV respectively in SGF (pH 1.2, 37℃) and PBS (pH 6.8, 37℃).

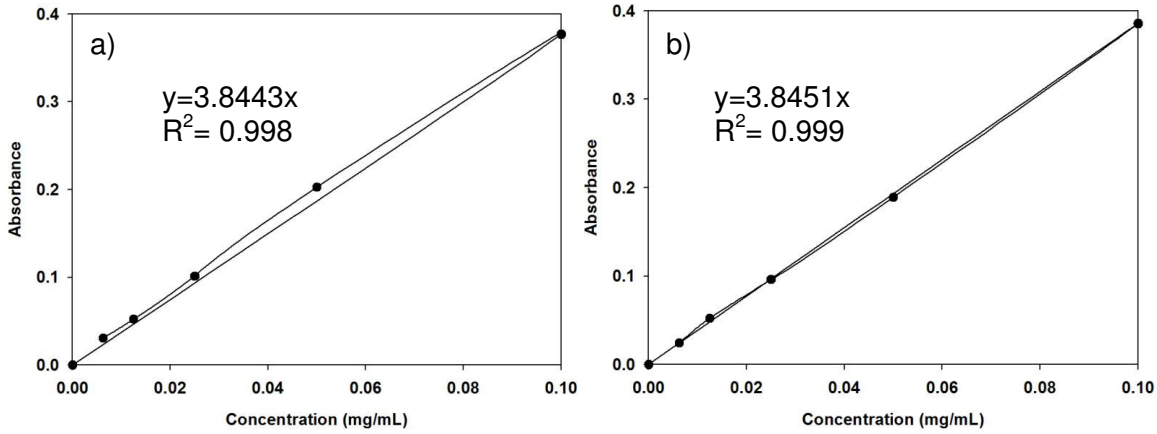

Figure 5.3: Calibration curve for ATN in a) PBS (pH 6.8, 37℃) and b) SGF (pH 1.2, 37℃).

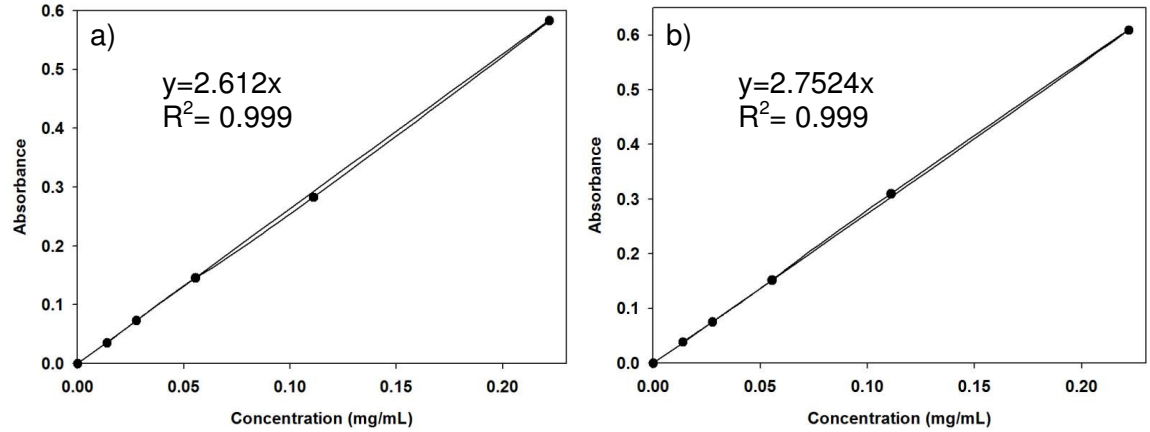

Figure 5.4: Calibration curves for ASA in a) PBS (pH 6.8, 37℃) and b) SGF (pH 1.2, 37℃).

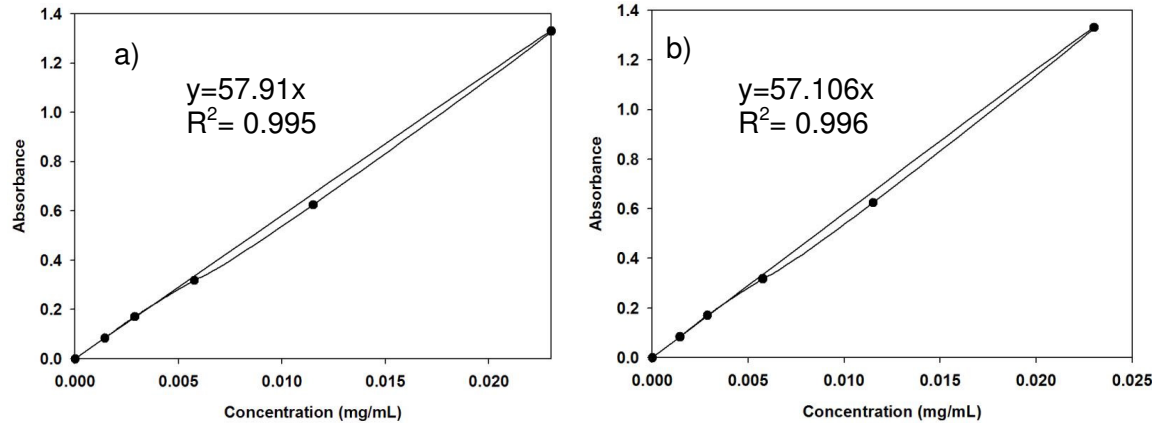

Figure 5.5: Calibration curves for SMV in a) PBS (pH 6.8, 37℃) and b) SGF (pH 1.2, 37℃).

5.3.5.2. Characterization of drug release behavior after the incorporation of ATN, ASA and SMV into the TLT

Drug release results obtained after dissolution studies showed desirable linear or near linear release profiles of all three drugs. Table 5.4 contains the respective *k* values and R^2 values obtained from the release of ATN, ASA and SMV from the optimized TLT formulation. Release of ATN from the TLT revealed that only half the loaded dose was released after 24 hours in PBS (pH 6.8, 37℃) (Figure 5.6) while the entire loaded dose was released in SGF (pH 1.2, 37℃). The *k* values obtained for the release of ATN were 0.0219 in PBS (pH 6.8, 37℃) and 0.0413 in SGF (pH 1.2, 37℃). The R^2 values computed were 0.8851 and 0.9983 IN PBS (pH 6.8, 37℃) and SGF respectively.

Table 5.4: Measured responses for the release of therapeutic regimen from optimized TLT formulation (in all cases N = 3).

Drug	*k* values (SGF) ± S.D.	*k* values (PBS) ± S.D.	R^2 values (SGF) ± S.D.	R^2 values (PBS) ± S.D.
ATN	0.0413 ± 0.0036	0.0219 ± 0.0025	0.9983 ± 0.0095	0.8851 ± 0.1074
ASA	0.0423 ± 0.0005	0.0416 ± 0.0000	0.9343 ± 0.0267	0.8966 ± 0.0233
SMV	0.0350 **±** 0.0009	0.0363 ± 0.0004	0.9487 ± 0.0059	0.9358 ± 0.0472

In terms of the release of ASA from middle PEO layer, a prolonged linear profile was obtained as displayed in Figure 5.7. Approximately 80% and 90% of the loaded dose was released after 24 hours in PBS (pH 6.8, 37℃) and SGF (pH 1.2, 37℃) respectively. The release of SMV from the s-PLGA outer layer displayed a similar linear extended release over 24 hours as illustrated in Figure 5.8. Near linear release profiles were noted in both SGF (pH 1.2, 37℃) and PBS (pH 6.8, 37℃). The fundamental presence of solid evidence of a controlled release pattern of the three drugs from the TLT authenticates potential of the TLT to provide linear or near linear release of a variety of drugs.

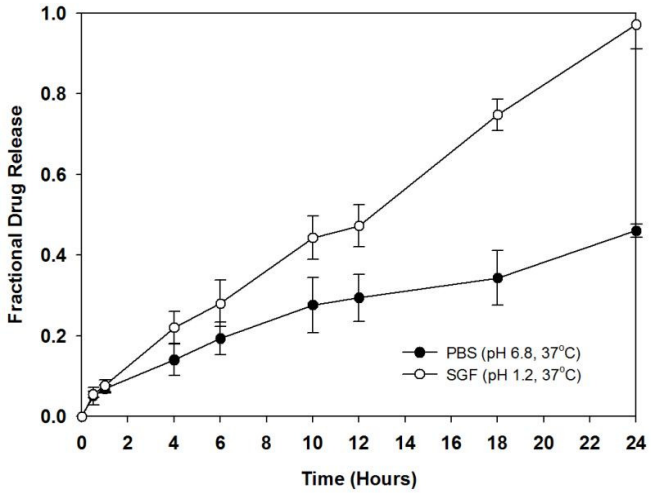

Figure 5.6: Drug release profile of ATN from optimized TLT formulation in SGF (pH 1.2, 37℃) and PBS (pH 6.8, 37℃).

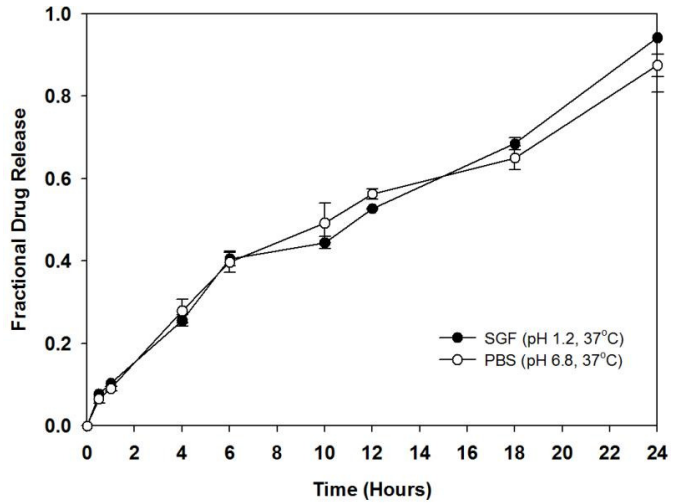

Figure 5.7: Drug release profile of ASA from optimized TLT formulation in SGF (pH 1.2, 37℃) and PBS (pH 6.8, 37℃).

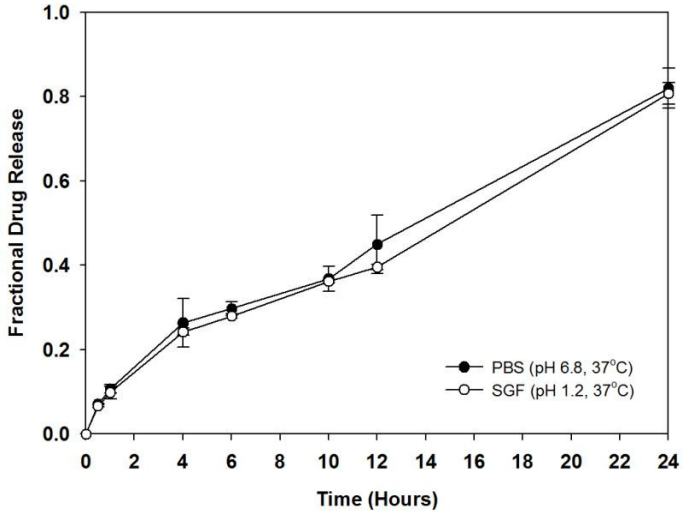

Figure 5.8: Drug release profile of SMV from optimized TLT formulation in SGF (pH 1.2, 37℃) and PBS (pH 6.8, 37℃).

5.3.6. Comparative *in vitro* dissolution analysis between the conventional therapeutic regimen tablets and the release of ATN, ASA and SMV from the optimized TLT formulation

Comparative results revealed that almost 100% of the drug was released in 0.5 to 1 hour for all three conventional tablets. Figures 5.9, 5.10 and 5.11 are drug release profiles of Tenormin® 50, DISPRIN CV®100 and Adco-Simvastatin 40 respectively. The rapid dissolution and burst release from the conventional tablets further supported the superiority of the TLT in terms of controlled and sustained release of the treatment regimen.

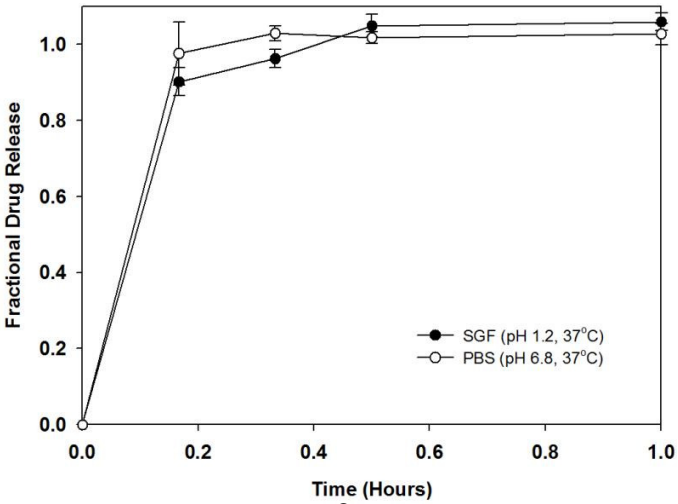

Figure 5.9: Drug release profiles of Tenormin® 50 in SGF (pH 1.2, 37℃) and PBS (pH 6.8, 37℃).

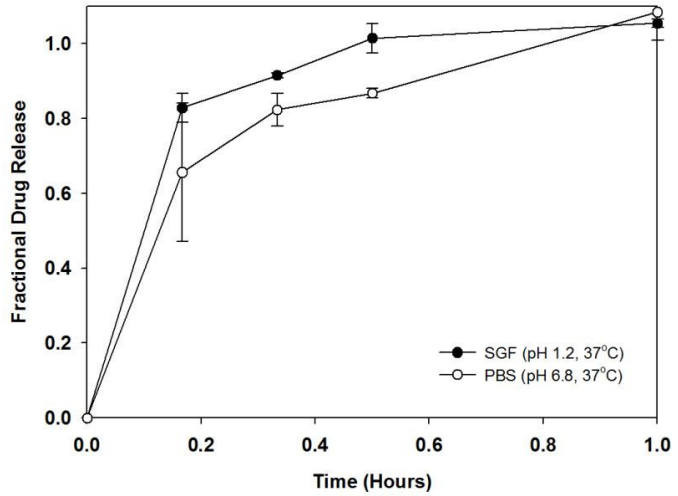

Figure 5.10: Drug release profiles of DISPRIN CV®100 in SGF (pH 1.2, 37℃) and PBS (pH 6.8, 37℃).

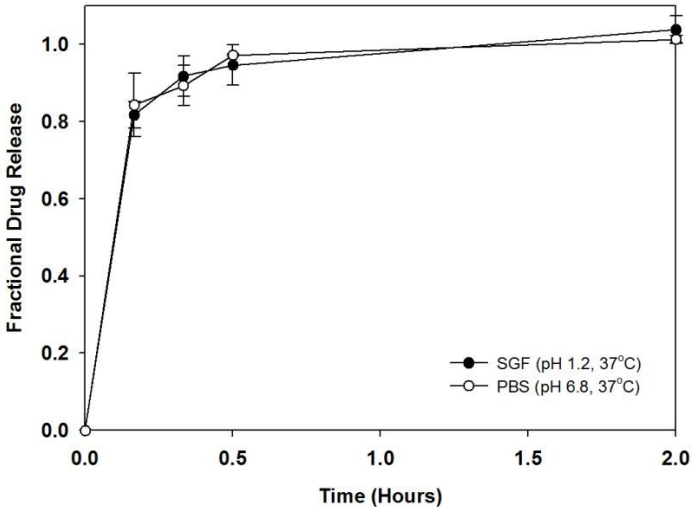

Figure 5.11: Drug release profiles of Adco-Simvastatin 40 in SGF (pH 1.2, 37℃) and PBS (pH 6.8, 37℃).

5.3.7. Benchtop Magnetic Resonance Imaging analysis of the optimized TLT formulation

The pattern that was displayed throughout the images at different time points was the ultimate disappearance of the middle PEO and lower s-PLGA cores due to the progressive swelling that occurs and the disappearance of the inner core (black area in images) due to erosion and decreasing intactness of the upper PA6,10 layer in the dissolution medium over 24 hours. A very clear succession is noticed (in Figure 5.12) with the increase in size of the lower two layers and the slight decrease in length and thickness of the upper layer. Figure 5.12 displays the images of the TLT at various time points during progressive dissolution study.

At 0.5 hours 6% of ATN was released, subsequently after an hour 8% of ATN was released. The data retrieved from MRI analysis shows a miniscule decrease in width and thickness of the outer layer between 0.5 and 1 hour. The change of size is associated with the disappearance of the core (black) of the PA6,10 layer. After 4 hours it was found that approximately 16% of ATN was released, this was associated with a marked variation in thickness of the PA6,10 layer. At 6 hours approximately 20% of ATN was released with a small change in thickness and width of the PA6,10 layer. At 10 hours, it was found that 26% of ATN was released with a noticeable decrease in thickness and width of the PA6,10 layer. After 12 hours, 30% was released with a further slight reduction of the PA6,10 layer. After 24 hours, it was found that almost 50% of ATN was released with a large decrease of substance of the PA6,10 layer.

At 0.5 hours 8% of ASA was released, which correlated with an increase in swelling and diameter of the middle PEO layer after 0.5 hours. After 1 hour, 10% of ASA was released noted with a further increase in diameter of the PEO layer. At 4 hours, almost 30% of ASA was released which was expected after a large increase in diameter swelling of the PEO layer. After 6 hours, 38% of ASA was released with a slight change of diameter from 4 hours. By 12 hours of dissolution time, almost 50% of ASA was released which was associated with a large increase in swelling and diameter of the PEO layer. At the end of 24 hours, 90% of ASA was released with a complete disappearance of the drug core and a large increase in diameter and swelling of the middle PEO layer. The release of SMV from the lower s-PLGA/PEO layer followed a similar trend to that if ASA, this was also noted with the same pattern of swelling and increase in diameter of the layer over 24 hours.

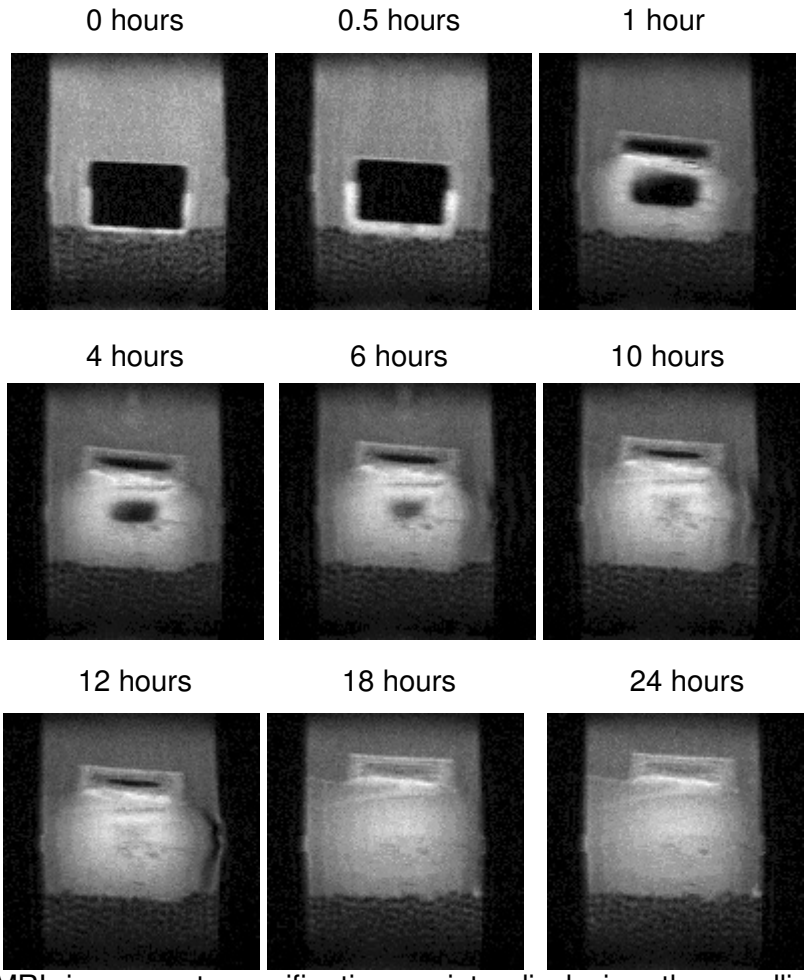

Figure 5.12: MRI images at specific time points displaying the swelling and erosion characteristics of the TLT during dissolution in PBS (pH 6.8, 37℃).

5.4. Concluding Remarks

The holistic analysis of the optimized TLT formulation generated data that confirms the robustness of the TLT. Porosity analysis cancelled out the presence of undesirable micropores after compression. Furthermore the TLT displayed excellent capability for controlling and prolonging drug release as compared to the conventional antihistamine tablets selected. The significant application of the cardiovascular treatment regimen to the TLT articulated the flexibility of the TLT to different drug actives as well as achieving a significantly desirable release of the selected therapeutic drug regimen. Retrospective analysis indicates that the TLT may be very beneficial for the positive treatment of chronic conditions.

CHAPTER 6
IN VIVO ASSESSMENT OF THE TRIPLE-LAYERED TABLET MATRIX IN THE LARGE WHITE PIG MODEL

6.1. Introduction

The use of appropriate animal models is undoubtedly an advantageous instrument for the determination of suitable therapeutic approaches for disease states in humans. *In vivo* studies provide useful and relevant information on the biocompatibility of treatment types, tolerance, drug release behavior and plasma drug levels in a biological environment. Large white pigs were selected for the *in vivo* assessment of the triple-layered tablet (TLT) matrices.

The Large White Pig model is undoubtedly advantageous over other animal models such as rats and mice for a more authentic validation and correlation of data analysis with human dosage. One of the major reasons for this, apart from the larger size of the animal, is the allowance for more frequent blood sampling in pigs than in rats or mice which only allow for daily blood sampling intervals. With more frequent blood sampling, a further comprehensive ability to identify and quantify altered or controlled drug release is essentially possible. It has been established that pigs have a similar gastrointestinal anatomy and physiology to humans (Oberle *et al.*, 1994; Anderson *et al.*, 2002). Furthermore, pigs are omnivores and their digestive characteristics would allow for a sufficient analogous comparison to humans. Another factor is the fact that pigs have been used in cardiovascular research (Crick *et al.*, 1998) which further confirms the application of such animals to *in vivo* analysis. The unequivocal widespread use of the pig model for drug delivery analysis ethically, further makes the selection of the Large White Pig model for the assessment of the TLT valid. Thus, this chapter involves the *in vivo* administration of the conventional drug products and the optimized TLT matrix formulation containing atenolol (ATN), aspirin (ASA) and simvastatin (SMV), for the assessment of the performance and tolerability of the TLT in the Large White Pig model.

6.2. Materials and Methods

6.2.1. Materials

Solvents used for UPLC–MS/MS measurements were of UPLC grade, and all other reagents were of analytical grade. Double deionized water was obtained from a Milli-Q system, (Milli-Q, Millipore, Johannesburg, South Africa). Control blank pig plasma was supplied by healthy

donors. HPLC grade Acetonitrile (ACN) was purchased from Microsep (Johannesburg, South Africa). Approval was received from the Animal Ethics Committee for the use of healthy Large White pigs in the *in vivo* release study. French gauge double lumen 35cm catheters (CS-28702) were purchased from Arrow Deutschland GmbH (Erding, Germany). Heparin vials (5000iu/5mL) and isotonic saline (1L) bags were purchased from Milpark Hospital Pharmacy (Johannesburg, South Africa). Pre-filters employed in the study were Acrodisc® 13mm 0.2µm filters obtained from Life sciences (Johannesburg, South Africa). A BEH Shield RP18, 1.7µm, 2.1×100mm column was obtained from Waters Corporation (Milford, MA, USA).

6.2.2. Methods

6.2.2.1. Habituation of pigs prior to drug administration

Healthy female Large White pigs were employed in the study. Pigs were housed in a farm unit and maintained under a 12 hour light dark cycle and fed a commercial diet. Figure 6.1 is a digital photograph showing the farm unit and housing of the pigs and the daily habituation process. Figure 6.4 displays the number of pigs required for the study. Habituation was necessary prior to *in vivo* studies in order to reduce the challenges associated with handling the animals for administration of formulations and blood sampling. The habituation involved visiting the animals twice a day and feeding them foods such as nuts and raisins.

Figure 6.1: Farm unit, housing, daily habituation process of feeding and behavioural learning of the Large White Pig model.

6.2.2.2. Surgical implantation of a chronic catheter into the left jugular vein of the pigs

It was established that the most efficient way to sample blood from the pigs was to insert a catheter into the left jugular vein. The procedure was performed by the chief veterinarian and the supporting staff of the Central Animal Services (CAS) at the University of the Witwatersrand. This method was chosen as it caused the least amount of distress to the

animal as opposed to the previous blood sampling method which involved drawing of blood from the marginal ear vein of the pigs. The pigs were anaesthetized and then transported to the operating room and prepared for surgery. The preparation prior to surgery involved administering injections of antibiotics and analgesic agents and shaving of the operating site around the jugular vein. The animals were under anaesthesia and constant oxygen supply for the duration of the procedure which was performed under aseptic conditions.

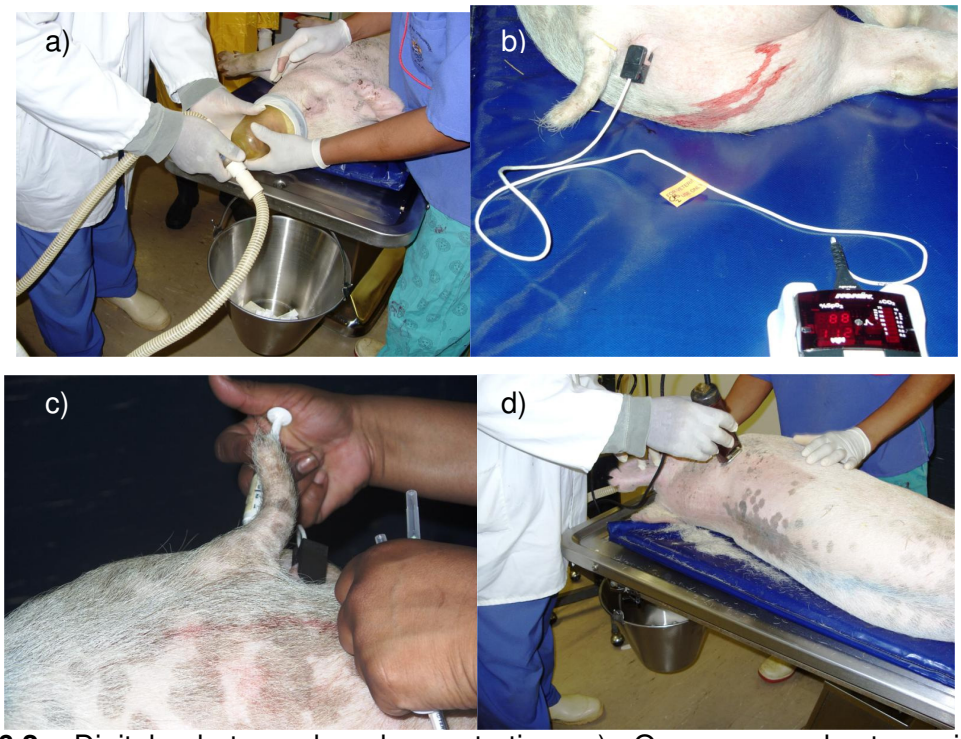

Figure 6.2: Digital photographs demonstrating a) Oxygen supply to animal after anaesthetization, b) Monitoring of heart rate, c) administration of injections and d) shaving of operating area.

Figures 6.2a, b, c and d are digital photographs demonstrating the preparation for surgical procedure involved. In brief, the procedure began with an incision made to the left lateral aspect of the neck in order to expose the jugular vein. Once the vein was isolated, the catheter was inserted 10cm into the lumen of the vein. The lumen of the catheter was then sutured to the wall of the vein ensuring security. The remaining aspect of the catheter was then placed subcutaneously with the ports exposed via an outlet made around the dorsal area of the scapula. The wound was subsequently sutured and the ports were fastened with sutures to the skin. Figure 6.3a is a digital photograph of the 7 French gauge double lumen 35cm catheter to be inserted into the left jugular vein during surgery. Following the procedure a ten day waiting period was necessary to allow the surgical wound to heal. During the waiting period, between each dosing of the animals and after each blood sample taken for the entire duration of the study, the catheters were flushed with 10mL of heparin in saline (5000i.u./L) twice a day to ensure that the catheters did not become blocked and that ease of blood sampling was achievable.

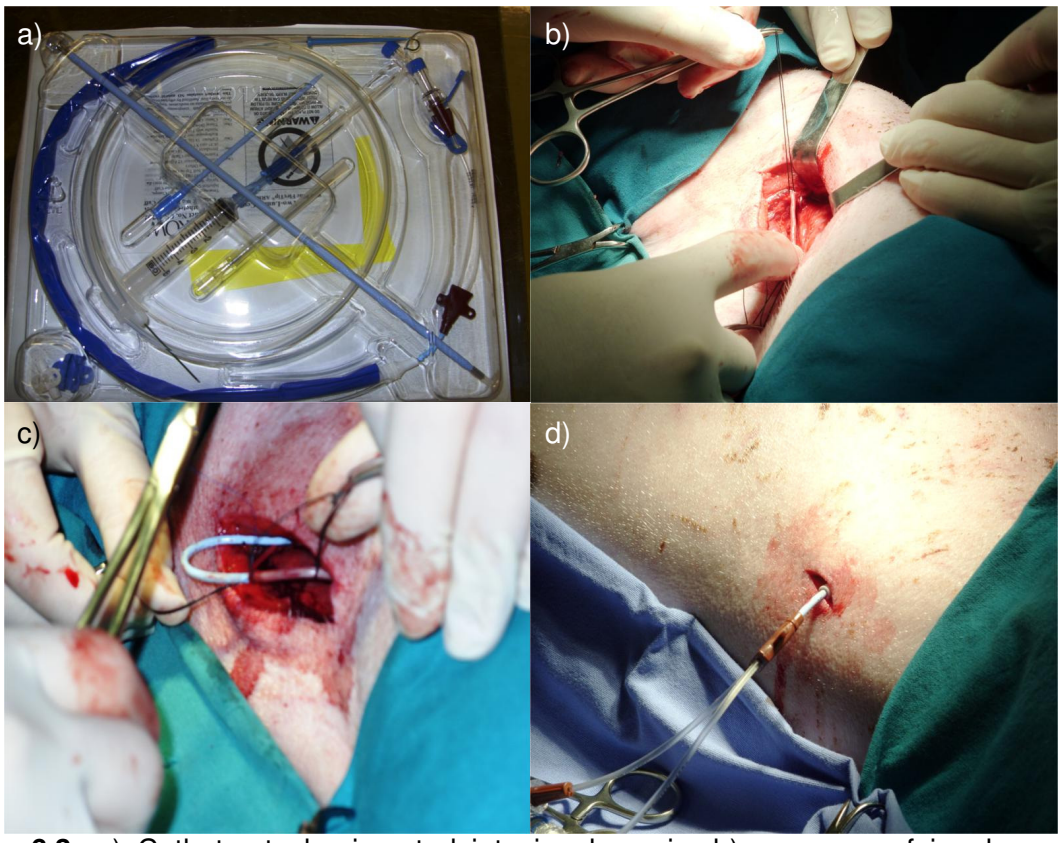

Figure 6.3: a) Catheter to be inserted into jugular vein, b) exposure of jugular vein for insertion, c) insertion of catheter into jugular vein and d) stitching up of wound with ports exposed for blood sampling.

6.2.2.3. Administration of the conventional tablets to the Large White Pig model

The dosing procedure was carried out in conjunction with the animal technicians at the CAS. The animals were injected with Ketamine HCl (40mg/kg) via the jugular vein catheter for anaesthetization. Once the animal was under anaesthesia it was moved to an open area and maintained under anaesthesia by topical procaine HCl (0.5%) and oxygenated. The animal was then lifted into an upright position and an intragastric tube was inserted via the mouth of the animal down into the gastric region. The conventional tablets (Tenormin® 50; DISPRIN CV®100 and Adco-Simvastatin 40) were placed at the end of the tube and flushed down with a small quantity of water simultaneously. The animal was then laid down and carried to the pen where it was then closely observed for proper breathing until the anaesthesia wore off and it was conscious and mobile.

6.2.2.4. Administration of the optimized TLT formulations to the Large White Pig model

The procedure was carried out in the same way as that of the conventional dosage forms previously after a 3-day washout period allowing for more accurate and uncontaminated results.

6.2.2.5. Blood sample collection from the jugular vein catheter port of the Large White Pig model

Blood samples for time point 0 hours were drawn prior to administration of the conventional dosage forms and TLT formulations to the pigs. Subsequent to administration and allowing for the anaesthesia to wear off, blood samples (5mL) were drawn from the jugular vein catheter ports at time intervals of 0; 2; 4; 6; 8; 10; 12; 16; 20 and 24 hours into heparin lined glass blood vials . Plasma was separated by centrifugation for 15 minutes at 3000rpm and stored at -70℃ until analysis. Figure 6.4 is a schematic diagram depicting the entire *in vivo* study sequential that was carried out.

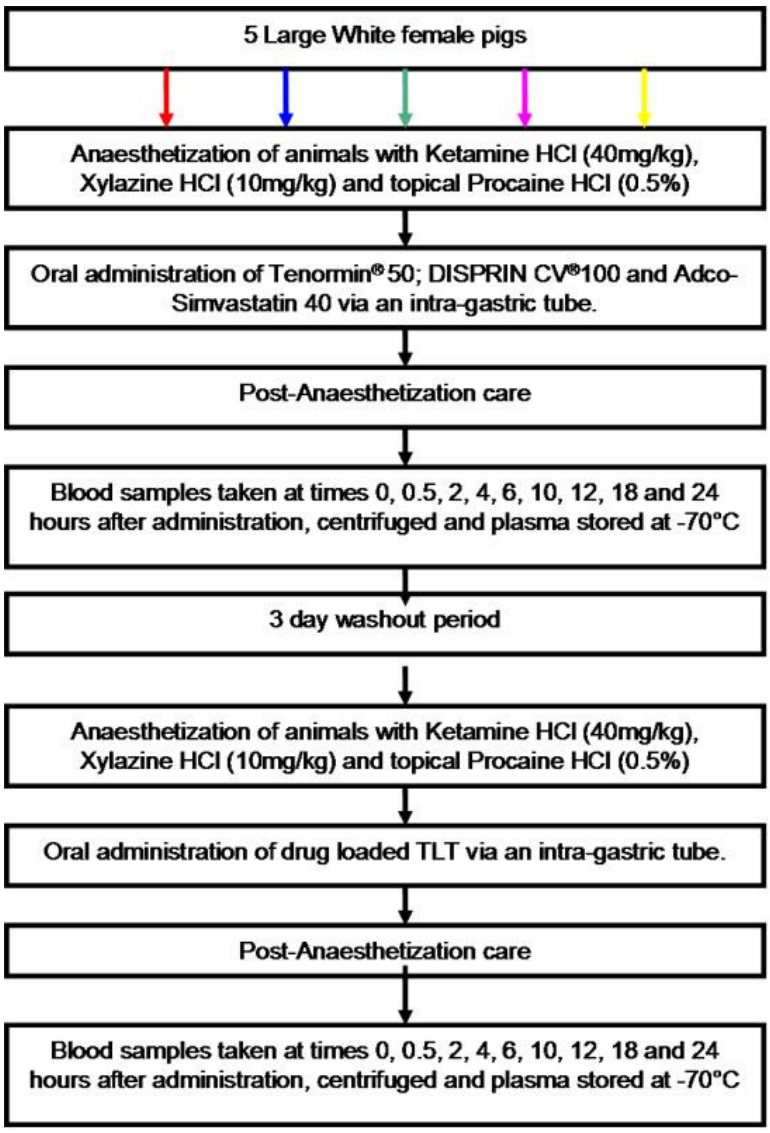

Figure 6.4: Schematic diagram depicting the number of pigs required and the steps involved during the *in vivo* studies.

6.2.2.6. Development of a method for sample analysis employing Ultra Performance Liquid Chromatography™

Ultra performance liquid chromatography (UPLC) was the technique utilized to determine the concentration of the model drugs in the plasma retrieved at the different time points. It is a renowned technique employed for the separation of compounds by means of peak identification using stationary phase column particles with a size below 2.5µm (Dongre *et al*., 2008). The fundamental concept is the running of samples through a column coupled with a PDA detector for the ultraviolet absorbance of the compounds. The utilization of column particles that are below 2.5µm results in a betterment of column efficiency. This subsequently leads to increased resolution of peaks and speedy analysis of samples (Jerkovich *et al*., 2003, Krishnaiah *et al*., 2010).

The Waters Acquity Ultra Performance Liquid Chromatography (UPLC) system (Waters, Milford, MA, USA) with a PDA detector was utilized in the study. The machine was equipped with a binary solvent manager that contained three lines (A, B_1 and B_2) for the flow of mobile phase solvents. Line A was for the exclusive use of inorganic solvents while lines B_1 and B_2 were for the exclusive use of organic solvents such as methanol and ACN. Separation was achieved on an Acquity UPLC C18 column (50×2.1mm, i.d., 1.7µm particle size, Waters). A method for the simultaneous determination of ATN, ASA and SMV was investigated; this involved the selection of appropriate mobile phases, flow rate, wavelength and injection volume.

After a series of attempts a suitable method to separate all three of the drugs was achieved. The mobile phases employed were 0.01%$^{v}/_{v}$ orthophosphoric acid (OPA) and acetonitrile (ACN). An isocratic method with the ratio of 65:35 (OPA: ACN) proved to be the most adequate at separating the drugs. Table 6.1 displays the separation method selected for the three drugs. Diphenhydramine (DPH) was selected as the internal standard for quantification. Mobile phases were prepared and filtered through 0.22µm Millipore filters and placed on the machine with the appropriate solvent flow lines placed in the two mobile phases. The initial step to UPLC analysis is priming the machine which includes washing of the pumps and lines. Two types of washing occurred, a weak wash (90%$^{V}/_{V}$ de-ionized water and 10%$^{V}/_{V}$ ACN) and a strong wash (10%$^{V}/_{V}$ de-ionized water and 90%$^{V}/_{V}$ ACN). Once the priming process is complete (2 cycles of 10 minutes each), the column must be equilibrated to the selected separation method, this constitutes loading the method on to the software and allowing the mobile phases to flow through the column while the environment of the column is changed according to the method.

Table 6.1: Method parameters for the simultaneous determination of ATN, ASA and SMV.

Parameter	Condition
Mobile Phase	0.01% OPA and ACN (65:35) isocratic gradient
Flow rate	0.5mL/min
Injection volume	5µL
Wavelength	210nm
Column Temperature	40℃

6.2.2.7. Selection of a suitable method for extraction of ATN, ASA and SMV from plasma for UPLC analysis

After various attempts at solid phase extraction (SPE) and liquid-liquid extraction for the adequate extraction of all three drugs from the plasma, SPE proved to be the least feasible option as it did not provide an adequately measurable result. As a result, the more optimal liquid-liquid extraction was further investigated. Liquid-liquid extraction involves the separation of different compounds according to their different affinities to solvents. The basic principle is the addition of a liquid solvent to another liquid solution containing the compound requiring separation (Muller *et al.*, 2008). During method development, blank plasma was spiked with the three drugs and IS. The method that was developed involved the addition of ACN to plasma and subsequent centrifugation (Optima® LE-80K, Beckman, USA) and reconstitution. ACN was employed due to its effective deproteinating capability and the high solubility of all four drugs in ACN. Figure 6.5 is a schematic describing the sequential process of liquid-liquid extraction of ATN, ASA, SMV and DPH.

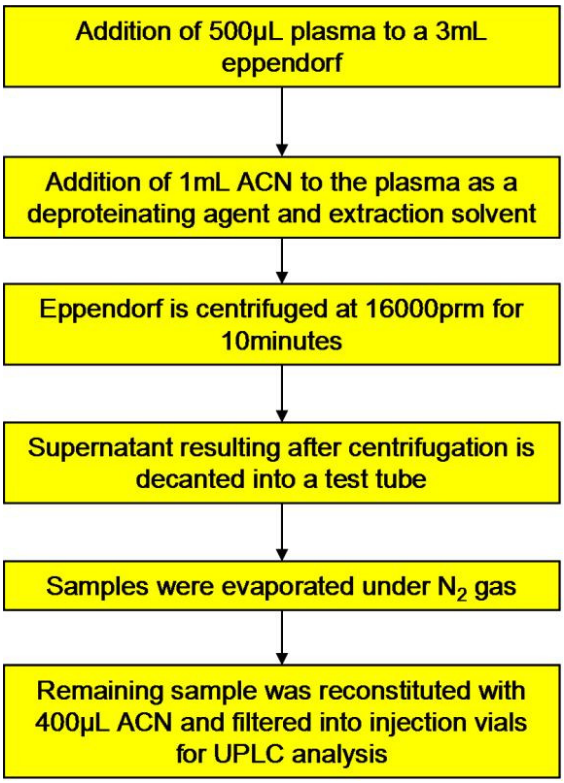

Figure 6.5: Schematic diagram depicting the sequential process the liquid-liquid extraction procedure selected for the extraction of ATN, ASA and SMV from plasma.

6.2.2.8. Preparation of calibration curves and limit of quantification for ATN, ASA and SMV in plasma

A standard stock solution (A) of 1mg/mL ATN, ASA and SMV was prepared. A second stock solution (B) of 0.1mg/mL was prepared from A. A micropipette was used to spike the blank plasma with specific quantities of ATN, ASA and SMV for calibration. A standard concentration of DPH was added to the different calibration samples followed by the extraction procedure described in Chapter 6, section 6.2.2.7. UPLC analysis was subsequently performed.

6.2.2.9. UPLC analysis of drug release after the in vivo administration of Tenormin®, Adco-Simvastatin 40 and Disprin CV® and the optimized TLT formulation

Once the suitable UPLC separation and plasma extraction procedures were optimized and subsequent to the preparation of calibration curves for the three drugs, it was necessary and feasible to run the plasma samples obtained from the *in vivo* animal study. The samples were prepared by spiking 500µL of plasma from each time point with a known concentration of IS and performing the extraction procedure mentioned in Chapter 6, section 6.2.2.7. Once the samples were prepared they were filtered in to ANSI482mL UPLC vials for analysis. UPLC analysis was carried out according to the UPLC separation method selected and mentioned in Chapter 6, section 6.2.2.6.

6.3. Results and Discussion

6.3.1. Behavior of pigs after insertion of a jugular vein catheter and after administration of the optimized TLT formulation

On the actual day of the surgical procedure where the catheters were inserted in to the jugular vein of the pigs, the pigs displayed no changes in behavior from prior to the surgical procedure. Subsequent to the wearing off of anaesthesia the animals displayed the usual levels of activity and appetite as previously experienced. The quantity of time required for them to get back on their feet and walk around was not lengthy. The blood sampling procedure was not complex or time consuming, further proving the feasibility of the use of the catheter. The administration of the TLT showed no adverse effects to the pig substantiating the biocompatibility of the system orally. The pigs displayed normal behavior in terms of activity and appetite, blood sampling after administration of the TLT was normal as well.

6.3.2. Validation of selected method for UPLC analysis of plasma samples

The method selected for plasma analysis proved to be ideal for the undisturbed simultaneous separation of ATN, ASA and SMV. The retention times obtained for ATN, ASA and SMV were approximately 0.45, 0.91 and 1.39 minutes respectively in ACN. Figure 6.6 is a chromatogram illustrating the peaks obtained for the three drugs at the different retention times.

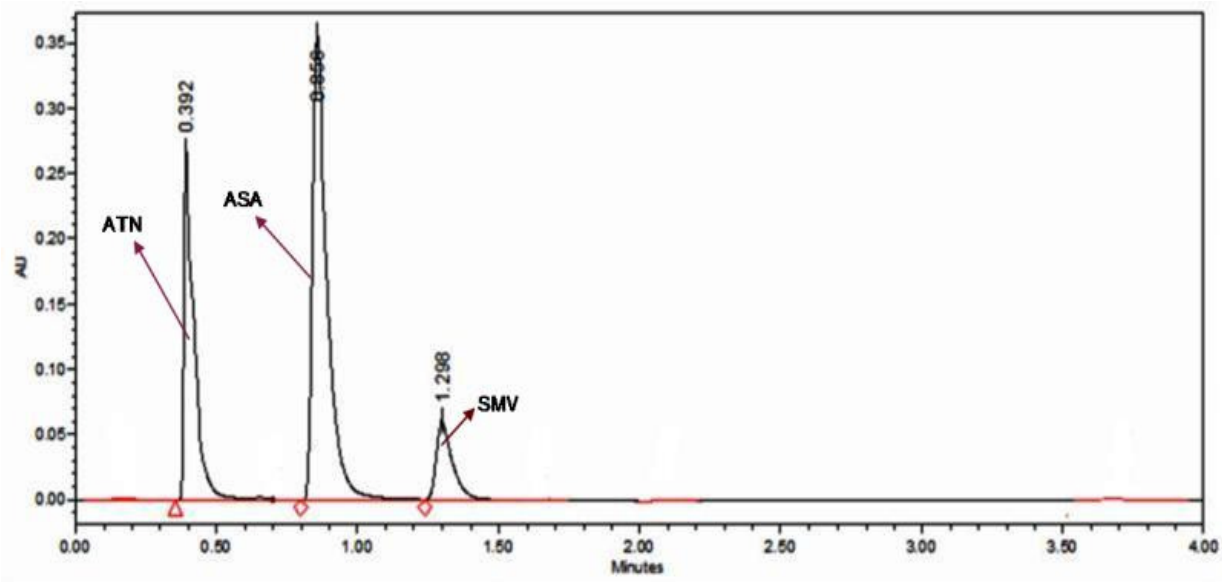

Figure 6.6: Chromatogram illustrating the separation peaks of ATN, ASA and SMV.

Figure 6.7 is a three-dimensional (3D) plot depicting the three peaks of ATN, ASA and SMV further illustrating the appropriate separation of the three drugs. 3D inspection was useful in determining the most favorable absorption wavelength for all three drugs with minimal interference. DPH was selected as it was the only drug that did not overlap or disturb the other drug peaks. The retention time for DPH was found to be approximately 0.7 minutes. Figure 6.8 is a chromatogram showing the peaks obtained for all the drugs including DPH. The extraction method selected produced a drug recovery of 73%, 78% and 82% for ATN, ASA and SMV respectively. This was calculated by comparing the area of drug peaks generated in ACN to those generated from the plasma extraction method with the same concentration of drug.

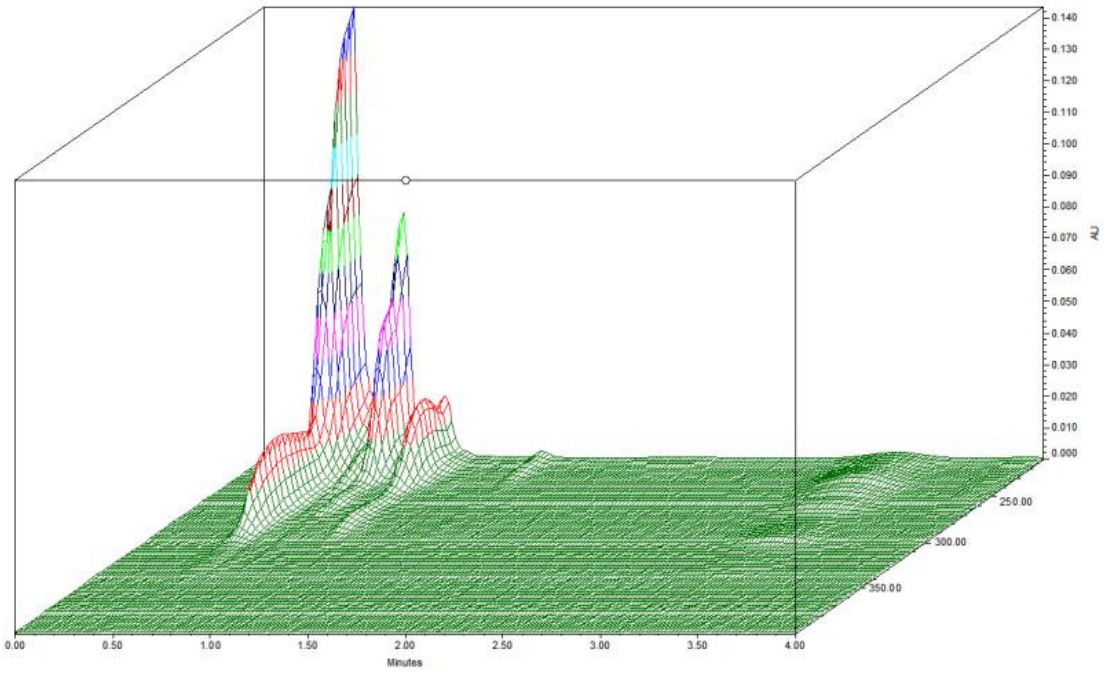

Figure 6.7: 3D chromatogram of ATN, ASA and SMV.

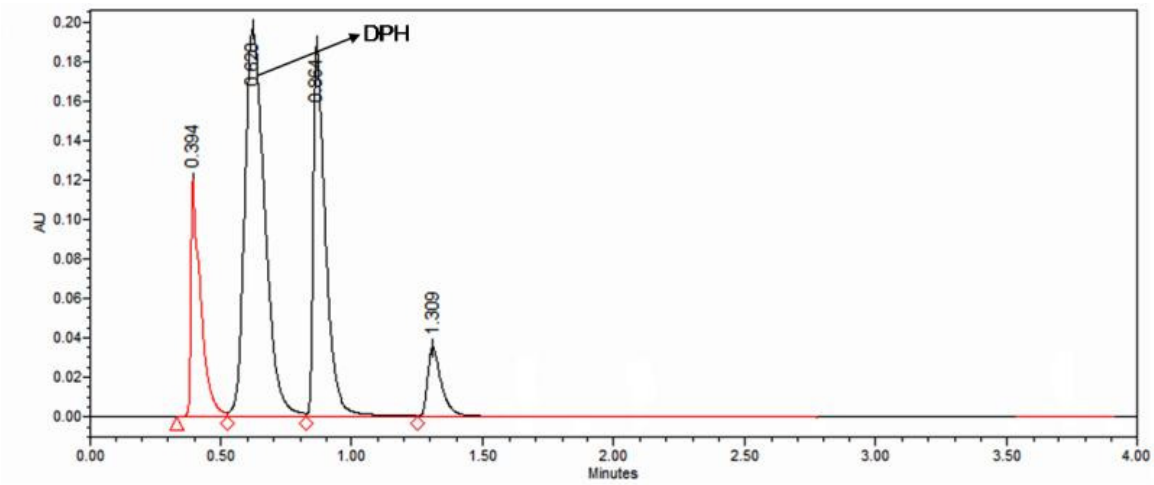

Figure 6.8: Chromatogram illustrating the separation peaks of ATN, ASA and SMV with DPH as the internal standard.

6.3.3. Liquid-liquid extraction and assessment of UPLC chromatographic separation method in plasma

Subsequent to the elucidation of the feasibility of the separation technique in ACN, it was then investigated for the separation of the drugs in plasma. A sample was prepared by spiking blank plasma with ATN, ASA, SMV and DPH. This mixture was then vortexed to allow for drug binding to the plasma. The extraction procedure described previously was then followed and the sample was injected for UPLC analysis. After UPLC analysis, it was observed that the process proved to be adequate in providing separate peaks of all four drugs with slightly shifted retention times. Figure 6.9 is a chromatogram displaying the four drug peaks after plasma extraction.

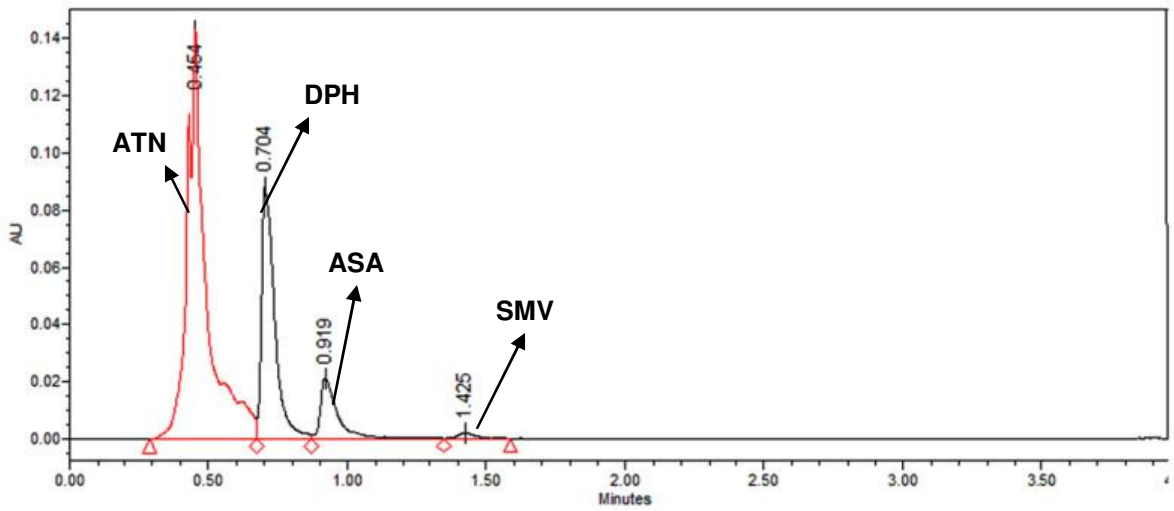

Figure 6.9: Chromatogram displaying the separation peaks of ATN, ASA, SMV and DPH as the internal standard after plasma extraction.

6.3.4. Calibration curves prepared for the quantitative analysis of ATN, ASA and SMV in plasma

Figures 6.10a, b and c are the calibration curves obtained in plasma for ATN, ASA and SMV respectively. The calibration ranges selected were 0-50000ng/mL for all three drugs.

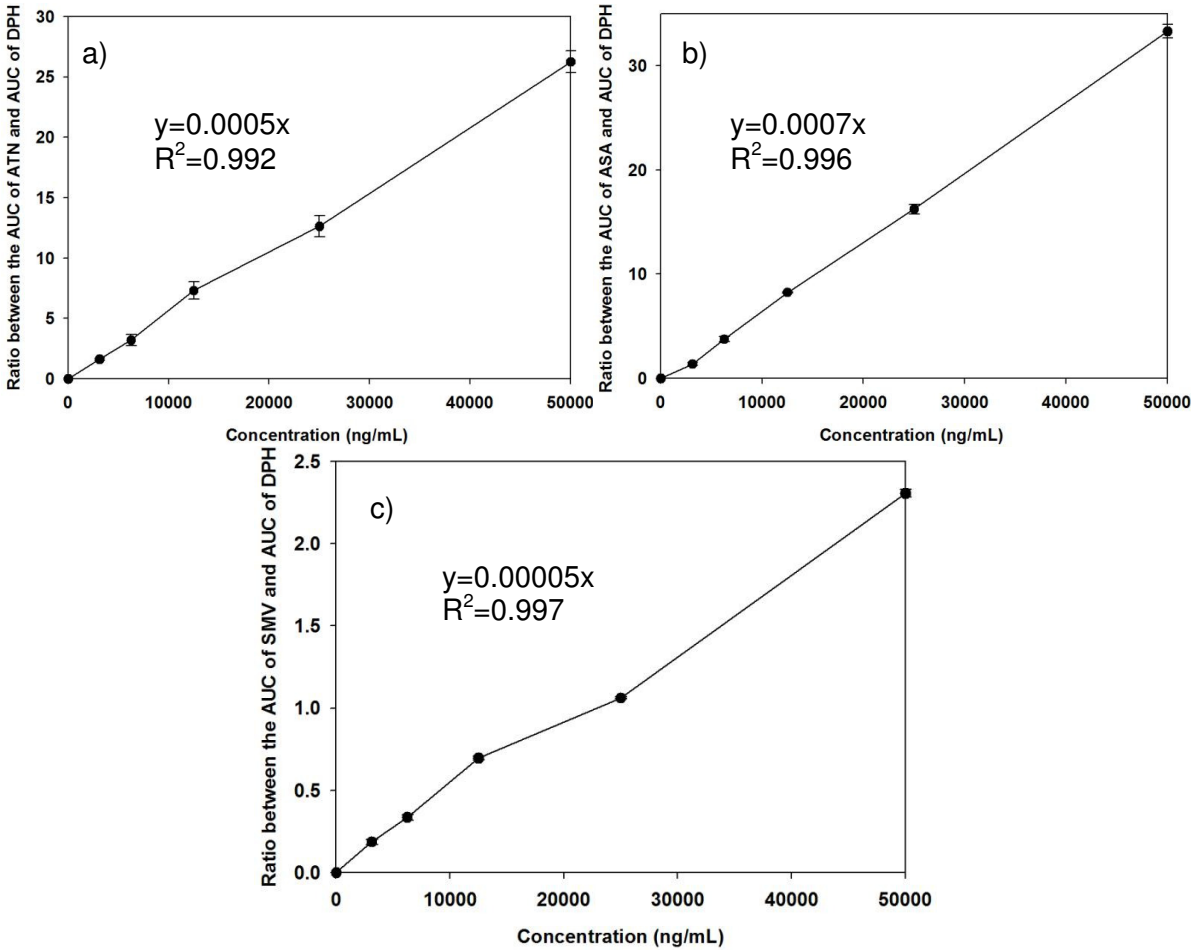

Figure 6.10: a) ATN calibration curve in plasma; b) ASA calibration curve in plasma and c) SMV calibration curve in plasma.

6.3.5. Assessment of *in vivo* drug release from Tenormin® 50; DISPRIN CV®100 and Adco-Simvastatin 40

The ultimate aim of the *in vivo* study was to develop a comparison in drug release behavior between the conventional dosage forms and the optimized TLT formulation. An adequate comparison was necessary *in vivo* following the confirmation of a superior release from the TLT *in vitro*. Figure 6.11a, b and c contains the drug release profiles of Tenormin® 50; DISPRIN CV®100 and Adco-Simvastatin 40 respectively in plasma. For Tenormin® 50 it was noted that there was an initial significant ascension of plasma concentration after 2 hours, with peak plasma concentrations (C_{max}= 816ng/mL) being reached at approximately 4 hours. This was followed by a swift reduction of plasma concentration for a further 8 hours.

With DISPRIN CV®100, a similar trend was observed with an increase of plasma concentration until a C_{max} of 2439ng/mL was reached at 8 hours followed by a steady descent of plasma concentration. The Adco-Simvastatin 40 release profile displayed much more miniscule plasma concentrations as compared to those of the previous two conventional tablets. The C_{max} of 13.5ng/mL was reached at 6 hours after administration.

Thus it can be confirmed that for all three conventional tablets, most of the drug was released by an initial burst before 8 hours after administration. This may due to the lack of controlling mechanisms present in the conventional tablets which are compressed powders of the drugs in question coupled with formulation excipients. Although large standard deviations were noticed, the pattern of drug release was found to be consistent.

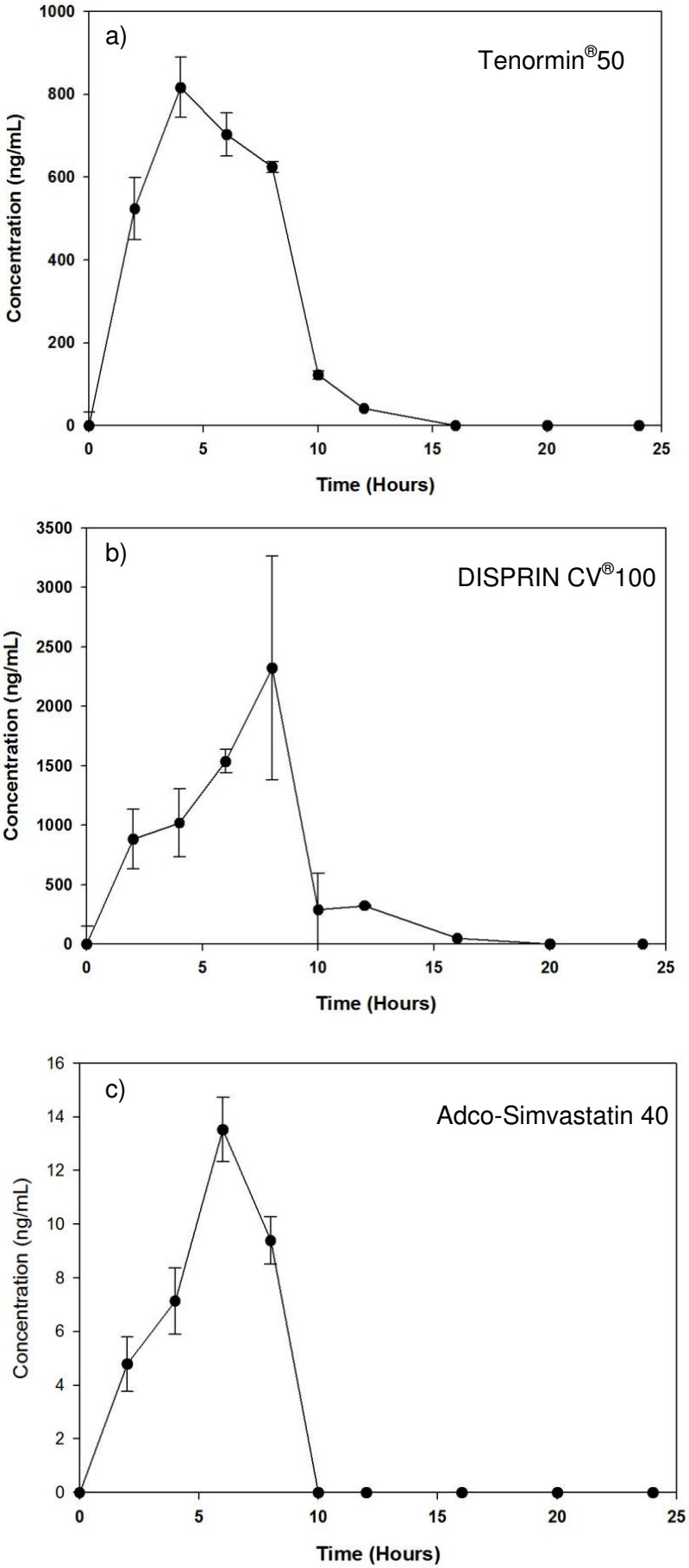

Figure 6.11: Plasma drug concentration profile depicting the release behavior over 24 hours of a) Tenormin® 50; b) DISPRIN CV®100 and c) Adco-Simvastatin 40 (N=5).

6.3.6. Assessment of *in vivo* drug release from the optimized TLT formulation

The stark comparative difference in drug release profiles between the conventional tablets and the optimized TLT formulation was immediately noted as illustrated in Figures 6.12a, b and c. With ATN, a gradual release of drug was noted at the onset. This steady increase in plasma concentration reached a C_{max} of 4443ng/mL after 2 hours. The plasma levels subsequently decreased at the end of 24 hours. For ASA, a C_{max} of 4195ng/mL was reached only at 24 hours, which was preceded by a steady increase in plasma concentration.

A similar pattern was observed with SMV, C_{max} (21ng/mL) was reached only 20 hours after administration. The very low therapeutic levels of the drugs that were reached may be due to the *in vivo* absorption and distribution characteristics of the drugs. According to literature, simvastatin has an overall low systemic oral bioavailaility (Bellosta *et al.*, 2004) which is confirmable with the low C_{max} of SMV that was obtained. Also, depending on the storage of the plasma that was collected, slight degradation of drug may have occurred even though temperature storage of -70℃ was maintained.

A prolonged release over a minimum 12 hours was achieved with all three drugs indicating a significant improvement on controlling plasma levels of each drug. The vast variance of TLT release profiles to that of the conventional tablets further authenticates the *in vitro* results obtained.

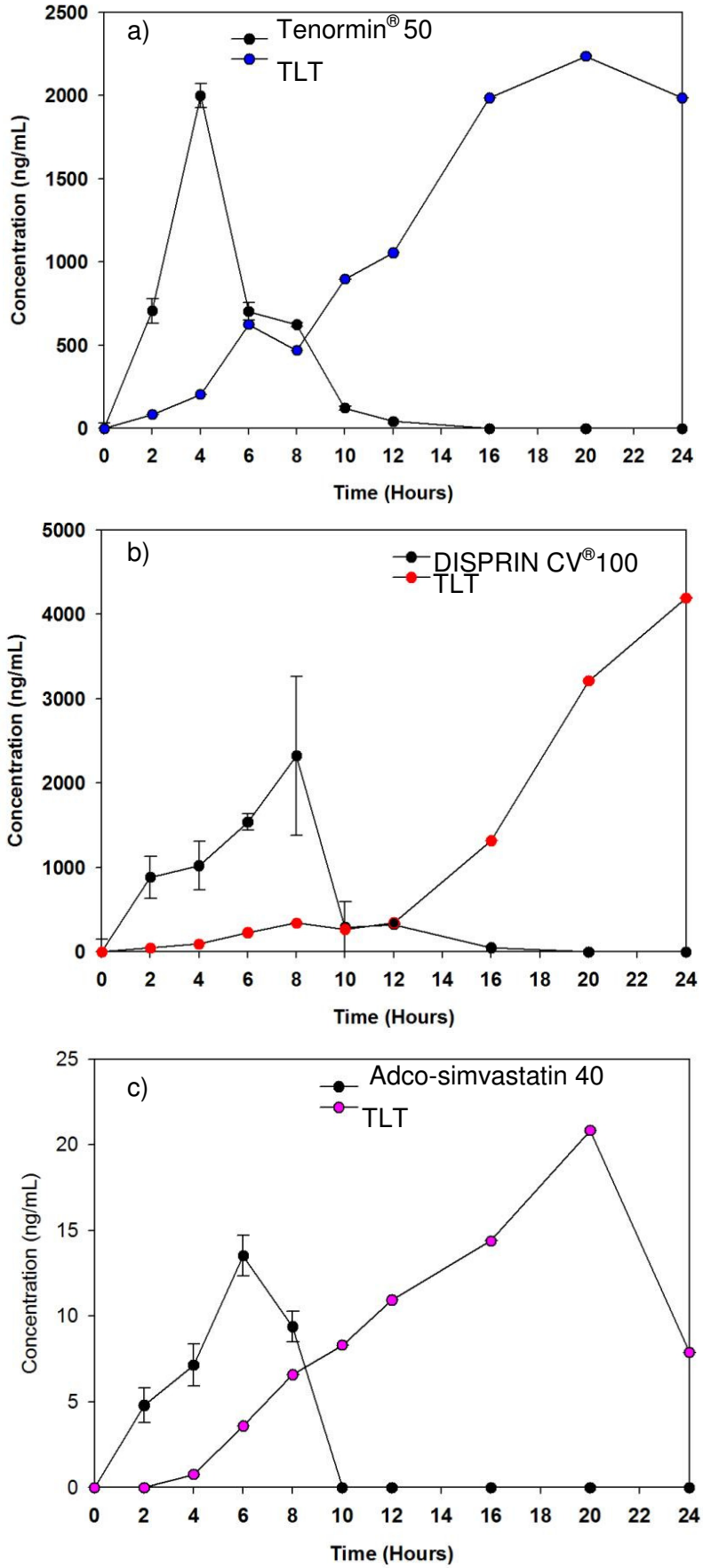

Figure 6.12: Comparative plasma drug concentration profiles of optimized TLT versus conventional tablets depicting drug release behavior over 24 hours of a) ATN versus Tenormin®50 ; b) ASA versus DISPRIN CV® and c) SMV versus Adco-simvastatin 40 (N=5).

6.4. Concluding Remarks

The aim of the *in vivo* study was to assess the drug release capability of the TLT in comparison to the conventional tablets Tenormin® 50; DISPRIN CV®100 and Adco-Simvastatin 40. The pig proved to be a feasible model for the study with the insertion of jugular vein catheters greatly improving the efficiency of the study. After completing the study and UPLC analysis of data, it was confirmed that the TLT formulation did in fact display a largely superior release profile in terms of sustained and controlled drug release to that of the conventional tablets. The TLT also displayed a lack of sharp plasma concentration fluctuations as compared to the conventional tablets. Although the release profile was less than desirable in comparison to *in vitro* study results, which may be attributed to first pass metabolism and erratic absorption of the drugs from the gastrointestinal tract, the TLT showed capability in controlling the plasma concentrations of the drugs. Further research may focus on developing more accurate analysis methods that may better qualify the TLT *in vivo*.

CHAPTER 7
CONCLUSIONS AND RECOMMENDATIONS

7.1. Conclusions

It is evident that new developments allowing for improved and cheaper treatment outcomes are essential in terms of modern healthcare. Seeing as though it is becoming increasingly difficult and expensive to develop novel drug molecules (Wen and Park, 2010), more prominence is being given to developing novel ways of delivering existing drugs. Due to the reality that pharmaceutical companies are faced with increasing challenges as a result of the higher cost of starting up product lines and decreased market shares (Lee, 2007), there is a decreased accomplishment of developing novel pharmaceutical drug actives. Therefore, developing advanced drug delivery technologies may allow for the extension of the use of existing pharmaceutical drug actives. The requirement of these novel pharmaceutical concepts is due to the prominent therapeutic failures that occur as a result of non compliance of the patient to multiple drug treatment regimens. The possible motives of non compliance have been elucidated to be pill burden and dose-dependent side-effects that occur with various multi-drug treatment regimens. Difficulty comprehending drug administration instructions also plays a role in failed therapeutic results especially with complex drug regimens that require a variety of tablets to be taken at various time intervals per day. As a result of these short comings, health resources are wasted leading to economic consequences. For example non-compliance with cardiovascular and antidiabetic medication is a sizeable problem.

Furthermore, the management of numerous infectious diseases such as Tuberculosis and HIV/AIDS is still limited due to poor treatment compliance (Munro *et al.*, 2007), this adds to the disease burden worldwide. The discovery and establishment of novel drug delivery systems that work effectively and efficiently to reduce dose dependent side-effects and pill burden is yet to be adequately fulfilled.

The crucial ambition of this research was to develop an oral triple-layered tablet system for the controlled zero-order delivery of any suitable therapeutic regimen, which is equipped to hold up to three drug actives with the focal-point honing in on the improvement of patient compliance and reduction of the occurrence of dose-dependent side-effects. The administration of one tablet once per day is understandably easier to comprehend by the patient than three tablets three times a day. The novelty of the proposal lies in the linear release of three different drugs from one TLT. This allowed for a constant amount of drug entering the blood stream reducing dose-dependent side-effects.

In vitro studies involved preliminary experimentation whereby novel polymers were synthesized and employed as drug matrices. TLT formulations were subjected to extensive *in vitro* release studies to assess the capability of providing zero-order release of all three water-soluble drugs. BHN as a measure of matrix hardness was another essential factor in determining the robustness of the TLT.

The Box-Behnken design was utilized in the TLT optimization process which focused on the drug release characteristics. Rate constants (*k* values) and correlation coefficients (R^2 values) were employed as the measured responses for 17 formulations. A solitary formulation was selected as the optimized formulation and the release profile of the three drugs were corroborated.

In addition, a novel drug regimen that comprised atenolol (50mg), simvastatin (40mg) and aspirin (100mg) was applied to the optimized TLT; *in vitro* drug release of this regimen was also assessed to determine the flexibility of the TLT to provide zero-order release of a cardiovascular therapeutic drug combination.

Furthermore, *in vivo* studies were performed on the optimized TLT. The TLT was administered to pigs and drug-release profiles were generated according to the concentration of drugs in plasma at predetermined time intervals. Results from *in vivo* studies showed a definite difference of plasma profiles between conventional tablets Tenormin®, DISPRIN CV® and Adco-simvastatin 40 and the optimized TLT formulation. The release was markedly noted to be more controlled and provided near zero-order to zero-order release. Thus, the TLT provided some degree of sustained and controlled release of the therapeutic regimen.

The TLT developed in the study showed flexibility in providing zero-order release of different drugs. Although a cardiovascular regimen was employed, the TLT is not limited to this. It may be applied to the delivery of various and appropriate disease treatment regimens. The oral administration of the TLT may therefore reduce the pill burden and dose-dependent side-effects of different treatment regimens.

7.2. Recommendations

With oral drug delivery being the least invasive mode of therapy, it can be concluded that more comprehensive research should be conducted to develop more efficient and applicable oral drug delivery systems utilizing existing drugs. Improved and dynamic drug delivery systems may prove to have a significant positive effect on patient therapeutic outcomes. The synthesis of “smart” polymers as drug matrices could be further analyzed and optimized to

decrease research time while increasing efficiency. The application of a gastro-retentive aspect to the TLT may prove to be advantageous for controlled release of Narrow Absorption Window drugs. This may also pose an advantage in providing controlled release of drugs for an extended period greater than 24 hours.

Although the *in vivo* animal study model proved to be efficient, it may be limited in the results that are computed from it. The reason for this may be the altered behavior of the TLT in a pig model according to a specific diet. Also, the molecular absorption of drug molecules from the gastrointestinal tract into plasma may need to be adequately investigated which is difficult in such a setting. Further emphasis should therefore be given to comprehensive *in vivo* analysis. Research should aim to develop modern techniques that allow for uncomplicated administration with minimal to no distress to the animals. Analytical techniques to best identify *in vivo* pharmacokinetic behavior and imaging may also be investigated and improved.

REFERENCES

Abdul, S., Poddar, S.S., 2004. A flexible technology for modified release of drugs:multi layered tablets, *Journal of Controlled Release*, ***97***, 393-405.

Anderson, D.L Bartholomeusz, F.D., Kirkwood,I.D., Chatterton, B.E., Summersides, G., Penglis, S., Kuchel, T., Sansom, L., 2002. Liquid Gastric Emptying in the Pig: Effect of Concentration of Inhaled Isoflurane, The Journal of Nuclear Medicine, ***43(7)***, 968-971.

Andjelić, S.; Yuan, J.; Jamiolkowski, D.D.; Diluccio, R.; Bezwada, R.; Zhang, H.;Mijovic, J., 2006. Hydrophilic absorbable copolyester exhibiting zero-order drug release. *Pharmaceutical Research*, ***23***, 821-834.

Apu A.S.; Pathan, A.H.; Shrestha, D.; Kibria G.; Jalil, R., 2009. Investigation of *in vitro* release kinetics of carbamazepine from Eudragit RS PO and RL PO matrix tablets, *Tropical Journal of Pharmaceutical Research*, 145-152.

Ayres J.W., 2004. Coated, Platform generating tablet, *US Patent,* 6 720 005.

Ayres, J.W., 2004. Coated, platform-generating tablet, *US Patent*, 6 733 784.

Barakat, N.S.; Elbagory, I.M.; Almurshedi, A.S., 2009. Controlled-release carbamazepine matrix granules and tablets comprising lipophilic and hydrophilic components. *Drug Delivery*, ***16***, 57–65.

Barringer L.F., Ledford W.T., 1993. Polymers having enhanced hydrophilicity and thermal regulated properties and process of producing the same, (WO/1993/025749).

Bellosta, S., 2004. Safety of Statins, focus on clinical pharmacokinetics and drug interactions, *Circulation*, **109**, 50-57.

Bernkop-Schnürch A., 2005. Mucoadhesive systems in oral drug delivery, *Drug Discovery Today,* ***2***, 83-87.

Bronzino J.D., 2000. The biomedical engineering handbook, CRC Press, ISBN 084930461X, 9780849304613, 39-10.

Brooke, D.; Walshkuhn, R.J., 1977. Zero-order drug delivery system: Theory and preliminary testing, *Journal of Pharmaceutical Sciences*, ***66***, 159-162.

Cao, X.; Lai, S.; Lee, L.J., 2001. Design of a self-regulated drug delivery device, *Biomedical Microdevices*, ***3***, 109-118.

Cheng, K.; Zhu, J.; Song, X.; Sun, L.; Junhong, Z., 1999. Studies of hydroxypropylmethylcellulose donut-shaped tablets, *Drug Development and Industrial Pharmacy*, ***25***, 1067-1071.

Cheng, P.; Chen, M.; Udipi, K., 2010. Dry diazeniumdiolation methods for producing nitric oxide releasing medical devices. *US Patent Application*, 20100159119.

Chidambaram, N.; Porter, W.; Flood, K.; Qui, Y., 1998. Formulation and characterisation of new layered diffusional matrices for zero-order sustained release. *Journal of Controlled Release,* ***52***, 149-158.

Chien, T.W., 1982. Fundamentals of controlled-release drug administration. In *Novel Drug Delivery Systems*; Swarbrick, J., Ed.; Marcel Dekker Inc: New York, USA, 465–574.

Chopra, S.K., 2002. Drug Delivery Systems Based on Geometric Configuration. In *Modified-Release Drug Delivery Technology*; Rathbone, M.J., Hadgraft, J., Roberts, M.S., Eds.; Marcel Dekker: New York, USA, 35–48. DOI: 10.1201/9780203910337.

Chopra, S.K., 2002. Drug Delivery Systems Based on Geometric Configuration. In *Modified-Release Drug Delivery Technology*; Rathbone, M.J., Hadgraft, J., Roberts, M.S., Eds.; Marcel Dekker: New York, USA, 35–48. DOI: 10.1201/9780203910337.ch4.

Chopra, S., Motwani, S.K., Iqbal, Z., Talegaonkar, S., Ahmad, F.J., Khar, R.K., 2007. Optimisation of polyherbal gels for vaginal drug delivery by Box-Behnken statistical design. *European Journal of Pharmaceutics and Biopharmaceutics*, ***67***, 120-131.

Cleave, J.P., 1965. Some geometrical considerations concerning the design of tablets. *Journal of Pharmacy and Pharmacology,* ***17***, 698-702.

Cobby, J.; Mayersohn, M.; Walker, G.C., 1974. Influence of shape factors on kinetics of drug release from matrix tablets I: Theoretical. *Journal of Pharmaceutical Scences*, ***63***, 725–732.

Colombo, P., 1993. Swelling-controlled Release in Hydrogel Matrices for Oral Route, *Advanced Drug Delivery Reviews*, ***11(1–2)***, 37–57.

Colombo, P.; La Manna, A.; Conte, U., 1989. System for the controlled-rate release of active substances, *US Patent*, 4839177.

Colombo, P.; Sonvic, G.; Colombo, G.; Bettini, R., 2009. Novel platforms for oral drug delivery, *Pharmaceutical Research*, ***26(3)***, 601-610.

Conte U, Maggi L., Colombo P, Manna L., 2005. Multilayered hydrophilic matrices as constant release devices, *Journal of Controlled release, **26**,* 39-47.

Conte, U.; Maggi, L., 2000. A flexible technology for the linear, pulsatile and delayed release of drugs allowing for easy accommodation of difficult in vitro targets, *Journal of Controlled Release, **64***, 263-268.

Conti, S.; Maggi, L.; Segale, L.; Ochoa Machiste, E.; Conte, U.; Grenier, P.; Vergnault G., 2007. Matrices containing NaCMC and HPMC: 2. Swelling and release mechanism study, *International Journal of Pharmaceutics, **333***, 143-151.

Corrigan, O.I., Li, X., 2009. Quantifying drug release from PLGA nanoparticulates, *European Journal of Pharmaceutical Sciences*, ***37***, 477-485.

Crick, S.J., Sheppard, M.N, Ho, S.Y., Gebstein, L., Anderson, R.H., 1998. Anatomy of the pig heart: comparisons with normal human cardiac structure, *Journal of Anatomy*, **193**, 105-119.

Crotts, G.; Park, T.G., 1995. Preparation of porous and nonporous biodegradable polymeric hollow microspheres, *Journal of Controlled Release, **35***, 91-105.

Danckwerts, M.P., 1994. Development of a zero-order release oral compressed tablet with potential for commercial tabletting production, *International Journal of Pharmaceutics, **112***, 37-45.

Dash, A.K., Cudworthll, G.C., 1998. Therapeutic applications of implantable drug delivery systems, *Journal of Pharmacological and toxicological methods*, ***40 (1)***, 1-12.

Dash, S.; Murthy, P.N.; Nath, L.; Chowdhury, P., 2010. Kinetic modeling on drug release from controlled drug delivery systems. *Acta Poloniae Pharmaceutica Drug Research,* ***67***, 217-223.

Davidson III, G.W.R. and Peppas, N.A. 1986. Relaxation-Controlled Transport in P(HEMA-co-MMA) Copolymers, *Journal of Controlled Release*, ***3***, 243–258.

Desai, S., 1996. Multilayer Controlled Release Tablets Containing both naproxen and naproxen sodium salt, *Euopean Patent*, 0656776.

Deshpande, A.A.; Rhodes, C.T.; Shah, N.S.; Malick, A.W., 1996. Controlled-release drug delivery systems for prolonged gastric residence: An overview, *Drug Development and Industrial Pharmacy,* ***22***, 531-539.

Dongre, V.G., Karmuse, P.P., Rao, P.P., Kumar, A., 2008. Development and validation of UPLC method for determination of primaquine phosphate and its impurities, *Journal of Pharmaceutical and Biomedical Analysis*, ***46(2)***, 236-242.

Doshi, M.M.; Joshi, M.D.; Mehta, B.P., 2007. Pharmaceutical composition for controlled drug delivery system, *US Patent*, 7 157 100.

Efentakis M, Politis S., 2006. Comparative evaluation of various structures in polymer controlled drug delivery systems and the effect of their morphology and characteristics on drug release, *European Polymer Journal,* ***42,*** 1183-1195.

Efentakis, M.; Peponaki, C., 2008. Formulation study and evaluation of matrix and three-layer tablet sustained drug delivery systems based on carbopols with isosorbide mononitrate. *AAPS PharmSci*, ***9***, 917-923.

Elan drug technologies, 2010. Spheroidal drug absorption system (SODAS®). http://www.elandrugtechnologies.com/oral_controlled_release/sodas [accessed August 26, 2010].

Faour, J.; Mayorga, J., 2006. Multi-layered osmotic device. *US Reissued Patent,* RE39069.

Fassihi, R.; Yang, L., 1998. Controlled release drug delivery system. *US Patent*, 5 783 212.

Ferreira, S.L.C., Bruns, R.E., Ferreira, H.S., Matos, G.D., David, J.M., Brandão, G.C., da Silva, E.G.P., Portugal, L.A., dos Reis, P.S., Souza, A.S., dos Santos, W.N.L., 2007. Box-

Behnken design: An alternative for the optimization of analytical methods. *Analytica Chimica Acta*, ***597***, 179-186.

Flanner, H.H.; Mcknight, L.C.; Burnside, B.A., 2005. System for osmotic delivery of pharmaceutically active agents, *US Patent*, 6838093.

Ford, J.L.; Rubenstein, M.H.; McCaul, F.; Hogan, J.E.; Edgar, P.J., 1987. Importance of drug type, tablet shape and added diluents on drug release kinetics from hydroxypropylmethylcellulose matrix tablets, *International Journal of Pharmaceutics, **40***, 233-234.

Frolov, S.V., Artemov, A.V. and Kiryukhin, S.M., 1999. Properties of polyamide fibres treated with Aqueous solutions of metal salts, *Fibre Chemistry*, ***31***, 95-98.

Fukui, J.; Uemura, K.; Kobayashi, M., Studies on applicability of press-coated tablets using hydroxypropylcellulose (HPC) in the outer shell for timed-release preparations, *Journal of Controlled Release, **68***, 215-223.

Gallardo, A.; Rodríguez, G.; Aguilar, M.R.; Fernández, M.; San Román, J., 2003. A Kinetic model to explain the zero-order release of drugs from ionic polymeric drug conjugates: Application to AMPS–Triflusal-Derived polymeric drugs, *Macromolecules*, ***36***, 8876–8880.

Garcia-Encina, D., Torres, B., Seijo, Vila Jato J.L., 1993. In vivo evaluation of nylon-coated diclofenac-resin complexes, *Journal of Controlled Release*, ***23***, 201–207.

Ghosh, T., Ghosh, A., 2011. Drug delivery through osmotic systems-an overview. *Journal of Applied Pharmaceutical Science*, 2011, ***1(2)***, 38-49.

Gohel, M.C.; Nagori, S.A., 2009. A novel colonic drug delivery system of ibuprofen. *Asian Journal of Pharmaceutics*, ***3***, 233-239.

Green, P.G., 1996. Iontophoretic delivery of peptide drugs, *Journal of Controlled Release*, ***41***, 33-48.

Guimarães, G.G.; Katsuki, G.I.; Zanardo, N.D.; Ribeiro, D.A.; Cavalcanti, O.A., 2008. Evaluation of pectin-HPMC as compression coating. I - A study of the swelling properties of coated tablet, *Revista Brasiliera Ciencias Farmaceuticas, **44***, 133-141.

Guo J.H., Carbopol polymers for pharmaceutical drug delivery applications, *Drug Delivery Technology. Retrieved 15 February 2008, http://www.drugdeliverytech.com/cgi-bin/articles.cgi*

Gupta, A., Saquing, C.D., Afshari, M., Tonelli, A.E., Khan S.A. and Kotek, R., 2009. Porous nylon-6 fibers via a novel salt-induced electrospinning method, *Macromolecules*, ***42***, 709-715.

Hardy, I.J.; Windberg-Baarup, A.; Neri, C.; Byway, P.V.; Booth, S.W.; Fitzpatrick, S., 2007. Modulation of drug release kinetics from hydroxypropyl methyl cellulose matrix tablets using polyvinyl pyrrolidone, *International Journal of Pharmaceutics*, ***337***, 246-253.

Harland, R.S.; Gazzaniga, A.; Sangalli, M.E.; Colombo, P.; Peppas, N.A., 1998. Drug/polymer matrix swelling and dissolution, *Pharmaceutical Research,* ***5***, 488-494.

Heller, J.; Pangburn, S.H.; Penhale, D.W.H., 1987. Use of bioerodible polymers in self-regulated drug delivery systems, In *Controlled-Release Technology, Pharmaceutical Applications;* Lee, P.I., Good, W.R., Eds.; ACS Symposium Series: Washington DC, USA, 172–187.

Herrlich, S.; Ziolek, S.; Hoefemann, H.; Zengerle, R.; Haeberle, S., 2009. Adjustable diffusion barrier for controlled drug release in spastic and pain therapy, In: *4th European conference of the international federation of medical and biological engineering*, ***22***, 2368-2371.

Hongtao, L.; Xiaochen, G.U., 2007. Correlation between drug dissolution and polymer hydration: A study using texture analysis, *International Journal of Pharmaceutics*, ***342***, 18-25.
Hsieh, D.S.T.; Rhine W.D.; Langer, R., 1983. Zero-order controlled release polymer matrices for micro and macromolecules, *Journal of Pharmaceutical Sciences*, ***72***, 17–22.

IntelGel$_x$ Corp., 2009. Innovative Drug Delivery Solutions. http://www.intelgenx.com/_assets/pdf/Rodman-Renshaw-Sept-2009.pdf [accessed August 26, 2010].

Iyer, K.; Jha, R.J.; Saoji, D.G., 2006. Cardiovascular therapeutic combinations, *WIPO Patent Application*, WO/2006/085128.

Jerkovich, A.D.; Mellors, J.S.; Jorgensen, J.W., 2003. The use of micrometer-sized particles in ultrahigh pressure liquid chromatography, *LC-GC North America*, ***21***, 600-610.

Karnachi, A.A., Khan, M.A., 1996. Box-Behnken design for the optimization of formulation variables of indomethacin coprecipitates with polymer mixtures, *International Journal of Pharmaceutics*, ***131 (1)***, 9-17.

Kaushal, A.M., Garg, S., 2003. An update on osmotic drug delivery patents, *Pharmaceutical Technology*, 38-97.Kim, C.J., 1995. Compressed donut-shaped tablets with zero-order release kinetics. *Pharmaceutical Research,* ***12***, 1045–1048.

Kim, C.J., 1999. Release kinetics of coated, donut-shaped tablets for water soluble drugs, *European Journal of Pharmaceutical Sciences,* ***12***, 237-242.

Kim, C.J., 2000. Coated tablet with long term parabolic and zero-order release kinetics, *US Patent*, 6110500.

Kim, C.J., 2005. Controlled release from triple layer, donut-shaped tablets with enteric polymers, *AAPS PharmSci,* ***6***, 429-436.

Kim, S.W.; Jun, S.S.; Jo, Y.G.; Koo, J.S.; Jun, Y.S., 2008. Combination formulation with controlled release comprising metformin and glimepiride, *WIPO Patent Application*, WO/2008/050987.

Kohan M. I., 1999. Polymer Data Handbook. Oxford University Press Inc, Oxford.

Kohlrausch A., 2005. Multilayer tablet patent, *US Patent*, 20050186274.

Kolawole O.A., Pillay V., Choonara Y.E., 2007. Novel polyamide 6, 10 variants synthesised by modified interfacial polymerization for application as a rate-modulated monolithic drug delivery system, *Journal of Bioactive and Compatible Polymers*, *22*, 218-313.

Krishnaiah, C.H., Reddy, R., Kumar, R., Mukkanti, K., 2010. Stability-indicating UPLC method for determination of Valsartan and their degradation products in active pharmaceutical ingredient and pharmaceutical dosage forms, *Journal of Pharmaceutical and Biomedical Analysis*, ***53(3)***, 483-489.

Krishnaiah, Y.S.R.; Karthikeyan, R.S.; Gouri Sankar, V.; Satyanarayana, V., 2002. Three-layer guar gum matrix tablet formulations for oral controlled delivery of highly soluble trimetazidine dihydrochloride, *Journal of Controlled Release*, ***81***, 45-56.

Kydonieus A.F., 1991. Treatise on controlled drug delivery: fundamentals, optimization, applications, Informa Healthcare, Eds: Marcel Dekker: New York, USA.

Landgraf W, Li N.H, Benson J.R., 2005. New polymer enables near zero order release of drugs, *Drug Delivery Technology*, ***5(2)***, 48-55.

Learoyd, T.P.; Burrows, J. L.; French, E.; Seville, P.C., 2009. Sustained delivery by leucine-modified chitosan spray-dried respirable powders, *International Journal of Pharmaceutics*, ***372***, 97-104.

Lee, P.I., 1985. Kinetics of drug release from the hydrogel matrices, *Journal of Controlled Release*, ***2***, 277-288.

Lee, R.J., 2008. Modern drug discovery and development-GTCbio's Third Annual Summit conferene report, *IDRUGS*, 11, 101-104.

Lewis G., 2001. Properties of crosslinked ultra-high-molecular-weight polyethylene, *Biomaterials, **22***, 371-401.

Li, H.; Hardy, R.J.; Gu, X., 2008. Effect of drug solubility on polymer hydration and drug dissolution from polyethylene oxide (PEO) matrix tablets, *AAPS PharmSci, **9***, 437-443.

Lingam, M.; Ashok, T.; Venkateswarlu V; Rao Y.M., 2006. Design and evaluation of a novel matrix type multiple units as biphasic gastroretentive drug delivery systems, *AAPS PharmSci, **9***, 1253-1261.

Liu, Q.; Fassihi, R., 2008. Zero-order delivery of a highly soluble, low dose drug alfuzosin hydrochloride via gastro-retentive system, *International Journal of Pharmaceutics, **348***, 27–34.

Longxiao, L..; Xiangning, X., 2008. Preparation of bilayer-core osmotic pump tablet by coating the indented core tablet, *International Journal of Pharmaceutics, **352***, 225-239.

Longxiao, L.; Binjie, C., 2006. Preparation of monolithic osmotic pump system by coating the indented core tablet, *European Journal of Pharmaceutics and Biopharmaceutics,* ***64*****,** 180-184.

Lopes C.M., Lobo J.M.S., Pinto J.F., Costa P., 2006. Compressed mini-tablet as a biphasic delivery system, *International Journal of Pharmaceutics,* ***303***, 93-100.

Losi, E.; Bettini, R.; Santi, P.; Sonvico, F.; Colombo, G.; Lofthus, K.; Colombo, P.; Peppas, N.A., 2006. Assemblage of novel release modules for the development of adaptable drug delivery systems, *Journal of Controlled Release*, ***111***, 212-218.

Maggi, L.; Shepard, T.; Rochdi, M.; Grenier, P.; Halbeisen, S.; Zimmer, R.; Conte, U. ,1997. A simulation approach for efficient development of a naproxen Geomatrix Quick/Slow formulation. In: *Proceedings of the 24th International Symposium on Controlled Release of Bioactive Materials*, Stockholm, Sweden, 327–328.

Martin del Valle, E.M.; Galan, M.A.; Carbonell, R.G., 2009. Drug delivery technologies: The way forward in the new decade, *Industrial and Engineering Chemistry Research*, ***48***, 2475–2486.

Mittal, G., Sahana, D.K., Bhardwaj, V., Ravi Kumar, M.N.V., 2007. Estradiol loaded PLGA nanoparticles for oral administration: Effect of polymer molecular weight and copolymer composition on release behavior *in vitro* and *in vivo*, *Journal of Controlled Release*, ***119***, 77-85.

Mit-uppatham, C., Nithitanakul, M. and Supaphol, P., 2004. Ultrafine electrospun polyamide-6 fibers: effect of solution conditions on morphology and average fiber diameter, *Macromolecular Chemistry and Physics*, ***205***, 2327-2338.

Müller, E., Berger, R., Blass, E., Sluyts, D. and Pfennig, A. 2008. Liquid–Liquid Extraction, In: *Ullmann's Encyclopedia of Industrial Chemistry*, Eds: Wiley-VCH Verlag GmbH & Co. KgaA, online, DOI: 10.1002/14356007.b03_06.pub2.

Mueller, K.F.; Heiber, S.J., 1985. Crosslinked, porous polymers for controlled drug delivery, *US Patent*, 4 548 990.

Munro, S.A., Lewin, S.A., Smith, H., Engel, M.E., Fretheim, A., 2007. Patient adherence to tuberculosis treatment: A systematic review of qualitative research, *PLoS Medicine*, ***4(7)***, e238.doi:10.1371/journal.pmed.0040238.

Nair, K.C.M., Thomas, S. and Groeninckx, G. 2001. Thermal and dynamic mechanical analysis of polystyrene composites reinforced with short sisal fibres, *Composites Science and Technology*, ***61***, 2519-2529.

Namdeo, B., 2008. Barrier layers in multilayered tablets, *Express Pharma.* www.expresspharmaonline.com/20080731/research03.shtml. [accessed October 24, 2010.]

Narasimhan, B.; Langer, R., 1997. Zero-order release of micro and macromolecules from polymeric devices: the role of the burst effect, *Journal of Controlled Release*, ***47***, 13–20.

Naveen, R., 2009. Biodegradable Polymers in Controlled Drug Delivery. *Pharmainfo.net*. http://www.pharmainfo.net/raghanaveen/biodegradable-polymers-controlled-drug-delivery. [accessed on May 03, 2010]

Nelson, K.G.; Smith, S.J.; Bennet, R.M. 1987. Constant-release diffusion systems: rate control by means of geometric configuration. In *Controlled-Release Technology, Pharmaceutical Applications;* Lee, P.I., Good, W.R., Eds.; ACS Symposium Series: Washington DC, USA, 324–340.

Nirmal, J.; Saisivam, S.; Peddanna, C.; Muralidharan, S.; Godwinkumar, S.; Nagarajan, M., 2008. Bilayer tablets of Atorvastatin calcium and Nicotinic acid: Formulation and evaluation, *Chemical and Pharmaceutical Bulletin*, ***56***, 1455-1458.

Oberle, R.L., Das, H., Wong, S.L., Chan, K.K., Sawchuk, R.J., 1994. Pharmacokinetics and metabolism of diclofenac sodium in Yucatan miniature pigs, *Pharmaceutical Research*, ***11(5)***, 698-703.

Okhamafe A., York P., 1989. Thermal characterization of drug/polymer and excipient/polymer interactions in some films coating formulation, *Journal of Pharmacy and Pharmacology*, ***41***, 1-6.

Patel, V.M.; Prajapati, B.G.; Patel, M.M., 2007. Formulation, evaluation, and comparison of bilayered and multilayered mucoadhesive buccal devices of propranolol hydrochloride. *AAPS PharmSci*, ***8***, Article 22.

Patra, C.N.; Kumar, A.B.; Pandit, H.K.; Singh, S.P.; Devi, M.V., 2007. Design and evaluation of sustained release bilayer tablets of propranolol hydrochloride. *Acta Pharmaceutica*, ***57***, 479-89.

Peppas L.B., 1999. Polymers in controlled drug delivery, *Medical Plastics and biomaterials Magazine.*

Peppas, N.A.; Sahlin, J.J., 1989. A simple equation for the description of solute release: III. Coupling of diffusion and relaxation, *International Journal of Pharmaceutics,* ***57,*** 162-172.

Phutane P.; Shidhaye S.; Lotlikar, V.; Ghule, A.; Sutar, S.; Kadam, V., 2010. *In vitro* evaluation of novel sustained release microspheres of glipizide prepared by the emulsion solvent diffusion-evaporation method, *Journal of Young Pharmacists,* ***2(1)***, 35-41.

Pillay V., Fassihi R., 1999. Electrolyte induced compositional heterogeneity: A novel approach for rate-controlled oral drug delivery, *Journal of Pharmaceutical Sciences*, ***88***, 1140-1148.

Porter, S.C., 2009. Novel Drug Delivery: Review of current trends with oral solid dosage forms, *American Pharmaceutical Review*, ***85***, 28-35.

Pryce Lewis, W.E.; Rowe, C.W.; Cima, M.J.; Materna, P.A., 2010. System for manufacturing controlled release dosage forms, such as zero-order release profile dosage form manufactured by three-dimensional printing, *US Patent*, 7820201.

Qiu, Y.; Chidambaram, N.; Flood, K., 1998. Design and evaluation of layered diffusional matrices for zero-order sustained-release, *Journal of Controlled Release,* ***51***, 123-130.

Rao, N.G.R., Yadav, A., Kulkarni, U., 2010. Formulation and evaluation of zero-order release glipizide bilayer matrix tablets using natural and synthetic polymers, *International Journal of Current Pharmaceutical Research*, ***2(1)***, 34-42.

Reed, R.C.; Dutta, S.; Liu, W., 2009. Once-daily dosing is appropriate for extended-release divalproex over a wide dose range, but not for enteric-coated, delayed-release divalproex: Evidence *via* computer simulations and implications for epilepsy therapy. *Epilepsy Research*, ***87***, 260-267.

Rhine, W.D.; Hsieh, D.S.T.; Langer, R., 1980. Polymers for sustained macromolecule release: procedures to fabricate reproducible delivery systems and control release kinetics, *Journal of Pharmaceutical Sciences*, ***69***, 265-270.

Rosca I.D., Watarib F., Uob M., 2004. Microparticle formation and its mechanism in single and double emulsion solvent evaporation, *Journal of controlled release,* ***99***, 271-280.

Rubinstein, A.; Friedman, M.; Baluom, M.; Tirosh, B., 2007. Controlled release oral drug delivery system, *US Patent*, 7189414.

Sakamoto, J.H.; van de Ven, A.L.; Godin, B.; Blanco, E.; Serda, R.E.; Grattoni, A.; Ziemys, A.; Bouamrani, A.; Hu, T.; Ranganathan, S.I.; De Rosa, E.; Martinez, J.O.; Smid, C.A.; Buchanan, R.M.; Lee, S.Y.; Srinivasan, S.; Landry, M.; Meyn, A.; Tasciotti, E.; Liu, X.; Decuzzi, P.; Ferrari, M., 2010. Enabling individualized therapy through nanotechnology. *Pharmacological Research*, ***62(2)***, 57-89.

Sandile, M.K., Roderick, B.W., 2006. Evaluation of rate of swelling and erosion of verapamil (VRP) sustained release matrix tablets, *Drug Development and Industrial Pharmacy*, ***32***, 1139-1148.

Sangalli, M.E.; Conte, U.; Gazzaniga, A.; La Manna, A., 1993. Inert monolithic device with central hole for constant release. In Proceedings of *International Symposium of Controlled Release Bioactive Materials*, ***20***, 316-317.

Santander-Ortega, M.J., Csaba, N., González, L., Bastos-González, D., Ortega-Vinuesa J.L., 2010. Protein-loaded PLGA–PEO blend nanoparticles: encapsulation, release and degradation characteristics, *Colloid and Polymer Science*, ***288***, 141-150.

Sershen, S.; West, J., 2002. Implantable, polymeric systems for modulated drug delivery, *Advanced. Drug Delivery Reviews,* ***54***, 1225-1235.

Shah, A. C., 1988. Design of oral sustained release drug delivery systems: *in vitro* / *in vivo* Considerations. In *Oral Sustained Release Formulation Design and Evaluation;* Yacobi A., Halperin-Walega E., Eds.; Pergamon: New York, USA, 35–56.

Shahiwala, A.; Misra, A., 2004. Pulmonary absorption of Liposomal Levonorgestrel, *AAPS PharmSci*, ***5(1)***, E13.

Shionogi Pharma, Inc. 2008. Once a day Sular® (Nisoldipine) with Geomatrix® delivery system for the treatment of hypertension. http://www.sular.com/html/geomatrix.html [accessed August 24, 2010].

Shivaraj, A.; Selvam, R.P.; Mani, T.T.; Sivakumar, T., 2010. Design and evaluation of transdermal drug delivery of ketotifen fumarate, *International Journal of Pharmaceutical and Biomedical Research*, ***1(2)***, 42-47.

Siahi, M.R.; Barzegar-Jalali, M.; Monajjemzadeh, F.; Ghaffar, I.F.; Azarmi, S., 2005. Design and evaluation of 1- and 3-layer matrices of verapamil hydrochloride for sustaining its release, *AAPS PharmSci*, ***6***, 626-632.

Sibambo S., Pillay V., Choonara Y.E., 2008. A Novel Salted-out and Subsequently Crosslinked Poly(Lactic-co-Glycolic Acid) Polymeric Scaffold Applied to Monolithic Drug delivery, *Journal of Bioactive and Compatible Polymers*, ***23***, 132-152.

Siegel, S.; Winey, K., 2008. Long-Term Delivery Formulations and Methods of Use Thereof, *US Patent Application*, 20080305140.

Siepmann, J.; Streubel, A.; Peppas, N.A., 2002. Understanding and predicting Drug delivery from hydrophilic matrix tablets using the "Sequential Layer" Model, *Pharmaceutical Research*, ***19,*** 306-314.

Singh, B.N.; Kim, K.H., 2000. Floating drug delivery systems: an approach to oral controlled drug delivery via gastric retention, *Journal of Controlled Release*, ***63***, 235-259.

SkyePharma, 2010. A chronotherapy focused-real time oral drug delivery. http://www.skyepharma.com/ [accessed August 26, 2010].

Song, C.X., Labhasetwar, V., Murphy, H., Qu, X., Humphrey, W.R., Shebuski, R.J., Levy, R.J., 1997. Formulation and characterization of biodegradable nanoparticles for intravascular local drug delivery, *Journal of Controlled Release*, ***43***, 197-212.

Song, F.; Zhang, L.; Yang, C.; Yan, L., 2009. Genipin-crosslinked casein hydrogels for controlled drug delivery, *International Journal of Pharmaceutics*, ***373***, 41-47.

Streubel, A.; Siepmann, J.; Peppas, N.A.; Bodmeier, R., 2000. Bimodal drug release achieved with multi-layer matrix tablets: transport mechanisms and device design, *Journal of Controlled Release*, ***69***, 455-468.

Sundy, E.; Danckwerts, M.P., 2004. A novel compression-coated doughnut-shaped tablet design for zero-order sustained release, *European Journal of Pharmaceutical Sciences*, ***22***, 477-485.

Survase, S.; Kumar, N., 2007. Pulsatile drug delivery: Current scenario, *Current Research and Information on Pharmaceutical Science*, ***8***, 27-33.

Tiwari, S.B., Rajabi-Siahoomi, A.R., 2008. Extended-release oral drug delivery technologies: monolithic matrix systems, *Methods in Molecular Biology*, **437**, 217-243.

Torres, D., Garcia-Encina, G., Seijo, B. and Vila-Jato, J.L.,1995. Formulation and *in vitro* evaluation of HPMCAP-microencapsulated drug-resin complexes for sustained release of diclofenac, *International Journal of Pharmaceutics, **121**,* 239-243.

Townsend A., Hunt K., Wyke S., 2003. Managing multiple morbidity in mid-life: a qualitative study of attitudes to drug use, *British Medical Journal, **327***, 7419.

Ullah, Ismat**,** Jain, Nemichand B., 1998. Pharmaceutical composition containing a combination of a statin and aspirin and method.

Vandamme, T.F.; Ellis, K.J., 2004. Issues and challenges in developing ruminal drug delivery systems*, Advanced Drug Delivery Reviews*, ***56***, 1415-1436.

Varelas, C.G.; Dixon, D.G.; Steiner, C.A., 1995. Zero-order release from biphasic polymer hydrogels, *Journal of. Controlled Release*, ***34***, 185-192.

Varma M.V.S., Kaushal A.M., Garg A., Garg S., 2004. Factors Affecting Mechanism and Kinetics of Drug Release from Matrix-Based Oral Controlled Drug Delivery Systems, *American Journal of drug delivery, **2(1)***, 43-57.

Varum, F.J.O.; Merchant, H.A.; Basit A.W., 2010. Oral modified-release formulations in motion: The relationship between gastrointestinal transit and drug absorption, *International Journal of Pharmaceutics, **395***, 1-2, 26-36.

Vermeiren, E.; Hearnshaw, H.; Van Royen, P.; Denekens, J., 2001. Patient adherence to treatment: three decades of research. A comprehensive review, *Journal of Clinical Pharmacy and Therapeutics*, ***26***, 331-342.

Vyas S. P., Sood A., Venugopalan P., Venkatesan N., 2000. Preparation and characterisation of microencapsulated gelospheres for controlled oral theophylline delivery, *Journal of Microencapsulation*, ***17***, 767-775.

Wen, H., Park, K., 2010. Oral Controlled Release Formulation Design and Drug Delivery: *Theory to Practice*, Hoboken, N.J.: Wiley©

Wilding, I.R.; Coupe, A.J.; Davis, S.S., 1991. The role of gamma scintigraphy in oral drug delivery, *Advanced Drug Delivery Reviews*, ***7***, 87-117.

Wu C., McGinity J.W., 1999. Non-traditional plasticization of polymeric films, *International Journal of Pharmaceutics,* ***177***, 15-27.

Wu, Y.S., Frijlink, H.W., van Vliet, L.J., Stokroos, I., van der Voort Maarschalk, K., 2005. Location-Dependent Analysis of Porosity and Pore Direction in Tablets, *Pharmaceutical Research*, ***22(8)***, 1399-1405.

Yang, L., Fassihi, R., 2000. Zero-order release kinetics from a self-correcting floatable asymmetric configuration drug delivery system, *Journal of Pharmaceutical Sciences*, ***85***, 170-173.

Yang, L., Venkatesh, G., Fassihi, R., 1997. Compaction simulator study of a novel triple-layer tablet matrix for industrial tabletting, *International Journal of Pharmaceutics*, ***152***, 45-52.

Yang, L.; Eshragh, J.; Fassihi, R., 1999. A new intragastric delivery system for the treatment of *Helicobacter pylori* associated gastric ulcer: *in vitro* evaluation, *Journal of Controlled Release*, ***57***, 215-222.

Yang, L.; Johnson, B.; Fassihi, R., 1998. Determination of continuous changes in the gel layer thickness of poly(ethylene oxide) and HPMC tablets undergoing hydration: A textural analysis study, *Pharmaceutical Research*, ***15***, 1902-1906.

Ye I.M.; Karasulu, H.; Ertan, G., 2003. Different geometric shaped hydrogel theophylline tablets: statistical approach for estimating drug release, *Il Farmaco*, ***57***, 939-945.

Yoo, J.W., Dharmala, K., Lee, C.H., 2006. The physicodynamic properties of mucoadhesive polymeric films developed as female controlled drug delivery system, *International Journal of Pharmaceutics*, ***309***, 139-145.

Yu, D.; Branford-White, C.; Ma, Z.; Zhu, L.M.; Li, X.Y.; Yang, X.L., 2009. Novel drug delivery devices for providing linear release profiles fabricated by 3DP, *International Journal of Pharmaceutics,* ***370***, 160-166.

Yu, R., Chen, H., Chen, T., Zhou, X., 2008. Modeling and simulation of drug release from multi-layer biodegradable polymer microstructure in three dimensions. *Simulation Modelling Practice and Theory*, ***16***, 15–25.

Zerbe H.G.; Krumme, M., 2002. Design Characteristics and Release Properties of a Novel Erosion-Controlled Oral Delivery System. In *Modified-Release Drug Delivery Technology*; Rathbone, M.J., Hadgraft, J., Roberts, M.S., Eds.; Marcel Dekker: New York, USA, 59-76. DOI: 10.1201/9780203910337.ch6

Zerbe, H.G.; Szabo, P., 2006. Oral dosage formulation. *US Patent Application*, 20060127478.